A novel model system for the study of anti-tumour T-cell memory

Thesis

A novel model system for the study of anti-tumour T-cell memory

Dissertation

submitted to the
Department of Biology
at The Open University in London
for the degree of

Doctor of Philosophy (PhD)

Yolanda Dagmar Mahnke, BSc

Sponsoring establishment:
German Cancer Research Centre (DKFZ), Heidelberg, Germany

internal examiner: Prof. B. Kyewski
external examiner: Prof. A. Dalgleish

submitted on 7th September 2001
viva on 4th October 2001

for my parents

and

grandparents

and Emmanuel

Abstract

A novel model system for the study of anti-tumour T-cell memory

Y. Mahnke, Dept. of Cellular Immunology, DKFZ, Heidelberg, Germany.

An adoptive immunotherapy (ADI) protocol was developed where the fate and requirements of long-term persisting memory T-cells can be monitored. Anti-tumour immune peritoneal exudate cells (iPEC) were produced by injecting a subtumorigenic dose of the highly metastatic, β-gal$^+$ T-lymphoma into the ear pinna of syngeneic DBA/2 mice, followed by an intraperitoneal challenge with irradiation-inactivated tumour cells. 33.9 % of CD8$^+$ iPEC were shown to be recognising the immunodominant peptide of β-gal (aa 876-884), and, consistently, the iPEC exerted specific lysis of β-gal$^+$ cells. Upon adoptive transfer into sublethally irradiated, ESbL-Gal tumour-bearing, athymic Balb/c nu/nu mice, they conferred protective and long-lasting anti-tumour immunity. ADI-treated animals were able to reject subsequent high dose tumour challenges, and memory T-cells appeared to be only partially affected by γ-irradiation. β-gal$^{876\text{-}884}$ peptide/MHC class I tetramer stainings identified the bone marrow as the major compartment for the long-term persistence of memory T-cells, as β-gal$^{876\text{-}884}$ specific T-cells occurred at elevated frequencies in this microenvironment as compared to the spleen and lymph nodes. In a "parking experiment", Ag-removal led to a decrease of tetramer-binding cells below background levels. Tumour-reactive memory T-cells could be reisolated from ADI-treated animals by recruitment to the peritoneal cavity via Ag-specific challenge at this anatomical site. Reisolated memory PEC (mPEC) retained their reactivity and conferred tumour protection even after multiple transfers to subsequent tumour-bearing nude mice.

The present model proved to be a valuable tool for the evaluation of the factors and mechanisms involved in the long-term maintenance of T-cell memory, and promises to yield further invaluable data in this field of research.

Contents

List of Figures

List of Tables

Introduction

1.1 General introduction on host responses to infectious agents

(Janeway and Travers 1996, Male 1994)

The function of the immune system is to protect the body from invading organisms, such as bacteria, viruses, fungi and parasites. Leukocytes, together with a number of accessory cells, are responsible for this defensive function. They are distributed throughout the body and large accumulations are found at sites where infectious agents have the potential to invade (e.g. skin and mucosal surfaces of the lung and gastrointestinal tract). Immune cells are also localised in lymphoid organs including the bone marrow, thymus, spleen and lymph nodes. They use both the blood stream and the lymphatic system to migrate between tissues. A co-ordinated response aiming at the elimination of pathogens with minimal damage to host tissues is achieved by interaction of the different cellular and soluble components of the immune system.

Immune responses can broadly be classified as belonging to either innate or adaptive immunity, although most immune responses involve elements from both systems. Innate or natural immune responses are not improved by repeated infection, and were classically not considered to be specific for particular pathogens. Such responses are dominated by phagocytes and natural killer cells (NK-cells), and by soluble factors including those of the complement system and acute phase proteins. In contrast to innate immunity, the key features of adaptive immune responses are specificity and memory, which is marked by enhanced responses upon repeated encounters with the same infectious agent. Such antigen (Ag)-specific immune responses are also referred to as acquired immune responses, with T-cells and antibodies constituting the main effector mechanisms.

Recently, a family of Toll-like receptors (TLRs) have been identified which confer some degree of specificity to innate immune responses and represent a critical link between innate and adaptive immunity. TLRs are pattern-recognition receptors which are differentially expressed on APCs and the ten members identified to date have a broad specificity for conserved molecular patterns shared by large groups of pathogens. For example, TLR4 recognises lipopolysaccharides, whereas TLR2 is specific for lipoproteins and glycolipids, and TLR9 binds bacterial DNA via unmethylated CpG motifs. The different TLRs activate similar but distinct signalling pathways, thus offering APCs a means of discriminating between different stimuli. How TLRs recognise their targets is still unknown, but binding of microbes or their products results in the activation of APCs, up-regulating the expression of co-stimulatory molecules and inducing the production of conditional cytokines (Akira et al. 2001).

In the following sections I will concentrate on the nature of T-cell immunology.

1.2 T-cell immunology

T-cells are lymphocytes which mature in the thymus. They can be subdivided into different populations based upon markers expressed on their cell surface, namely into $CD4^+$ and $CD8^+$ T-cells. Functionally, they can be classified according to their cytokine response profiles as being either TH1 or TH2 type cells, the former comprising inflammatory $CD4^+$ T-cells and $CD8^+$ cytotoxic T-lymphocytes (CTL), and the latter involving $CD4^+$ helper T-cells and $CD8^+$ suppressor T-cells.
The multiple functions of T-cells include (i) recognition and destruction of infected cells, (ii) activation of phagocytes to destroy pathogens they have taken up, (iii) provision of B-cell help, and (iv) control of immune responses, mainly by production of soluble mediators (cytokines).

1.2.1 The T-cell receptor

T-cell progenitors originate from the bone marrow and mature in the micro-environment of the thymus to express a functional T-cell antigen receptor (TCR), with which they recognise antigenic peptide presented on proteins encoded by genes of the major histocompatibility complex (MHC) expressed on the surface of Ag presenting cells (APC).
In order to be able to recognise the enormous variety of possible infectious agents encountered in a lifetime, the TCR genes have evolved to provide a comparable diversity of Ag receptors for T-cells. Each T-lymphocyte expresses only one type of TCR and can therefore recognise only a limited number of antigens. Every T-cell clone differs from the next in respect to its TCR. As a consequence, T-cells can, on a population level, recognise virtually every antigenic peptide presented in conjunction with a self MHC molecule.
On most T-cells (> 90 %), the TCR heterodimer is composed of an α- and a β-chain, while a small sub-population of T-cells express a γδTCR. In the following paragraph, the structure of the β-chain will be discussed in more detail.
The TCR β-chain consists of a constant (Cβ), a joining (Jβ), a diversity (Dβ), and a variable (Vβ) segment (Fig. 1.1), each being encoded by more than one gene. The TCR genes are subject to allelic exclusion so that a unique receptor is expressed at the surface of a given T-cell clone. It is the Vβ together with the Vα region that constitute the peptide/MHC recognition site of the TCR. There are 24 murine Vβ region genes, but some of these do not encode a functional Vβ-chain while others are clonally eliminated in some mouse strains due to superantigen mediated deletion during thymic selection of T-cells (Table 1.1).

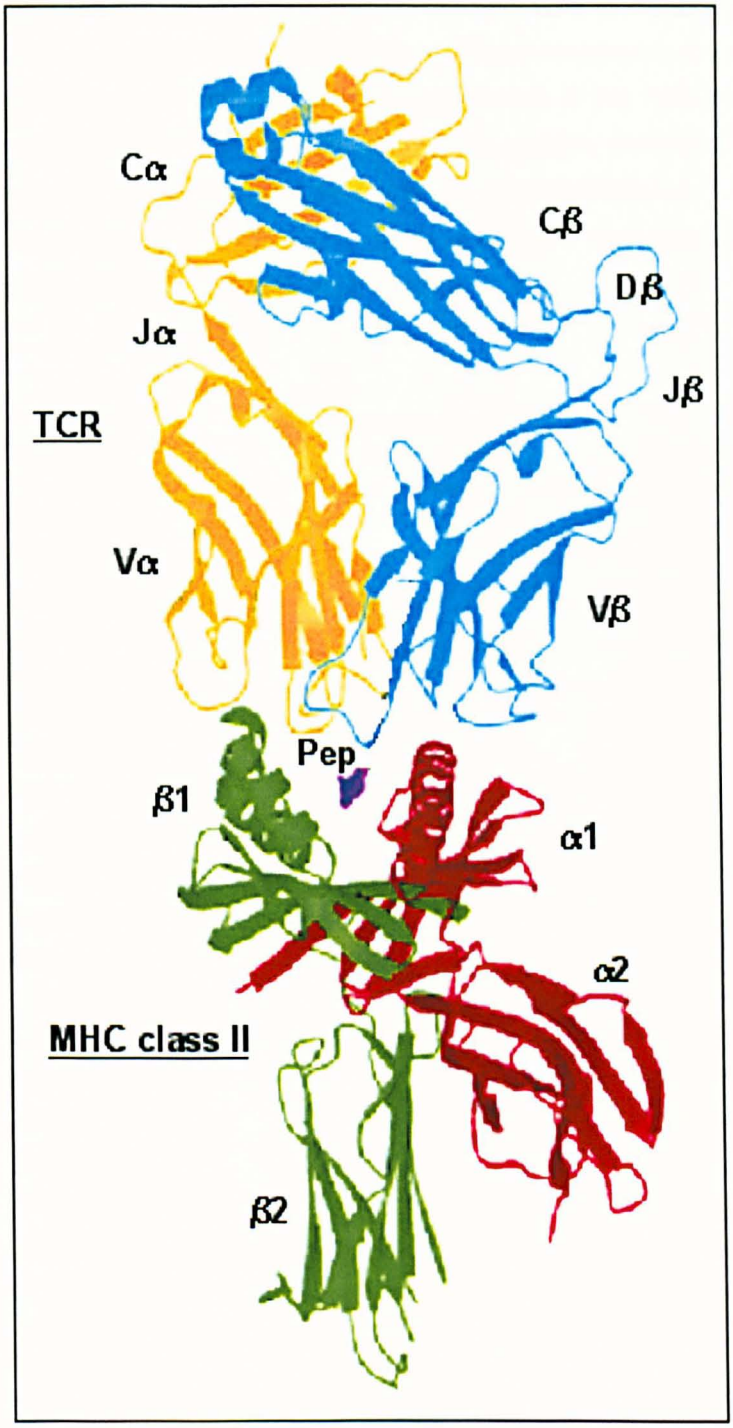

Fig. 1.1 Ribbon diagram of an αβTCR / peptide / MHC class II complex. During interaction of an APC with a T-cell, the TCR (α-chain: yellow, β-chain: blue) recognises antigenic peptide (Pep) in combination with an MHC complex, here a class II complex (α-chain: red, β-chain: green). TCR-segments are indicated as follows: V: variable region; C: constant region; J: joining segment; D: diversity segment. Adapted from Hennecke et al. 2000.

The total number of different Ag-specificities present in the mature T-lymphocyte population is referred to as the T-cell repertoire. During an immune response, interaction between a peptide/MHC complex and the variable part of the TCR may lead to clonal expansion of T-cells carrying the appropriate TCR. Thus, immunodominant epitopes may lead to the activation of T-cells expressing certain TCR α- or β-chains, resulting in the skewing of the TCR-Vα or -Vβ repertoire. T-cell responses to defined Ags or epitopes can range from a highly diverse TCR-repertoire to the dominance of a particular TCR-Vβ family or even a single TCR (Döffinger et al. 1997). Likewise, a study on the TCR-Vβ repertoire in shigellosis patients revealed a temporary skewing in both the $CD4^+$ and $CD8^+$ T-cell compartments (Islam et al. 1996).

TCR-Vβ chain	comment	reason for elimination	reference
Vβ1	expressed		
Vβ2	expressed		
Vβ3	clonally eliminated	*Mtv*-1, -3, -6, -13	Hodes et al. 1996
Vβ4	expressed		
Vβ5.1	clonally eliminated	*Mtv*-8 *	McMahan et al. 2000
Vβ5.2	clonally eliminated	*Mtv*-8 *	McMahan et al. 2000
Vβ5.3	pseudogene		Abu-Hadid et al. 1996
Vβ6	clonally eliminated	*Mtv*-7, -43	Hodes et al. 1996
Vβ7	clonally eliminated	*Mtv*-7, -43	Hodes et al. 1996
Vβ8.1	clonally eliminated	*Mtv*-7, -43	Hodes et al. 1996
Vβ8.2	expressed		
Vβ8.3	expressed		
Vβ9	clonally eliminated	*Mtv*-7, -43	Hodes et al. 1996
Vβ10	expressed		
Vβ11	clonally eliminated	*Mtv*-8, -11	Hodes et al. 1996
Vβ12	clonally eliminated	*Mtv*-8, -11	Hodes et al. 1996
Vβ13	expressed		
Vβ14	expressed		
Vβ15	expressed		
Vβ16	expressed		
Vβ17	pseudogene		Abu-Hadid et al. 1996
Vβ18	expressed		
Vβ19	pseudogene		Abu-Hadid et al. 1996
Vβ20	clonally eliminated	I-E	Six et al. 1991

Table 1.1 TCR-Vβ chain expression in DBA/2 mice. Endogenous proviruses are encoded in *Mtv*-loci of mouse mammary tumour viruses (MMTV). * affects only $CD4^+$ T-cells. Vβ5 chains are reportedly deleted in response to *Mtv*-9, but this is not expressed in DBA/2 (Hodes et al. 1996).

1.2.2 T-cell activation

T-cell responses are initiated in secondary lymphoid organs such as lymph nodes and spleen, where naïve T-cells encounter Ag-loaded professional APCs. Macrophages, B-cells, and dendritic cells (DCs) represent the professional APCs of the immune system, but DCs are the only ones capable of activating naïve T-cells. They are activated by endogenous or exogenous danger signals to capture, process, and present Ag along with co-stimulatory signals. In order to generate a productive immune response, conditioned DCs can be a temporal bridge between Ag-specific $CD4^+$ helper and $CD8^+$ cytotoxic T-cells. In a dynamic system, the DC initially stimulates the $CD4^+$ T-cell, which, in turn, stimulates and "conditions" it to differentiate into a state where it can then provide direct co-stimulation to the CTL (Ridge et al. 1998).

Exogenous (foreign) and endogenous proteins from the cell itself, which are localised in the cytoplasm are processed into peptides and transported into the endoplasmatic reticulum (ER), where they are loaded onto MHC class I molecules. The peptide/MHC molecular complexes are transported to the cell surface for Ag-presentation to $CD8^+$ T-cells, which are then activated and elicit their effector functions. In contrast to MHC class I, MHC class II molecules classically present peptides from exogenous proteins. Such Ags are taken up by phagocytosis, macropinocytosis, or receptor-mediated internalisation and are processed by proteases in intracellular vesicles, called lysosomes. The MHC class II complexes, either newly synthesised or recycled from the cell surface, are loaded in specialised compartments of the endosomal pathway termed MIICs (MHC class II compartments), from where they are transported to the cell surface for Ag-presentation to $CD4^+$ T-cells. This classical link of protein-origin and type of MHC involved in presentation is not strictly true, and it has been shown that MHC class I molecules can indeed present peptides from exogenous sources in a process termed cross-priming (Lanzavecchia et al. 1996). Likewise, MHC class II molecules can also present peptides derived from endogenous proteins (Pieters et al. 1997).

Ag-recognition of peptide/MHC complexes via the TCR/CD3 complex is the first step in T-cell activation. This interaction results in the up-regulation of CD40L on the T-cells, which in turn causes an up-regulation of the co-stimulatory molecules CD80, CD86, and ICAM-1 (intracellular adhesion molecule-1) on the APC via interaction with CD40. These interact with their ligands expressed on the T-cell's surface (CD28 for CD80 and CD86; LFA-1 (lymphocyte function-associated Ag-1) for ICAM-1), thus providing the second signal required for full T-cell activation, induction of proliferation and effector functions, and prevention of anergy or tolerance induction. The recently discovered CD28-related inducible co-stimulatory molecule (ICOS) that is expressed on activated T-cells, and which interacts with the CD80/CD86-related B7h on APCs, has been shown to be essential for T-cell activation and function, $ICOS^{-/-}$ T-cells exhibiting reduced proliferation and defective cytokine production upon activation (Dong et al. 2001).

1.2.3 Termination of an immune response: return to homeostasis and rescue of T-cells from apoptosis

Following activation, rare Ag-specific T-cells undergo an enormous and rapid expansion. At the resolution of the immune response when the Ag has been cleared, most of the T-cells involved in the response will be eliminated by apoptosis. This is a physiologic effect necessary in the return to cellular homeostasis. During this process, the rescue of some activated T-cells from apoptosis is essential for the establishment of long-term Ag-specific T-cell memory.

Two hypotheses have been proposed for the origin of memory T-cells (Fig. 1.2). One, referred to as the linear differentiation model, predicts that memory T-cells are the progeny of CTLs that escape activation-induced cell death (AICD), while the second, known as the decreasing potential model, proposes that weak antigenic stimulation could result in the development of memory T-cells which differentiate through a lineage parallel to effectors (Ahmed et al. 1996). Substantial evidence has recently been provided to support the linear differentiation model. Purified H-Y specific pre-CTLs adoptively transferred to H-Y negative hosts after having undergone 0 to 1 cell divisions did not produce any H-Y specific memory T-cells, while cells transferred after 9 divisions developed into long-term (3 weeks) surviving memory T-cells. Naïve $CD8^+$ T-cells thus have to undergo a certain number of cell divisions in the presence of the stimulating Ag in order to mature into CTLs which can further differentiate into long-term surviving memory T-cells (Opferman et al. 1999).

Recently, a new aspect has been added to the linear differentiation model in that not all CTLs appear to be equally predisposed for further maturation into memory T-cells. In fact, CTL which exert high cytolytic activity during an immune response were found to succumb to suicide by degranulation of their perforin/granzyme granules, while those cells that exert low cytolytic activity could later form part of the memory compartment. It has, therefore, been proposed that CTL which arrive early at the site of infection and are thus confronted with high Ag-levels would perform cytolysis, killing infected or abnormal cells, as well as themselves. In contrast, those cells that arrive later when Ag-levels have waned would not perform cytolysis and, instead, differentiate into memory cells (Opferman et al. 2001). Consequently, subjecting all responding T-cells to prolonged antigenic stimulation would result in full differentiation and a subsequent total elimination of the responding T-cell pool. No memory T-cells would develop under such conditions (Sprent et al. 2001), which would actually argue in favour of the decreasing potential model.

In addition to the death by suicide, Ag-stimulated T-cells can be killed by either AICD or cytokine deprivation. TCR-ligation on cells that are already in cycle results in AICD, involving a secondary interaction between CD95 (Fas/Apo-1) on the APC and CD95 ligand (CD95L) which is up-regulated on T-cells following activation. T-cells can thus be killed by over-stimulation. The second mechanism, cytokine deprivation, usually occurs during the resolution phase of an immune response when cytokines that signal through the interleukin-2 (IL-2) receptor (IL-2R) γ-chain (γ-chain cytokines: IL-2, IL-4, IL-7, IL-15) disappear from the site of inflammation. Such apoptotic clearance involves the down-regulation of intracellular apoptosis-inhibitory proteins (AIP), such as Bcl-2 and Bcl-x_L. Although the continuous presence of γ-chain cytokines can prevent apoptosis of

activated T-cells by inducing a high expression of Bcl-2 and Bcl-x_L, they simultaneously induce clonal expansion (Akbar et al. 1997).

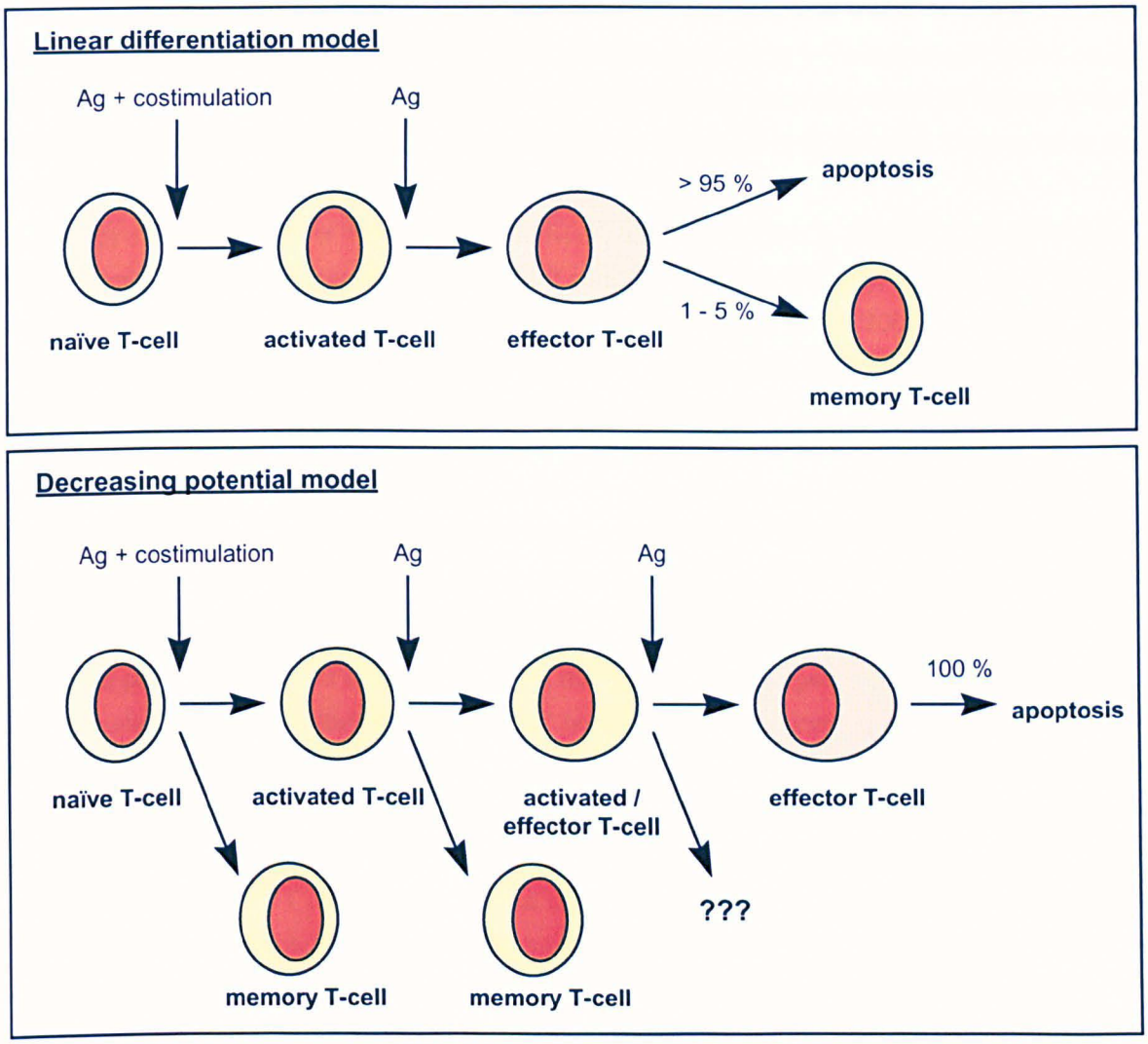

Fig. 1.2 Proposed pathways for the origin of memory T-cells. The top panel shows the linear differentiation pathway, while the lower panel illustrates the alternative decreasing potential hypothesis.
Adapted from Ahmed et al. 1996.

As early as 1990, Scott and colleagues proposed a fibroblast derived factor to be implicated in the retention of primed T-cells. They observed that IL-2 dependent T-cell lines that die upon IL-2 deprivation could be rescued by co-culture with fibroblasts of inflamed synovia or even by culture in fibroblast-conditioned medium (FCM = fibroblast culture supernatant) (Scott et al. 1990). Meanwhile, this stromal cell derived survival factor has been identified as being interferon-β (IFN-β), which does not cause cellular proliferation, and enhances the survival of primed T-cells by up-regulating the expression of Bcl-x_L but not Bcl-2. As a result, activated T-cell blasts are converted to a resting memory state by IFN-β (Pilling et al. 1999). Additionally, IFN-β prevents the translocation

of protein kinase C-δ (PKC-δ) from the cytoplasm to the nucleus, where it would be cleaved by caspase-3 to produce the apoptosis-inducing active PKC-δ enzyme. IFN-β also induces up-regulation of the intracellular antioxidant molecule glutathione, which further contributes to increased cell survival (Akbar et al. 2000). Although the anti-apoptotic effect of IFN-β could be mediated indirectly by IL-15 induction, this is not the case, as IL-15 (a γ-chain cytokine) would cause the T-cells to proliferate. It thus induces survival without inducing secondary cytokine release (Akbar et al. 2000). Survival and quiescence are induced only in a fraction of all activated T-cells due to the limited availability of the rescue factor IFN-β.

A recently cloned member of the AIP family, survivin, has been shown to prevent AICD by inhibiting the terminal effector caspases-3 and -7. While it could be demonstrated that survivin does not play a role in the maintenance of memory T-cells *per se* (Kornacker et al. 2001), it remains to be investigated whether this molecule might be involved in rescuing activated T-cells during the return to cellular homeostasis following an immune response.

1.2.4 T-cell memory

Immunological T-cell memory is characterised by the persistence of Ag-primed T-cells over extended periods of time. At a time point when the effector phase against an infection is over and the immune system has returned to a state of homeostasis, the surviving Ag-specific T-cells are termed memory T-cells and are present in elevated precursor numbers (Hou et al. 1994). They differ from naïve cells, having less stringent requirements for activation as they are less dependent on co-stimulation and require lower Ag-concentrations for activation (Feuerer et al. 2001). As a consequence, memory T-cells exhibit a more rapid and vigorous response to Ag-stimulation than do their naïve counterparts. Nevertheless, memory T-cells have been demonstrated to have a unique phenotype, in that they produce cytokines and commit to proliferation as rapidly as effector cells, while resembling naïve T-cells in their slower development of cytolytic function (Bachmann et al. 1999).

Whether Ag-persistence is required for the maintenance of memory T-cells has long been debated. In the early 1990s, the opinion was that this pool requires continuous restimulation provided by the persistence of Ag from the inoculum, cross-reactive Ag, non-specific pro-inflammatory stimuli or idiotype networks (Beverley et al. 1990). Several publications indicated that the presence of Ag is necessary in order to preserve the memory T-cell pool specific for that given Ag. As an example, Gray and Matzinger argued that the maintenance of T-cell memory for the minor histocompatibility Ag H-Y is only short-lived in the absence of Ag (Gray et al. 1991).

More recently, data have accumulated indicating that long-term survival of memory T-cells is indeed possible without the continuous presence of Ag, and it has been postulated that $CD8^+$ T-cell memory can survive in the absence not only of Ag (Müllbacher et al. 1994), but also of syngeneic MHC molecules (Tanchot et al. 1997), and that survival signals are provided by Ag non-specific stimuli (Sprent et al. 1997, Tanchot et al. 1998). Additionally, $CD4^+$ and $CD8^+$ memory T-cell pools have been demonstrated to be regulated independently (Varga et al. 2001).

Most of the work has been done on viral systems where low-level Ag may persist in specialised depots, such as follicular dendritic cells (FDC), or other as yet unidentified places. FDC have been shown to express non-phagocytic Fc-receptors (Fc-R) that allow them to hold unprocessed Ag : Ab immune complexes (ICs) on their surface for prolonged periods of time (Kelsoe 2000). Some of the retained ICs are converted into IC-coated bodies, called iccosomes, which can be endocytosed by germinal centre B-cells (Qin et al. 2000). These then process the iccosomal Ag and present it to T-cells, which in turn provide the help necessary for growth and differentiation of B-cells.

Such depots of Ag may play a role in the maintenance of B-cell memory and $CD4^+$ memory T-cells, but not for $CD8^+$ memory T-cells. Furthermore, as the continuous processing for MHC-presentation of a non-replicating Ag places a time limit on its availability for sustaining T-cell memory (Müllbacher et al. 1994), such specialised depots will be exhausted at some point in time.

In order to exclude the possibility of Ag-persistence on FDC to influence the results, many researchers have taken to using adoptive transfer systems, where purified virus-specific T-cells generated either *in vitro* or *in vivo* are transferred to animals negative for the Ag of choice (Bruno et al. 1995, Veiga-Fernandes et al. 2000).

Many model systems applied for T-cell memory research make use of transgenic T-cells. Such systems do not, however, reflect physiologic conditions, as transgenic T-cells will not undergo the same selective pressures as do T-cells under normal conditions, where T-cell clones compete with each other for survival factors and space.

1.2.5 Tools for the detection and isolation of Ag-specific T-cells

Identification of memory T-cells according to the differential expression of cell surface molecules has often proved to be rather inconclusive. In the murine system, there is no clear phenotypical distinction between effector and memory T-cells, although CD44 and CD62L expression are classically used to differentiate naïve from effector/memory T-cells, where $CD44^{hi}$ $CD62L^{lo}$ would mark the effector/memory phenotype.

Differential expression of the various isoforms of the lymphocyte marker CD45 has also been exploited. In the human system, this is quite reliable with the high molecular weight isoform CD45RA being expressed on naïve T-cells and the low molecular isoform CD45R0 on effector/memory T-cells. Analysis of the chemokine receptor-7 (CCR7) expression on $CD45R0^+$ cells further allows to differentiate between central memory ($CCR7^+$, resting) and effector memory ($CCD7^-$, cycling) cells (Sallusto et al. 1999). In mice, the high molecular weight isoform CD45RB is commonly expressed on all lymphocytes, with very high expression levels on naïve T-cells. Following T-cell activation, CD45RB expression is down-regulated, and most memory T-cells are negative for this molecule. Nevertheless, there exist a sub-population of memory T-cells with a "revertant" $CD45RB^{hi}$ phenotype (Table 1.2). Furthermore, this differential expression of CD45RB on naïve vs. memory T-cells appears to apply only to the $CD4^+$ compartment.

memory primed	memory revertant
low mol. wt. isoforms of CD45R	high mol. wt. isoforms of CD45R
Ag-dependent	Ag-independent
cycling	quiescent
rapid responder (2° kinetics)	slow responder (1° kinetics)
short lived	long lived
effector-like	*naïve-like*

Table 1.2 Characteristics of the two proposed CD4$^+$ memory T-cell types. Effector-like CD4$^+$ memory T-cells can revert to a naïve-like phenotype and *vice versa*. Adapted from Bell et al. 1998.

The cell surface markers could be used to differentiate between effector and memory T-cells when taking the time factor into consideration, defining all effector-phenotype T-cells present over one month after Ag-priming as memory T-cells. Nevertheless, this does not allow the identification of Ag-specific memory T-cells, as immune responses to environmental Ags, both in experimental and untreated control animals, will result in an increased frequency of memory phenotype T-cells with age. This will also occur under specific pathogen free (SPF) animal holding conditions, where responses can be elicited against food Ags.

Different approaches have been tested to circumvent this problem. As mentioned in 1.2.4, transgenic models have been widely used for T-cell memory research (Zimmermann et al. 1996, Bachmann et al. 1999, Opferman et al. 1999, Veiga-Fernandes et al. 2000, Kaech et al. 2001) as they reduce the problem of how to identify memory T-cells *in vivo* and how to purify them for *ex vivo* analysis. However, the major drawback of such model systems is that they do not reflect physiological conditions.

Another approach has been the quantification of Ag-specific memory cells by functional analysis. To this end, laborious limiting dilution assays have been set up where decreasing amounts of T-cells were cultured in the presence of Ag before evaluating Ag-reactivity in a ^{51}Cr-release assay (Lau et al. 1994), while Brosterhus and colleagues detected Ag-specific T-cells based on cytokine secretion after *in vitro* stimulation (Brosterhus et al. 1999).

More recently a novel technology for the detection of Ag-specific T-cells has emerged, namely the use of peptide/MHC tetrameric complexes. With the application of tetramers it was demonstrated that a significant fraction of herpes virus specific human CD8$^+$ T-cells revert from a CD45RO$^+$ to a CD45RA$^+$ state after priming. Such memory revertants resembled naïve T-cells in respect to their cell surface phenotype and recirculation pattern. However, unlike naïve T-cells they had very short telomeres and exhibited high expression levels of CD11a, indicating a history of activation and high cell turnover as well as a high level of differentiation (Faint et al. 2001).

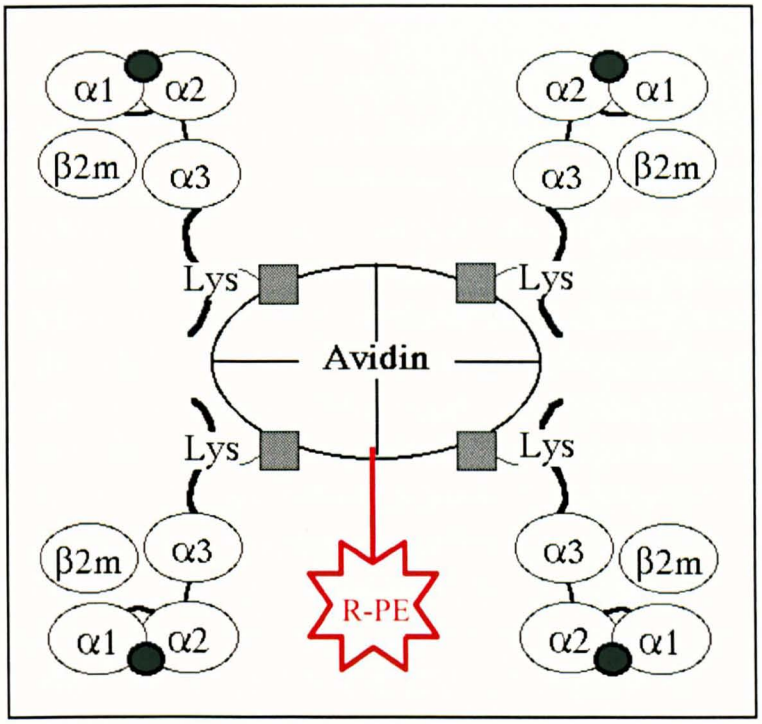

Fig. 1.3 Schematic representation of a peptide/MHC class I tetrameric complex. The MHC complexes are loaded with specific peptide sequences (●) and linked to streptavidin via linker peptides (bold lines) and biotin (■). α_1-α_3: domains of MHC class I α-chain; β2m: β_2-microglobulin; Lys: biotinylated lysine residue of the linker peptide.
Adapted from Altman and Safrit, HIV Molecular Immunology Database.

In combination with FACS analysis, peptide/MHC tetramers have thus proved to be valuable tools in the identification and characterisation of Ag-specific T-cells directly *ex vivo*, as well as in the purification of such cells for subsequent *in vitro* analyses.

1.3 Tumour-host interactions

1.3.1 Tumour immunology

At the basis of all anti-cancer immunotherapeutic strategies lies the assumption that malignant cells differ from their healthy precursors in the expression of so called tumour-associated Ags (TAA). The emergence of tumours and tumour metastases are, therefore, sometimes viewed as a failure of the immune system to mount a productive response for the elimination of abnormal cells.
$CD4^+$ helper T-cells as well as $CD8^+$ CTL are involved in cell-mediated tumour rejection. Many antigenic tumours develop immune escape mechanisms by somatic mutations. The selection of Ag loss variants (Bosslet et al. 1982), abnormalities in the expression and/or function of components of the Ag-processing and -presenting machinery (Alimonti et al. 2000, Seliger et al. 2000), expression of inhibitory molecules such as the non-classical Ags HLA-G and HLA-E (Carosella et al. 1999), and production of inhibitory cytokines such as IL-10 and TGF-β (tumour growth factor-β) (Finke et al. 1999) represent only some of the strategies for immunosurveillance escape used by tumour cells. In cases where Ag-presentation via MHC molecules is functional, deficiencies in the expression of co-stimulatory molecules can result in the induction of T-cell anergy and tolerance of the tumour, as TCR recognition of the tumour cells occurs, but the secondary signal required for T-cell activation is missing (Zheng et al. 1999). The expression of Fas ligand (FasL) on many types of tumour cells together with increased resistance to Fas-mediated apoptosis results in the induction of apoptosis in tumour infiltrating lymphocytes (Fas counterattack) as well as in the induction of tumour tolerance. This has lead to the assumption that cancers might represent sites of immune privilege (O'Connell et al. 1999).

1.3.2 Tumour immunotherapy

Most solid primary tumours can be removed surgically, but if malignant cells have already metastasised, patients often suffer a relapse. Early diagnosis is, therefore, essential to prevent dissemination of tumour cells from the primary source, which can result in the formation of metastases in vital organs, eventually causing a loss of function of the affected organ and death of the patient.
The most widely used non-surgical cancer treatments include radiotherapy, and chemotherapy, both acting non-specifically on proliferating tissues. They cause dramatic side effects, as they also affect healthy proliferating tissues, such as the bone marrow, intestinal epithelia, skin, and hair follicles. Additionally, the immune system is impaired or partly depleted. As a consequence, biological therapies, such as gene therapy or immunotherapy, are taking on an increasingly important role in the treatment of cancer, in that they are potentially more specific and reduce the likelihood of unwanted side effects.
The goal of anti-cancer immunotherapies is to break tumour resistance to immune attack (see 1.3.1), and to induce productive cell-mediated immune responses against abnormal cells. Cancer

patients have T-cells that are specific for TAA of the autologous tumour (Feuerer et al. 2001), but such cells are often anergised and non-reactive, and one immunotherapeutic goal is to provide the correct activation signals for these cells. Different approaches of immunotherapy include unspecific (application of cytokines or bacterial products), passive (Ab-therapy), adoptive (use of tumour-reactive immune cells), and active (e.g. modulation of autologous tumour cells to attain increased immunogenicity) immunotherapies. Examples for the latter two are given in the following chapters.

1.3.2.1 Adoptive immunotherapy (ADI) and introduction to ADI systems in the ESb T-lymphoma model

For cancer therapy, a broad spectrum of cell-based adoptive immunotherapies (ADI) using various types of anti-tumour effector cells are being evaluated, including lymphokine activated killer cells, large granular lymphocytes, or tumour infiltrating lymphocytes. One problem has been the poor efficiency of tumour targeting by effector cells cultured *in vitro* (Schirrmacher 1995a). *In vivo* models have been set up to study the factors involved in the efficient priming and tumour targeting of tumour reactive CTL.

Recently, a syngeneic murine model system of ADI against the highly metastatic DBA/2-derived T-lymphoma ESb has been developed, where whole-body irradiated, tumour-bearing DBA/2 mice were treated by transfer of *in situ* activated peritoneal exudate cells (PEC) from ESb-immunised DBA/2 mice (Schirrmacher et al. 1991, Schirrmacher et al. 1994b, Schirrmacher 1995b). It was demonstrated that the site of tumour inoculation is of critical importance in determining the type of systemic immune response generated and the clinical outcome, namely whether tumour growth or tumour resistance is obtained. Tumour growth was observed after injection of ESb cells at any anatomical site tested, except when tumour inoculation was carried out in the ear pinna. Here, the otherwise highly aggressive cells proved non-metastatic and non-tumourigenic. In comparison to a subcutaneous site, the ear pinna was shown to be superior in inducing a type 1 cytokine response after tumour injection, which could explain the difference in clinical outcome (Jurianz et al. 1998). Tumour cell integrity and viability were essential for the generation of tumour-reactive $CD8^+$ CTL both *in vitro* and *in vivo* (Schirrmacher et al. 1993).

A main metastatic target of the ESb T-lymphoma is the liver, and it could be shown that syngeneic ADI resulted in the clustering of $CD4^+$ and $CD8^+$ T-cells with a subset of host macrophages expressing the lymphocyte adhesion molecule sialoadhesin (Sn). These Sn^+ macrophages proved essential to the therapeutic success (Müerköster et al. 1999).

1.3.2.2 Active specific immunisation (ASI)

DNA-vaccination and somatic gene therapy are gaining increasing importance, as they promise to be a relatively simple and economic procedure for the induction of Ag-specific immune responses *in vivo*. They can be applied to achieve gene transfer, gene repair, or gene deletion. Different ways of

gene transfer include the injection of naked DNA, protein vectors, viral vectors, or DNA-liposome complexes (lipofection).

In experimental animals, the superiority of the ear pinna over muscle tissue as a site for DNA vaccination has been demonstrated (Förg et al. 1998). Transfection of the skin proved to be an efficient route of immunisation, possibly because this, alongside mucosal surfaces, is the physiologic site where most exogenous antigens are normally encountered. It has been reported that many cell types within the dermis and epidermis, including keratinocytes, macrophages and Langerhans' cells, take up and express the injected DNA (pCMVβ, coding for β-gal) without any preference (Förg et al. 1998). Although only a small proportion of DCs are transfected after ear pinna immunisation with naked DNA, a general activation of all DCs in the draining lymph node is observed, providing optimal conditions for effective T-cell activation (Akbari et al. 1999).

As for cellular injections in the ear pinna, the reasons for this as a privileged site for immunisation with plasmid DNA might be twofold. Local concentration of antigen in a restricted area connected with one major lymph node (*superfiscia cervicalis*) may result in fast stimulation of naïve T-cells by antigen-loaded DCs. Secondly, mechanical irritation by needle injection may induce local cytokine secretion and activate and recruit additional antigen-presenting cells. Additionally, the unmethylated CpG motifs present in bacterial plasmid DNA are known to exert potent immunostimulatory activity by inducing macrophages to produce IL-12, which in turn activates T- and NK-cells (Pisetsky 1996). They are, therefore, referred to as immunostimulatory DNA sequences (ISS). Such ISS could be shown to circumvent the need of $CD4^+$ helper T-cells in the induction of CTL activity by "licensing" the APC (see 1.2.2) for CTL-activation (Cho et al. 2000) via binding to TLR9 (see 1.1, Akira et al. 2001).

1.3.3 Tumour dormancy

Micrometastases are microscopic (< 2 mm) deposits of malignant cells that are segregated spatially from the primary tumour and have no specific blood supply. This might limit their growth as they depend on the passive diffusion for oxygen and nutrient supply (Kell et al. 2000). In patients with epithelial malignancies, such as breast, gastric and colorectal carcinoma, as well as squamous cell carcinomas of the head and neck, bone marrow micrometastases have been found to be a predictor of poor prognosis.

If proliferation and death rates are matched and angiogenesis is not induced, tumour cells can remain in a dormant state for long periods of time. By definition, tumour dormancy is a state in which potentially lethal tumour cells persist for a prolonged period of time in a clinically normal host with little or no increase in the tumour cell population. The microenvironment where they are located may affect the behaviour of tumour cells, and it has been shown that the persistence of tumour cells in a dormant state is closely associated with host immune responses (Matsuzawa et al. 1996). Lymph nodes and bone marrow appear to be privileged sites where tumour cells are proliferating, evidenced by expression of the S-phase specific proliferation marker Ki67, but prevented from expanding on a population level by an active host immune response involving $CD8^+$ T-cells (Müller et al. 1998). Immunologically controlled tumour dormancy thus represents a delicate balance

between the immunological properties of tumour cells and the status of the host immune system, tumour cell immunogenicity and cell-mediated immunity playing significant roles in its establishment and maintenance. Dormant tumour cells thus resemble clinical situations such as minimal residual disease or stable disease, where tumour foci may exist for prolonged periods of time under host control without enlargement.

Extracellular matrix (ECM) components such as the basement membrane play an important role in tumour dormancy (Pogány et al. 2001). They provide differentiation and survival signals (e.g. growth factors), as well as death neutralising signals to cells (e.g. increasing repair of DNA-damage following UV-radiation), and reduce the proliferative capacity of tumour cells. Taken together, the overall effect is a balance between tumour cell proliferation and apoptosis, the hallmark of tumour dormancy.

Tumour dormancy is a key limiting event in the treatment of malignant diseases, as the persistence of neoplastic cells represents a constant source for tumour recurrence and clinical relapse. The tumour dormancy state is, therefore, also included in the term minimal residual disease. Alterations in the host immune status, as well as tumour cell changes leading to increased malignancy or therapy resistance can both be involved in breaking the tumour dormant state. Nevertheless, the induction of long-lasting tumour dormancy might be a useful approach for the treatment of cancer patients, since it circumvents highly aggressive treatment strategies applied to eliminate even the last tumour cell (Morecki et al. 1996).

Dormant tumour cells provide persistent Ag-stimulation, potentially playing an important role in the long-term maintenance of anti-tumour immunity. It was shown that long-term protection was not achieved by vaccination with irradiated tumour cells, which persist for only a few weeks (< 3 weeks) in host bone marrow as compared to several months in the case of non-irradiated cells (Khazaie et al. 1994).

1.4 Structural and functional characterisation of the bone marrow

(Krstic 1994)

The bone marrow consists of two components. One is the bone marrow stroma, which is composed of arterioles, blood sinuses, adipose cells, and macrophages, and provides the blood supply, as well as growth factors to the bone marrow parenchyma. The parenchyma is the second component, and consists exclusively of haematopoietic cells at various stages of development, differentiation and maturation. These fill up the spaces within the meshwork of the vascular stroma.

The bone marrow is a primary lymphoid organ where haematopoiesis takes place. All blood cells are derived from the bone marrow, and B-cell, granulocyte, platelet, monocyte, thrombocyte, and erythrocyte maturation occurs in this special microenvironment. The bone marrow sinuses are lined by flattened endothelial cells which can produce openings to facilitate the release of mature blood elements into the circulation. Incorrectly developed blood elements are phagocytosed and destroyed by the numerous macrophages.

While the central role of the bone marrow in the successful development of the various immune system components is unquestioned, its potential of exerting secondary immune functions has hardly been addressed. Mature lymphocytes found in the bone marrow are mainly B-lymphocytes, but low numbers of T-cells are also found (1-2 % in mice; 30-50 % of mononuclear cells in humans). Early investigations have shown that the majority of all Ig-secreting cells are actually localised in the bone marrow. In this microenvironment, induction of Ig-production is slower initially, but overall longer lasting than that observed in other lymphoid compartments (Benner et al. 1981). It has been proposed that the bone marrow microenvironment can also support primary T-cell immune responses in a situation of disrupted lymphocyte trafficking in splenectomised animals, where the bone marrow assumed the functions usually attributed to the spleen (Tripp et al. 1997). Whether or not such primary T-cell responses also occur under physiologic conditions has not been investigated to date.

1.5 Athymic nude mice

Nude mice have a congenital aplasia of the thymus resulting in a quantitative and functional T-cell deficiency. This makes them a useful research tool for immunological and oncological studies. Athymic mice exhibit numerous immune system defects, including a reduced lymphocyte population which is almost entirely composed of B-cells. As a result, their susceptibility to infections is elevated.

As mice age, there is a gradual and partial development of limited T-cell function due to extrathymic maturation of bone marrow cells. Such extrathymic T-cells are also present in normal, euthymic animals, where reciprocal regulation between these T-cells and thymus-derived T-cells might occur. Extrathymic T-cells, also referred to as TCR^{int} T-cells due to their intermediate expression levels of the TCR/CD3 complex, are few in number and comprise both αβ ($CD4^+$, $CD8^+$ or $CD4^-CD8^-$) and γδT-cells. Like NKT-cells, they respond quickly to corresponding Ags, and are primitive T-cells which do not undergo selection. As a consequence, they harbour autoreactive "forbidden" clones, which can mediate autoreactive cytotoxicity to rapidly dividing self-cells. An increase in the number of extrathymic T-cells with age might, therefore, be important for the elimination of abnormal self-cells, such as virally infected cells and malignant tumour cells, which appear in the body with ageing (Abo 2001).

Although T-cells in nu/nu mice may arise from thymic rudiments, extrathymic differentiation is considered the major pathway of T-cell development in these animals. Extrathymic T-cell maturation can occur in several microenvironments, the most important being the intestinal epithelium (Emoto et al. 1996) and liver (Emoto et al. 1997). It is known that, during the foetal stage, the liver is a haematopoietic organ. In the adult liver, pluripotent stem cells still remain, which, by hepatocyte-derived IL-7, are induced to differentiate into TCR^{int} T-cells. After migration to the sinusoidal lumen, these undergo functional maturation stimulated by Kupffer cell-derived IL-12, IL-15, and IL-18 (Abo 2001).

Though T-cells can develop in nude mice along extrathymic pathways, T-cell numbers and function never reach levels comparable to those in normal mice.

1.6 Aims of this thesis

The mechanisms underlying long-term maintenance of T-cell memory are still poorly understood. In the centre of debate lies the question whether or not Ag-persistence is required (1.2.3). Most work on T-cell memory has been dealing with responses to soluble or viral Ag. While it is not clear whether T-cells specific for either soluble, viral, or cell-bound Ag have different requirements for survival, this needs to be analysed.
In the present work I set out to develop a novel model system to study anti-tumour T-cell memory. To this end, a graft-versus-leukaemia ADI system was established, comprising athymic nu/nu mice as therapy recipients where the fate of Ag-specific memory T-cells can be followed *in vivo* and *ex vivo*. The different components of this system were analysed, namely:

- T-lymphoma lines which were used as a source of tumour cells for the ADI were characterised concerning the expression of cell surface markers. Their migration kinetics after ear pinna injection in the primary syngeneic host were analysed.

- primary kinetics of $CD8^+$ T-cells specific for the H-$2L^d$-restricted immunodominant peptide of β-galactosidase (β-gal) were followed using peptide/MHC tetrameric complexes.

- immune peritoneal exudate cells used in the transfer were analysed for content of various immune cell populations, as well as for tumour specific cytotoxic activity.

- ADI-recipient mice were monitored for long-term survival.

- memory T-cells were tested for long-term survival, *in vivo* localisation, and requirement for Ag-persistence.

The final chapter of my work focuses on DNA-vaccination, which has emerged to be a promising tool in the design of new therapeutic strategies against a wide spectrum of diseases. As a hallmark of a good vaccine is not only its ability to prime a productive immune response, but also to induce long-term survival of T-cell memory, I addressed the question as to whether or not this is provided by DNA-vaccination.

1.7 Rationale for choice of model system

ADI with immune T-cells (e.g. effector CTL, central memory or effector memory T-cells) requires MHC-compatibility between donor and host. If this is not the case, the therapy may not be effective, and there is the risk of GvH-development. In response to host alloantigens, in particular allo-MHC, sensitised donor $CD4^+$ and $CD8^+$ T-cells can recruit macrophages to cause a severe hypoplasia of host lymphocytes (Kataoka et al. 2001) as well as pathological damage, especially in the skin, gut epithelium and liver. This is referred to as acute GvH disease (GvHD). In the chronic form of GvHD, alloreactive $CD4^+$ donor T-cells act as helpers of host B-cells, leading to B-cell activation and autoantibody production. Such complications are overcome by using ADI recipients which are either completely syngeneic or, if allogeneic, do not differ in the MHC gene complex.

In addition, athymic nude mice provide an optimal environment for the study of the fate of adoptively transferred Ag-specific T-cells, as, by nature, they are T-cell deficient. Adoptively transferred T-cells will thus occur at higher frequencies than in normal mice.

The present system is superior to the multiple transgenic T-cell models used for T-cell memory research, as it mimics physiological conditions where memory T-cell clones have to compete for survival factors and space. In this situation, the presence or absence of Ag might, therefore, be more critical to the maintenance of Ag-specific T-cells than it is in transgenic systems.

Materials

2.1 Apparatus

	commercial name, formula or clone	company or reference
Automatic Gamma Counter		Wallac, Turcu (FI)
AxioCam, camera for microscopy with Axioplan 2		Carl Zeiss, Göttingen (D)
Axioplan 2 imaging microscope		Carl Zeiss, Göttingen (D)
Centrifuge, Minifuge T		Heraeus, Hanau (D)
Cytospin centrifuge		Shandon, Pittsburgh (USA)
Electrophoresis system, Easy-Cast		Owl Separation Systems, Portsmouth (USA)
ELISA reader		Labsystems, Helsinki (FI)
FACScan		BD Biosciences, Heidelberg (D)
FACSvantage		BD Biosciences, Heidelberg (D)
Gammacell 1000, Caesium^{137}	(for cells)	Gammaster, Ede (NL)
Gammatron F80S, Cobalt^{60}	(for animals)	Siemens, Braunschweig (D)
Heating block, Grant QBT2		Neolab, Heidelberg (D)
Hybridisation oven		Bachofer, Reutlingen (D)
Laminar flow, SterilGARD Hood		The Baker Company Inc., Sanford (USA)
Liquid Scintillation Analyser, Tri-Carb 2100 TR		Packard, Groningen (NL)
Magnet stands, MPC-E-1 and MPC-L		Dynal, Hamburg (D)
Midi MACS Separation Unit		Miltenyi Biotec, Bergisch Gladbach (D)
Minigel migration trough, Mupid-21		Eurogentec, Seraing (B)
Nuaire US Autoflow Incubator		Nuaire, Plymouth (USA)
OctoMACS Separation Unit		Miltenyi Biotec, Bergisch Gladbach (D)
Phase contrast microscope		Carl Zeiss, Göttingen (D)
Roentgen film developing machine, Cuvix 160		Agfa, Köln (D)
Rotation device		Heidolph, Schwabach (D)
Spectrophotometer, GeneQuant pro		Amersham Pharmacia Biotec, Freiburg (D)
Ultracentrifuge L8-M		Beckman, Krefeld (D)
UV-lamp		Konrad Benda, Wiesloch (D)
UV Stratalinker^{TM} 2400		Stratgene, Heidelberg (D)
Vertical shaker, HS 501 digital		IKA Labortechnik, Staufen (D)
3 CCD video camera for ELISPOT with Axioplan 2		Sony Deutschland GmbH, Köln-Ossendorf (D)

2.2 Single-use items

	commercial name, formula or clone	company or reference
BioMax MS-1 roentgen film		Kodak, Stuttgart (D)
cell scraper		TPP, Trasadingen (CH)
cover glasses for microscope slides, various sizes		R. Langenbrinck, Emmendingen (D)
cryogenic vials, 2.0 ml		Corning B.V., Schiphol-Rijk (NL)
cytospin filter mats		Shandon, Pittsburgh (USA)
ELISA plates, flexible, 96-well		BD Biosciences, Heidelberg (D)
Eppendorf tubes 0.5/ 1.0/ 2.0 ml		Eppendorf, Köln (D)
FACS-tubes		Greiner, Frickenhausen (D)
gauze, 60 µm		Fritz Eckert GmbH, Waldkirchen (D)
gel-blotting paper, 3 MM Whatman paper		Schleicher & Schnell, Dassel (D)
Hybond^{TM}-N^{+} hybridisation transfer membrane		Amersham Pharmacia Biotec, Freiburg (D)
low-binding protein filter, 0.22 µm		Millipore, Eschborn (D)
microscope slides		R. Langenbrinck, Emmendingen (D)
MultiScreen plates, 0.45 µm cellulose ester membranes		Millipore, Eschborn (D)
needles, sterile; 20 G, 25 G, 27 G		BD Biosciences, Heidelberg (D)
NucTrap® probe purification columns		Stratagene, Heidelberg (D)
Petri dishes, bacteriological quality		Greiner, Frickenhausen (D)
Petri dishes, tissue-culture quality		TPP, Trasadingen (CH)
polystyrene tubes, 6.5 x 38 mm		BD Biosciences, Heidelberg (D)
pony vials		Packard, Groningen (NL)
QIAshredder		Qiagen GmBH, Hilden (D)
round-bottomed tubes, 5.0 ml		Greiner, Frickenhausen (D)
scalpel		PfM Ag, Köln (D)
separation columns; MS^{+}, LS^{+}		Miltenyi Biotec, Bergisch Gladbach (D)
sterile filters, 0.45 µm		Millipore, Eschborn (D)
syringe, sterile		Terumo, Louvain (B)
tissue culture flask; 25 cm^3, 75 cm^3, 150 cm^3		TPP, Trasadingen (CH)
tissue culture plates, round- & flat-bottomed; several sizes		TPP, Trasadingen (CH)

2.3 Reusable items

	commercial name, formula or clone	company or reference
BioMax MS intensifying screen		Kodak, Stuttgart (D)
centrifugal tubes, 500 ml		Nalgene, Rochester, NY (USA)
Erlenmeyer flasks, 500 ml		Fisher Scientific, Nidderau (D)
film exposure cassette		Appligene, Heidelberg (D)
glass tubes, 10 x 50 mm		neoLab, Heidelberg (D)
hybridisation bottles		Hybaid, Teddington, Middlesex (UK)
Neubauer chamber		Fisher Scientific, Nidderau (D)

2.4 Chemicals

agarose, electrophoresis grade		Life Technologies, Karlsruhe (D)
alkaline phosphatase conjugate substrate kit		BioRad, Hercules (USA)
ammonium acetate	$NH_4C_2H_3O_2$	Merck, Darmstadt (D)
ammonium chloride	NH_4Cl	Merck, Darmstadt (D)
assay diluent for OptEIA™ Sets		PharMingen, Hamburg (D)
bovine serum albumin	BSA	Sigma, Deisenhofen (D)
5-bromo-6-chloro-3-indolyl-β-D-galactopyranoside	X-gal, $C_{14}H_{15}BrClNO_6$	Roche Molecular Biochemicals, Mannheim (D)
chloroform	$CHCL_3$	Merck, Darmstadt (D)
diethyl pyrocarbonate	DEPC, $C_6H_{10}O_5$	Sigma, Deisenhofen (D)
N,N-dimethylformamide	DMF, C_3H_7NO	Merck, Darmstadt (D)
dimethyl sulfoxide	DMSO, C_2H_6OS	Merck, Darmstadt (D)
1,4-dithiothreitol	DTT, $C_4H_{10}O_2S_2$	Life Technologies, Karlsruhe (D)
Dynabeads® mRNA DIRECT™ buffer set		Dynal, Hamburg (D)
ethanol p.a.	C_2H_6O	Sigma, Deisenhofen (D)
ethidium bromide, 10 mg/ml	$C_{21}H_{20}N_3Br$	Sigma, Deisenhofen (D)
ethylene diaminotetraacetate	EDTA, $C_{10}H_{16}N_2O_8$	Life Technologies, Karlsruhe (D)
Ficoll, density: 1.077	Biocoll	Biochrom KG, Berlin (D)
fluorescein di-β-D-galactopyranoside	FDG, $C_{32}H_{32}O_{15}$	Molecular Probes, Leiden (NL)
formaldehyde, 37%	CH_2O	Merck, Darmstadt (D)
glacial acetic acid	$C_2H_4O_2$	Merck, Darmstadt (D)
glutaraldehyde, 25%	$C_5H_8O_2$	Merck, Darmstadt (D)
glycerol	$C_3H_8O_3$	Merck, Darmstadt (D)
glycogen		Merck, Darmstadt (D)

	commercial name, formula or clone	company or reference
heparin-sodium, 5.000 I.U./ml		B. Braun Melsungen AG, Melsungen (D)
hydrochloric acid	HCl	J. T. Baker B.V., Deventer (NL)
isoamyl alcohol	$C_5H_{12}O$	Merck, Darmstadt (D)
isopropanol p.a.	C_3H_8O	Sigma, Deisenhofen (D)
Kaiser's glycerol gelatine		Merck, Darmstadt (D)
ketamine hydrochloride, 50 mg/ml	ketanest, $C_{13}H_{16}ClNO$	Parke-Davis GmbH, Berlin (D)
lithium chloride	LiCl	Merck, Darmstadt (D)
loading buffer, 6x		MBI Fermentas, St. Leon-Rot (D)
magnesium chloride	$MgCl_2$	Sigma, Deisenhofen (D)
magnesium sulfate	$MgSO_4$	Merck, Darmstadt (D)
β-mercaptoethanol	C_2H_6OS	Merck, Darmstadt (D)
Nonidet P-40	NP-40	Sigma, Deisenhofen (D)
paraffin wax		Vogel, Medizinische Technik & Elektronik, Giessen (D)
phenol	C_6H_6O	Merck, Darmstadt (D)
phosphate buffered saline	PBS	Biochrom KG, Berlin (D)
polyoxyethylene sorbitan monolaurate	Tween 20	Gerbu, Gaiberg (D)
potassium chloride	KCl	Merck, Darmstadt (D)
potassium ferricyanide	$K_3Fe(CN)_6$	Sigma, Deisenhofen (D)
potassium ferrocyanide	$K_4Fe(CN)_6 \times 3\ H_2O$	Sigma, Deisenhofen (D)
potassium hydrogen carbonate	$KHCO_3$	Merck, Darmstadt (D)
propidium iodide	PI, $C_{27}H_{34}N_4I_2$	Sigma, Deisenhofen (D)
sodium acetate	$NaC_2H_3O_2$	Merck, Darmstadt (D)
sodium azide	NaN_3	Merck, Darmstadt (D)
sodium bicarbonate	$NaHCO_3$	Merck, Darmstadt (D)
sodium carbonate	Na_2CO_3	Merck, Darmstadt (D)
sodium chloride	NaCl	Merck, Darmstadt (D)
sodium chromate	$Na_2{}^{51}CrO_4$	NEN, Bad Homburg (D)
sodium deoxycholate		Sigma, Deisenhofen (D)
sodium dodecyl sulfate	SDS, $NaC_{12}H_{25}O_4S$	Merck, Darmstadt (D)
sodium hydrogenphosphate	$NaHPO_4$	Merck, Darmstadt (D)
sodium hydroxide	NaOH	J. T. Baker B.V., Deventer (NL)
spermidine		Sigma, Deisenhofen (D)
sulphuric acid	H_2SO_4	Merck, Darmstadt (D)
tetramethylbenzidine (TMB) microwell peroxidase substrate system		KPL, Gaithersburg (USA)

	commercial name, formula or clone	company or reference
trihydroxymethyl aminomethane	Tris, $C_4H_{11}NO_3$	Sigma, Deisenhofen (D)
Tris-HCl, 1M, DNA/RNA-free	$C_4H_{11}NO_3$	Sigma, Deisenhofen (D)
trypan blue	$C_{34}H_{24}N_6O_{14}S_4Na_4$	Merck, Darmstadt (D)
xylazine hydrochloride, 2%	rompun, $C_{12}H_{16}N_2S$	Bayer AG, Leverkusen (D)

2.5 Media and media supplements

ampicillin	$C_{16}H_{19}N_3O_4S$	Sigma, Deisenhofen (D)
foetal calf serum	FCS	Biochrom KG, Berlin (D)
geneticin®	G418 sulphate, $C_{20}H_{40}N_4O_{10} \times H_2SO_4$	Life Technologies, Karlsruhe (D)
gentamicin		Life Technologies, Karlsruhe (D)
L-glutamin, 200 mM	$C_5H_{10}N_2O_3$	Life Technologies, Karlsruhe (D)
granulocyte/macrophage colony-stimulating factor	GM-CSF	own production; see cell line Ag8653
N-2-hydroxyethylpiperazine-	HEPES, $C_8H_{18}N_2O_4S$ -N'-2-ethanesulfonic acid	Life Technologies, Karlsruhe (D)
β-mercaptoethanol	C_2H_6OS	Life Technologies, Karlsruhe (D)
penicillin/streptomycin, 10,000 IU/ml / 10,000 µg/ml		Life Technologies, Karlsruhe (D)
phytohemagglutinin	PHA-P	Sigma, Deisenhofen (D)
RPMI 1640		Life Technologies, Karlsruhe (D)
tryptone peptone	bacto-tryptone	Difco, Heidelberg (D)
X-vivo 20, serum-free medium		BioWhittaker, Verviers (B)
yeast extract	bacto-yeast extract	Difco, Heidelberg (D)

2.6 Cells

		commercial name, formula or clone	company or reference
Established murine cell lines			
Eb 288	Heidelberg subline of the methyl-cholanthrene induced T-lymphoma L5178Y/E of the DBA/2 mouse; low metastatic variant		Schirrmacher et al. 1979
ESb 289	spontaneous, high metastatic variant of Eb 288		Schirrmacher et al. 1979
ESb-L	more aggressive form of ESb 289, isolated from a liver metastasis		Krüger et al. 1994a
ESbL-Gal	bacterial *lacZ* gene transduced ESb-L subline (clone: L-Cl.5s); highly metastatic		Krüger et al. 1994a
P815	methyl-cholanthrene induced mastocytoma of the DBA/2 mouse; non-metastasising		Matter et al. 1976
P815-Gal	bacterial *lacZ* gene transduced subline of P815, commonly known as P13.1		Carbone et al. 1990
Ag8653	murine GM-CSF producing cell line		Zal et al. 1994
Primary murine tumour cell lines			
ESbL-Gal-BM	ESbL-Gal variant isolated from the bone marrow of ESbL-Gal-immunised DBA/2		
ESbL-Gal-ET	ESbL-Gal variant isolated from an ear tumour		
ESbL-Gal-ST	ESbL-Gal variant isolated from a spleen tumour		
ESbL-Gal-TT	ESbL-Gal variant isolated from a throat tumour		
Bacteria			
DH5α competent cells		*E.coli*	Clontech, Heidelberg (D)

2.7 Experimental animals

DBA/2 mice, female	H-2L^d	Charles River, Sulzfeld (D)
Balb/c nu/nu mice, female	H-2L^d	Iffa Credo, l'Arbresle (FR)
CD1 Swiss nu/nu mice, female	outbred	Charles River, Sulzfeld (D)

2.8 Antibodies and ELISA-Sets

commercial name,	formula or clone	company or reference
anti-β7 integrin chain, purified	FIB27	BD PharMingen, Hamburg (D)
anti-CD2 (LFA-2), purified	RM2-5	BD PharMingen, Hamburg (D)
anti-CD3ε, FITC-conjugated	145-2C11	BD PharMingen, Hamburg (D)
anti-CD4, CyChrome-conjugated	GK1.5	BD PharMingen, Hamburg (D)
anti-CD8α, CyChrome-conjugated	53-6.7	BD PharMingen, Hamburg (D)
anti-CD8α, FITC-conjugated	53-6.7	BD PharMingen, Hamburg (D)
anti-CD11a (LFA-1), purified	Tib 213	Prof. P. Altevogt, DKFZ, Heidelberg (D)
anti-CD11c (integrin α_x), FITC-conjugated	N418	BD PharMingen, Hamburg (D)
anti-CD19, FITC-conjugated	6D5	Beckman Coulter, Krefeld (D)
anti-CD45R/B220, R-PE-conjugated	RA3-6B2	BD PharMingen, Hamburg (D)
anti-CD62L (L-selectin), FITC-conjugated	Mel-14	BD PharMingen, Hamburg (D)
anti-CD80 (B7.1), R-PE-conjugated	16-10A1	BD PharMingen, Hamburg (D)
anti-CD86 (B7.2), R-PE-conjugated	RMMP1	BD PharMingen, Hamburg (D)
anti-CD90.2 (Thy1.2), FITC-conjugated	53-2.1	BD PharMingen, Hamburg (D)
anti-F4/80, FITC-conjugated	F4/80	Serotec, Eching (D)
anti-H-2D^d (MHC class I), R-PE-conjugated	34-2-12	BD PharMingen, Hamburg (D)
anti-H-2L^d (MHC class I), culture supernatant	19.191	Prof. G. Hämmerling, DKFZ, Heidelberg (D)
anti-I-A^d (MHC class II), R-PE-conjugated	AMS-32.1	BD PharMingen, Hamburg (D)
anti-ICAM-1, purified	YN.1/1.7	Prof. P. Altevogt, DKFZ, Heidelberg (D)
anti-PSGL-1, culture supernatant	2PH-1	Prof. P. Altevogt, DKFZ, Heidelberg (D)
PanNK mAb, FITC-conjugated	DX5	BD PharMingen, Hamburg (D)
donkey anti-rat IgG (H+L), R-PE-conjugated		Dianova, Hamburg (D)
CD90 (Thy1.2) MACS MicroBeads		Miltenyi Biotec, Bergisch Gladbach (D)
Dynabeads® mouse CD4 (L3T4)		Dynal, Hamburg (D)
Dynabeads® mouse CD8 (Lyt-2)		Dynal, Hamburg (D)
murine IFN-γ ELISPOT Kit		Diaclone, Besançon Cedex (FR)
OptEIA™ mouse IFN-γ Set		BD PharMingen, Hamburg (D)
OptEIA™ mouse IL-2 Set		BD PharMingen, Hamburg (D)
OptEIA™ mouse IL-4 Set		BD PharMingen, Hamburg (D)
OptEIA™ mouse IL-5 Set		BD PharMingen, Hamburg (D)
OptEIA™ mouse IL-6 Set		BD PharMingen, Hamburg (D)
OptEIA™ mouse IL-10 Set		BD PharMingen, Hamburg (D)

	company or reference
OptEIA™ mouse IL-12 (p70) Set	BD PharMingen, Hamburg (D)
OptEIA™ mouse TNF-α Set	BD PharMingen, Hamburg (D)

2.9 Proteins, peptides, and tetramers

H-2L^d-TPHPARIGL tetramer, R-PE-conjugated	NIAID Tetramer Facility and NIH AIDS Research and Reference Reagent Program, Bethesda (USA)
ovalbumin, FITC-conjugated	Molecular Probes, Leiden (NL)
TPHPARIGL, β-gal peptide 876-884	Gavin et al. 1993
YPHFMPTNL, MCMV pp89 peptide 168-176	Reddehase et al. 1989

2.10 Enzymes, including kits for molecular biology

Eco RV, 20,000 U/ml + NEBuffer 3 + BSA, 10 mg/ml	New England Biolabs GmbH, Schwalbach/Taunus (D)
Platinum Taq + 10x PCR buffer + 25 mM $MgCl_2$	Life Technologies, Karlsruhe (D)
proteinase K	Roche Molecular Biochemicals, Mannheim (D)
QIAquick Gel Extraction Kit	Qiagen GmBH, Hilden (D)
REDTaq™ DNA Polymerase + 10x REDTaq PCR buffer	Sigma, Deisenhofen (D)
RNeasy Mini Kit	Qiagen GmBH, Hilden (D)
SuperScript™ II RNase H$^-$ Reverse Transcriptase	Life Technologies, Karlsruhe (D)
SuperScript™ Choice System for cDNA Synthesis	Life Technologies, Karlsruhe (D)
T4 polynucleotide kinase	MBI Fermentas, St. Leon-Rot (D)
Xho I, 20,000 U/ml + NEBuffer 2 + BSA, 10 mg/ml	New England Biolabs GmbH, Schwalbach/Taunus (D)

2.11 PCR-primers, nucleotides, oligonucleotides, and plasmids

	company or reference
[γ-^{32}P]-ATP	Amersham Pharmacia Biotec, Freiburg (D)
100 bp DNA ladder	Life Technologies, Karlsruhe (D)
dNTP, 10 mM	Amersham Pharmacia Biotec, Freiburg (D)
Dynabeads® Oligo $(dT)_{25}$	Dynal, Hamburg (D)
λ DNA/*Eco* 91I (*Bst* EII) Marker	MBI Fermentas, St. Leon-Rot (D)
oligo $(dT)_{18}$ and other oligonucleotides	Life Technologies, Karlsruhe (D)
pCMVβ	Clontech, Heidelberg (D)
PCR-primers	Life Technologies, Karlsruhe (D)
riboATP	Roche Molecular Biochemicals, Mannheim (D)

2.12 Additional software

Axiovision 3.0	Carl Zeiss, Göttingen (D)
CELLQuest	BD Biosciences, Heidelberg (D)
KS ELISPOT	Carl Zeiss, Göttingen (D)

Methods

3.1 Cell culture

3.1.1 Cell culture conditions

RPMI media

			complete	minimal nutrient
RPMI 1640				
FCS	5	% (v/v)	+	--
β-mercaptoethanol	0.05	mM	+	+
L-Glutamine	2	mM	+	--
HEPES	10	mM	+	+
penicillin	50	IU/ml	+	+
streptomycin	50	µg/ml	+	+

Passaging of cells occurs under sterile conditions in a laminar flow. All cell culture incubations are carried out at 37°C, 5% CO_2 and 96% humidity. Centrifugation steps during cell handling are for 5 minutes at 250 x *g* unless indicated otherwise.
Foetal calf serum (FCS) is heat-inactivated by a one-hour incubation at 56°C.

Eb-derived cell lines, including the ESbL-Gal-variants, as well as P815, P815-Gal, and Ag8653 are incubated in complete RPMI with 3 passages per week. The adherent lines P815, P815-Gal, and Ag8653 are mechanically detached using a cell scraper.
With the β-galactosidase (β-gal) expressing cell lines ESbL-Gal, the variants thereof, and P815-Gal, G418 is applied at 500 µg/ml during the first passage. This selective agent is toxic to both prokaryotic and eukaryotic cells, unless they contain the neomycin resistance gene *neo*. In ESbL-Gal and P815-Gal the *neo* gene was introduced together with the *lacZ* gene, which codes for β-gal.

3.1.2 Freezing and thawing of cells

Ag8653 and primary dendritic cells (DCs, 3.1.9.2) are washed once and taken up in X-vivo 20 medium, containing 10 % DMSO, while all other cells are taken up in RPMI with 40 % FCS and 10 % DMSO. Cells are transferred to cryogenic vials in a total volume of 1 ml at a concentration of 2×10^6 - 1×10^7 cells before freezing them at -70°C. 24 hours later, the vials are transferred to a liquid nitrogen tank.

Cells are thawed with pre-warmed medium, diluted 1:20 and spun down by centrifugation. The pellet is taken up in fresh medium and given to a medium-sized tissue culture flask.

3.1.3 Determination of viable cell numbers by trypan blue exclusion

Trypan blue staining solution

ddH_2O with	
trypan blue	0.16 % (w/v)
NaCl	0.90 % (w/v)

Trypan blue is used to differentiate viable from non-viable cells, due to its property to pass through holes which open up in the plasma membrane of dead cells, while remaining excluded from live cells.
For cell counting, a cell sample is mixed with trypan blue staining solution at a desired dilution factor and allowed to fill a Neubauer chamber (haemacytometer) by capillary action. The unstained cells are counted in 4 large corner squares and the cellular concentration calculated using the following formula:

$$\text{cells / ml} = \text{average cell count per square} \times \text{dilution factor} \times 10^4$$

Overall cell viability of a cell sample is calculated as follows:

$$\%\ \text{cells viability} = \text{total viable cells (unstained)} \div \text{total cells (stained + unstained)} \times 100$$

3.1.4 Preparation of cell lysates

1×10^6 ESbL-Gal/ml phosphate buffered saline (PBS) are lysed by repetitively freezing at -198°C in liquid N_2 and thawing at r/t. The sample is centrifuged for 10 minutes at 2000 x *g* and the soluble lysate obtained is stored at -20°C until use.

3.1.5 Isolation of cells from murine lymphoid organs

For pathological analyses or isolation of cells or organs, experimental animals are killed with CO_2.

3.1.5.1 Preparing a single cell suspension from murine bone marrow

Femurs and tibiae are removed from experimental mice and excess muscle tissue is removed mechanically with the help of paper towels. Both ends of the bones are cut off with a scalpel so that the bone marrow plugs can be flushed out with cold PBS, using a syringe with a 27 gauge needle. A single cell suspension is obtained by vigorous pipetting with a 1 ml Pasteur pipette. The resulting suspension is washed once with cold PBS before use. Where needed, lysis of erythrocytes is carried out (see 3.1.10).

3.1.5.2 Preparing a single cell suspension from murine spleen

All excess connective tissue is removed from isolated spleens with the help of forceps. The spleens are then placed into a folded 60 µm gauze inside a 60 mm Petri dish containing 3 ml PBS. A sterile plunger from a 2 ml syringe is used to crush the organ, thereby producing a single cell suspension. In order to extract a maximum number of splenocytes, the gauze is rinsed twice with fresh PBS. The cells are pelleted by centrifugation in a 15 ml centrifugal tube, the supernatant is discarded, and erythrocytes are lysed as described under 3.1.10.

3.1.5.3 Preparing a single cell suspension from murine lymph nodes and thymus

The preparation method is analogous to that described for spleens, except that erythrocyte lysis is not required. A single washing step is sufficient after dissociation of the organs.

3.1.5.4 Isolation of peripheral blood leukocytes

Heparin buffer

PBS with	
heparin	50.0 I.E./ml
FCS	2.0 % (v/v)
sodium azide	0.1 % (v/v)

For the isolation of peripheral blood lymphocytes (PBL) from freshly killed animals, blood is isolated by puncturing the heart with a syringe and 27 gauge needle, while with live animals, blood is

obtained from the eye vein with the help of a glass capillary. In both cases, the blood is mixed well with 200 µl of heparin buffer in a 1.5 ml Eppendorf tube, and then pipetted into a 10 x 50 mm glass tube containing 1 ml Ficoll. After a 20 minute centrifugation step at 900 x *g* without brake, the PBL-containing interphase is pipetted off and washed once in PBS.

3.1.5.5 Harvesting anti-ESbL-Gal immune peritoneal exudate cells (iPEC)

For the production of anti-ESbL-Gal immune PEC, naïve DBA/2 mice are primed with 5 x 10^4 ESbL-Gal i.e. (in the ear pinna) and restimulated on d7 with 1 x 10^7 100 Gy irradiated ESbL-Gal i.p. (intraperitoneally, see 3.2.2) (Schirrmacher et al. 1991). 3 days after the second tumour inoculation, the animals are killed and the fur removed from the abdomen. PEC are isolated by thoroughly flushing the peritoneal cavity with 10 ml ice-cold, sterile PBS using a 10 ml syringe and 20 gauge needle. The cells are washed once with sterile PBS and are ready for use. The cells obtained thus will be referred to as d3 iPEC.

For the isolation of anti-ESbL-Gal specific memory cells from DBA/2 or Balb/c nu/nu mice, the animals are restimulated with 1 x 10^7 100 Gy irradiated ESbL-Gal i.p. after a minimum of 30 days post primary tumour inoculation (and ADI, in the case of Balb/c nu/nu mice). Again, PEC are isolated 3 days later. The cells obtained in this way will be referred to as mPEC (memory PEC).

3.1.6 Short-term cultures of immune cells for the production of culture supernatants

PEC are isolated from ESbL-Gal-primed and i.p. restimulated DBA/2 mice, washed twice in pre-warmed complete RPMI and taken up in fresh medium at a concentration of 2 x 10^6 cells/ml. They are then plated out in a sterile, round-bottomed 96-well plate at 200 µl/well and incubated under standard tissue culture conditions. After 24 hours, the plates are centrifuged for 3 minutes at 160 x *g*, and the supernatants are transferred to 0.5 ml Eppendorf tubes. These are stored at -20°C until use.

3.1.7 Isolation of dormant ESbL-Gal from the bone marrow

6 weeks after priming DBA/2 mice with 5 x 10^4 ESbL-Gal i.e. a single cell suspension is prepared from the bone marrow as described under 3.1.5.1. The cells are washed twice in pre-warmed, pure RPMI 1640, taken up in 30 ml minimal nutrient medium supplemented with 10 µg/ml gentamycin, and given to a medium-sized tissue culture flask. This is placed in a 37°C incubator in an upright position in order to prevent the growth of adherent cells (e.g. macrophages). After 2 days of culture, 500 µg/ml G418 are added to select for β-gal expressing cells. Another 2 days later, the culture medium is changed to complete medium, and the cells are allowed to expand for 2-3 weeks

undisturbed. Cytospins are prepared as described under 3.6.1 for determination of β-gal expression intensity by X-gal staining (see 3.6.2).

3.1.8 Isolation of ESbL-Gal-variants from solid tumours

Solid tumours are excised under sterile conditions, rinsed twice with sterile PBS and a ~6 mm^3 fragment of each tumour is placed in a separate 20 x 150 mm Petri dish containing 20 ml minimal nutrient medium supplemented with 10 µg/ml gentamycin. Using a sterile scalpel, the tumour fragment is chopped into small pieces in order to enable the release of tumour cells into the medium. After two days of culture under standard cell culture conditions, the tumour fragments are removed and the cells washed once, taken up in 20 ml minimal nutrient medium containing 500 µg/ml G418, and transferred to a medium-sized tissue culture flask. Another 2 days later, the culture medium is changed to complete medium, and the cells are allowed to expand for 10 days undisturbed. Cytospins are prepared as described under 3.6.1 for determination of β-gal expression intensity by X-gal staining (see 3.6.2).

3.1.9 Preparing dendritic cells for antigen presenting functions

3.1.9.1 Production of GM-CSF containing cell culture supernatant

The GM-CSF producing cell line Ag8653 is cultured in X-vivo 20 medium. Twice a week, the culture supernatant is collected and cells are passaged. The GM-CSF containing supernatant is tested for effectiveness in stimulating outgrowth of DCs (see 3.1.9.2) from murine bone marrow against a supernatant of known effectiveness.

3.1.9.2 Growth of dendritic cells from naïve bone marrow

Myeloid-lineage DCs are grown from the bone marrow of naïve DBA/2 mice following a slightly altered version of the protocol proposed by Lutz et al. 1999. Briefly, bone marrow is isolated under sterile conditions as described in 3.1.5.1, and seeded at 2 x 10^6 cells/Petri dish (10 cm, bacteriological quality) in 10 ml X-vivo 20 medium containing 10 % GM-CSF supernatant (see 3.1.9.1). After 3 days of culture under standard tissue culture conditions another 10 ml medium, 10 % GM-CSF are added. At day 6 and day 8 of culture, 10 ml of the culture are collected in a 15 ml centrifugal tube. The cells are pelleted by centrifugation, the supernatant discarded, and the cells are re-suspended in 10 ml medium, 10 % GM-CSF (5 % GM-CSF on day 8 in order to prevent maturation of growing DCs) and transferred back to the culture dish. Immature DCs are harvested on day 10 - 11 of culture by aspiration of the non-adherent fraction and gently flushing the dish with fresh medium. Adherent cells remaining in the culture dish are mainly macrophages and fibroblasts.

Samples of the collected cells are tested by FACS analysis for their ability to macropinocytose antigen (a property of immature but not of mature DCs) (see 3.1.9.3), as well as for expression of CD11c and MHC class II (see 3.4.1.1).

3.1.9.3 Loading dendritic cells with antigen

In order to determine the maturation stage of DCs cultured under the above conditions (3.1.9.2), 1 x 10^6 cells are incubated with 0.5 mg/ml FITC-conjugated ovalbumin (OVA-FITC) in FACS buffer (see 3.4.1.1) for 15 minutes at 37°C. A control sample is incubated at 4°C. Both are washed three times, and taken up in 100 µl FACS buffer. The mean fluorescence intensity as determined by FACS analysis reflects uptake of the soluble OVA-FITC (Merkenschlager et al. 1999).
For Ag-presentation purposes, DCs are seeded out in a 6-well plate at a concentration of 1 x 10^6 in X-vivo 20 medium and co-cultured o/n under cell culture conditions with 0.2 µg peptide/ml. The cells are washed twice with fresh medium, and the Ag-pulsed DCs are ready for T-cell stimulation in an ELISPOT assay (3.5.2).

3.1.10 Red blood cell lysis

Erythrocyte lysis buffer

ddH_2O with	
NH_4Cl	0.15 M
$KHCO_3$	1.00 M
Na_2EDTA	0.10 mM

pH 7.2-7.4; sterile filter; store at 4°C

For the lysis of erythrocytes in *ex vivo* isolated single cell suspensions, pelletted cells are taken up in erythrocyte lysis buffer (~1 ml/10^8 cells, depending on the erythrocyte content in the sample). After a 1 minute incubation at r/t the cells are washed twice in medium or PBS.

3.2 Animal experiments

3.2.1 Holding conditions for experimental animals

All animal experiments are carried out under controlled specific pathogen free (SPF) conditions. DBA/2 and CD1 Swiss nu/nu mice are held in the central animal facilities of the DKFZ, 'barrier IV', while Balb/c nu/nu mice are housed in isolators.

3.2.2 Inoculations and anaesthesia

Cells or DNA are taken up in sterile PBS and injected using a 1 ml syringe and a 27 gauge needle. The inoculation volume for injections in the ear pinna (i.e.) and intradermally (i.d.) in the shaved flank is 50 µl, while for intravenous (i.v., in the lateral tail vein) injections it is 100 µl. Intraperitoneal (i.p.) tumour challenges are administered with a 10 ml syringe and 25 gauge needle in an inoculation volume of 1 ml.

Anaesthetic (R/K)

rompun (muscle relaxant)	20 % (v/v)
ketanest (general anaesthetic)	20 % (v/v)
PBS	60 % (v/v)

Animals are anaesthetised by injection of 100 µl R/K i.p.

3.2.3 Isolation of normal mouse serum

For the isolation of normal mouse serum (NMS), naïve DBA/2 mice are killed and their blood is isolated by puncturing the heart with a syringe and 27 gauge needle. The blood is transferred to 1.5 ml Eppendorf tubes and incubated for 2 hours at room temperature before a 5 minute centrifugation at 2200 x *g*. The serum is removed, aliquoted, and frozen at -20°C until use.

3.2.4 Whole-body irradiation

Prior to tumour inoculation, Balb/c nu/nu mice receive sub-lethal whole-body irradiation at a dose of 4.5 Gy from a Co^{60} source.

3.2.5 Therapy model

Whole-body irradiated (d-1) Balb/c nu/nu mice are tumour-inoculated with 1 x 10^5 ESbL-Gal i.v. (d0). Adoptive immunotransfer (ADI) occurs on d1 by injection of 1 x 10^7 d3 iPEC (see 3.1.5.5) i.v., while negative control animals remain without ADI treatment.

3.2.6 Delayed-type hypersensitivity (DTH) reaction

Ear pinna immunised mice were challenged with 50 µl ESbL-Gal lysate (3.1.4) in the contralateral ear pinna, and the DTH-reaction was evaluated 2 days later by classification of redness and swelling of the ear as previously described (Schirrmacher et al. 1994c). Table 3.1 summarises the grading system used for evaluation.

	erythema	swelling
grade 0	no	no
grade 1	yes	no
grade 2	yes	<0.5 mm
grade 3	yes	>0.5 mm

Table 3.1 Grading system for evaluation of DTH-reactions in the ear pinna.

3.3 Molecular biology

3.3.1 Large-scale pCMVβ DNA preparation

pCMVβ is a mammalian expression vector designed for high level expression of β-gal in mammalian cells. Alongside the full-length *Escherichia coli* (*E. coli*) β-galactosidase gene *lacZ* with eukaryotic translation initiation signals, the pCMVβ plasmid carries a polyadenylation signal from SV40 (Simian Virus 40) as well as the ampicillin resistance gene *Amp*^{r}.

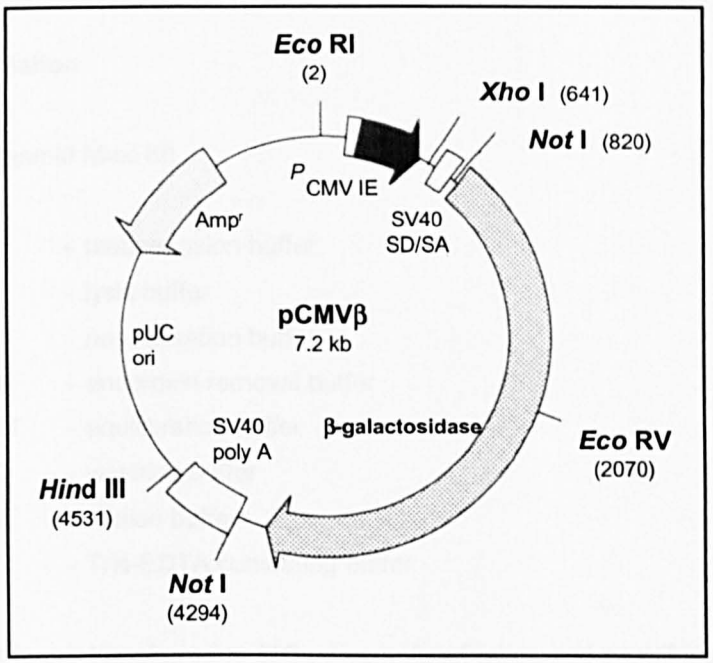

Fig. 3.1 The pCMVβ plasmid.

3.3.1.1 Expansion of bacterial cultures

Luria-Bertani (LB) medium

ddH_2O with	
bacto-tryptone	1.0 % (w/v)
bacto-yeast extract	0.5 % (w/v)
NaCl	1.0 % (w/v)

The solutes are dissolved completely using a magnetic stirring apparatus before correcting the pH to 7.0 with 5N NaOH. The volume is adjusted to 1 litre with ddH_2O, and the solution is sterilised by autoclaving for 20 minutes at 15 lb/in^2 on liquid cycle. LB-medium is stored at 4°C until use.

DH5α competent cells are an *Escherichia coli* (*E. coli*) line which can efficiently be transformed with large plasmids. pCMVβ-transformed DH5α cells were obtained from Dr. K. Chlichlia who had carried out the transformation according to the manufacturer's instructions.

pCMVβ-transformed DH5α cells are stored in LB medium, 15 % glycerol at -189°C. To recover bacteria for culture, the frozen surface of an aliquot is scraped with a sterile inoculation loop. The bacteria are inoculated into 250 ml LB medium containing 100 µg/ml ampicillin, and incubated o/n at 37°C under shaking at 250-300 rpm in a 500 ml Erlenmeyer flask covered with aluminium foil.

3.3.1.2 DNA-isolation

Qiagen Endofree Plasmid Maxi Kit

Buffers:

P1	- resuspension buffer
P2	- lysis buffer
P3	- neutralisation buffer
ER	- endotoxin removal buffer
QBT	- equilibration buffer
QC	- washing buffer
QN	- elution buffer
TE	- Tris-EDTA containing buffer

The bacterial cultures are transferred to 500 ml centrifugal tubes and centrifuged for 10 minutes at 6000 x *g*. The supernatant is discarded, while the pellet is resuspended in 10 ml ice-cold P1 buffer, containing RNase A, and transferred to a 50 ml centrifugal tube. The probe is removed from the ice before adding 10 ml P2 lysis buffer containing SDS and NaOH. The probe is mixed by repeatedly inverting the tube. After an incubation step of 5 minutes at r/t, 10 ml ice-cold P3 buffer is added. The sample is mixed immediately. The outlet nozzle of a QIAfilter column (contained in the kit) is blocked with a cap before giving the lysate onto the column. Following a 10 minute incubation at r/t, the cap is removed and the lysate it gently filtered into a 50 ml collection tube. 2.5 ml ER buffer is added to the flow-through. The sample is mixed by inverting, and incubated for 30 minutes on ice.
A QIAGEN-tip 500 (supplied in the kit) is equilibrated by applying 10 ml QBT buffer and allowing the column to empty into a tub by gravity flow. The filtered lysate is given onto the QIAGEN-tip and allowed to enter the resin by gravity flow. The column is washed twice with 30 ml QC buffer before eluting the DNA into a 15 ml centrifugal tube with 15 ml QN buffer. The DNA is precipitated with 10.5 ml isopropanol, and the sample is centrifuged for 30 minutes at 15.000 x *g* at 4°C. The supernatant is decanted and the DNA-pellet is washed with 5 ml endotoxin-free 70 % ethanol p.a.. The sample is centrifuged for another 10 minutes at 15.000 x *g* at 4°C, and the supernatant discarded. The pellet is air-dried for 5-10 minutes before redissolving the DNA in 350 µl endotoxin-free TE buffer.

Optical density (OD) of a diluted sample is measured at 260 nm using a spectrophotometer, and the DNA-content of the solution is calculated using the following formula:

$$OD_{260\ nm} \times 0.05 \times \text{dilution factor} = \mu g/\mu l\ DNA$$

3.3.2 pCMVβ digestion with *Xho* I and *Eco* RV

The purified pCMVβ DNA is cleaved using specific restriction endonucleases in order to determine whether the plasmid is intact and has not lost the *lacZ* insert. Cleavage with *Xho* I should occur after base pair 641, while *Eco* RV should cut after base pair 2070, yielding fragments of 1429 bp and 5771 bp (see Fig. 3.1 pCMVβ plasmid).

10 units *Xho* I, 10 units *Eco* RV, 2 µl 10x NEBuffer 2 as well as 0.2 µg BSA are added to 1.0 µg pCMVβ and the mixture is filled up to a total volume of 20 µl with ddH_2O. After incubating the sample for 1h at 37°C, the restriction reaction is terminated by a 20 minute incubation step at 80°C. The result is analysed by gel electrophoresis as described under 3.3.7, using an 0.8 % agarose gel.

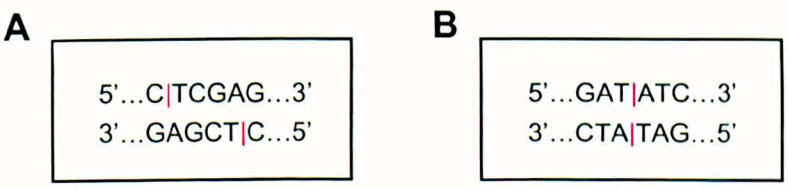

Fig. 3.2 Recognition sequences and cleavage sites (|) of the restriction endonucleases *Xho* I (A) and *Eco* RV (B).

3.3.3 RNA-isolation

3.3.3.1 Isolation of total RNA from murine cells

RNeasy Mini Kit

Buffers:
- RLT - lysis buffer for tissues and cells
- RW1 - washing buffer
- RPE - ethanol containing buffer

For isolation of total RNA from 5 x 10^6 to 1 x 10^7 suspension cells, the cells are pelleted by centrifugation, and resuspended in 600 µl RLT lysis buffer containing 1 % β-mercaptoethanol (v/v). The lysate is homogenised by applying it onto a QIAshredder column sitting in a 2.0 ml collection tube, and centrifuging it for 2 minutes at 15.000 x *g*. 600 µl 70 % ethanol p.a. is added to the homogenised lysate, which is then applied to an RNeasy mini spin column sitting in a 2.0 ml collection tube. To bind the RNA in the filter, the probe is centrifuged for 15 seconds at 8.000 x *g*, and the flow-through is discarded. The filter column is washed, first with 700 µl RW1 buffer, then with 500 µl RPE buffer. For a final washing step, 500 µl RPE buffer are given onto the filter, and the column is centrifuged for 2 minutes at 15.000 x *g*. The column is placed in a fresh 1.5 ml collection tube, 30 µl RNase-free H_2O are given directly onto the filter membrane, and the sample is centrifuged for 1 minute at 8.000 x *g*.

The flow-through contains the eluted RNA. Optical density (OD) of a diluted sample is measured at 260 nm using a spectrophotometer, and the RNA-content of the solution is calculated using the following formula:

$$OD_{260\,nm} \times 0.04 \times \text{dilution factor} = \mu g/\mu l\ RNA$$

3.3.3.2 Isolation of mRNA from small cell numbers

Dynabeads Oligo $(dT)_{25}$

Binding buffer

ddH_2O with		
Tris-HCl, pH 7.5	100	mM
LiCl	500	mM
EDTA, pH 8.0	10	mM
DTT	5	mM
SDS	1	% (v/v)

NP-40 lysis buffer

Tris-HCl, pH 7.5, with		
NP-40	1.0	% (v/v)
NaCl	0.14	M
KCl	5.0	mM

Washing buffer 1

ddH_2O with		
Tris-HCl, pH 7.5	10	mM
LiCl	150	mM
EDTA	1	mM
SDS	0.2	% (v/v)

Washing buffer 2

= washing buffer 1 without SDS

For mRNA-isolation from small cell numbers ($\leq 1.0 \times 10^6$ cells) the following protocol is applied:
250 µg Oligo $(dT)_{25}$ Dynabeads / 1×10^6 cells are transferred to a clean 1.5 ml Eppendorf tube, which is then placed in an MPC-E-1 magnet stand. When the solution is clear, the supernatant is removed, and the tube is removed from the magnet stand. The magnetic beads are then taken up in 200 µl binding buffer.
Cells are pelleted by centrifugation, resuspended in 100 µl NP-40 lysis buffer, and placed on ice for 1 minute. The sample is centrifuged for 30 seconds at 13,000 x *g*.
Pre-conditioned Oligo $(dT)_{25}$ Dynabeads are placed on the magnet stand, the supernatant is removed, and beads are taken up in 100 µl binding buffer after removing the tube from the magnet. The cell lysate is added and annealing is carried out under rotation for 5 minutes at room temperature. The sample is washed twice with 200 µl washing buffer 1 and twice with 350 µl washing buffer 2 before taking up the bead-coupled mRNA in 30 µl H_2O-DEPC.
The mRNA can directly be used for cDNA-synthesis in the solid phase, i.e. coupled to the beads.

3.3.4 RNA- and DNA-precipitation

2 volumes ice-cold 100 % ethanol p.a., one tenth of a volume 3 M sodium acetate (pH 5.5), as well as 1 µl glycogen are added to the RNA or DNA sample and incubated o/n (minimum 1 hour) at -20°C. The mixture is centrifuged for 1 hour at 15,000 x *g* in a 4°C cold desk-top centrifuge, the liquid decanted and any remaining ethanol allowed to evaporate. The RNA or DNA is taken up in 300 µl ice-cold 70 % ethanol p.a. and pelleted by a 10 minute centrifugation step at 15,000 x *g* at 4°C. The liquid is again decanted and remaining ethanol allowed to evaporate. The RNA or DNA is then taken up in a desired amount of H_2O-DEPC.

3.3.5 cDNA-synthesis

3.3.5.1 Synthesis of single-stranded cDNA (ss cDNA)

SuperScript II

H_2O-DEPC	
ddH_2O	1 l
DEPC	1 ml

0.5 µg oligo $(dT)_{12-18}$ is added to 1 µg RNA, which is adjusted to a total volume of 12 µl with H_2O-DEPC in an 0.5 ml Eppendorf tube. The mixture is heated for 10 minutes at 70°C, then quick-chilled on ice and briefly centrifuged. 4 µl 5x First Strand Buffer, 2 µl 0.1 DTT as well as 1 µl 10 mM dNTP mix are added. After 2 minutes incubation at 42°C, 1 µl SuperScript II is given to the solution, and the incubation is continued for another 50 minutes. In order to inactivate the reverse transcriptase and thus terminate cDNA-synthesis, the temperature is raised to 70°C for 10 minutes.
The ss cDNA is ready for use in a polymerase chain reaction (PCR).

3.3.5.2 Preparation of circularised, double-stranded cDNA (ds cDNA)

SuperScript™ Choice System for cDNA Synthesis

The following mixture is incubated for 2 hours at 16°C:

18 µl	first strand cDNA, ~1 mg (synthesised as described under 3.3.5.1)
93 µl	H_2O-DEPC
30 µl	5x Second Strand Buffer
3 µl	10 mM dNTP Mix
1 µl	*E. coli* DNA ligase (10 units/µl)
4 µl	*E. coli* DNA polymerase I (10 units/µl)
1 µl	*E. coli* RNase H (2 units/µl)

2 µl T4 DNA polymerase (5 units/µl) is added to produce blunt ends, and the incubation is extended for another 5 minutes, before terminating the reaction by quick-chilling on ice. The DNA is purified by adding 10 µl 0.5 M EDTA, as well as 150 µl phenol : chloroform : isoamyl alcohol (25:24:1). After a 5 minute centrifugation at 14,000 x *g* at r/t, 140 µl of the upper, aqueous layer is transferred to a sterile 1.5 ml reaction tube. The DNA is precipitated as described in 3.3.4, and taken up in 40 ml H_2O-DEPC.
For circularisation, the 40 µl ds cDNA, 5 µl 10x circularisation buffer, and 5 µl T4 DNA ligase C3 (1 U/µl) are mixed and incubated o/n at r/t. A 15 minute incubation at 68°C terminates the reaction. The ds cDNA is kept on ice until use in PCR.

10x circularisation buffer

ddH_2O with	
Tris, pH 7.5	500 mM
$MgCl_2$	100 mM
0.1 DTT	10 mM
riboATP	5 mM

3.3.6 Polymerase chain reaction (PCR)

3.3.6.1 Conventional PCR

1.0 µg ss cDNA is given to a mixture of 5 µl 10x REDTaq PCR buffer, 200 µM dNTP, 250 pmol sense primer, and 250 pmol antisense primer. H_2O-DEPC is added to a total volume of 47.5 µl. After a hot start of 5 minutes at 95°C, 2.5 µl REDTaq DNA polymerase (= 2.5 units) are added per PCR probe. PCR amplification is carried out with 30 cycles of 95°C (30 seconds), varying annealing

temperatures as indicated in Table 3.2 (30 seconds), and 72°C (60 seconds). The PCR reaction is terminated by incubating the probes for 10 minutes at 72°C.

primer	sequence 5' → 3'	annealing temperature	reference
Vβ1	CTG AAT GCC CAG ACA GCT CCA AGC	56°C	Pannetier et al. 1993
Vβ2	TCA CTG ATA CGG AGC TGA GGC	60°C	Pannetier et al. 1993
Vβ4	GCC TCA AGT CGC TTC CAA CCT C	60°C	Pannetier et al. 1993
Vβ5.1	CAT TAT GAT AAA ATG GAG AGA GAT	55°C	Pannetier et al. 1993
Vβ5.2	AAG GTG GAG AGA GAC AAA GGA TTC	55°C	Pannetier et al. 1993
Vβ8.1	CAT TAC TCA TAT GTC GCT GAC	56°C	Pannetier et al. 1993
Vβ8.2	CAT TAT TCA TAT GT GCT GGC	55°C	Pannetier et al. 1993
Vβ8.3	TGC TGG CAA CCT TCG AAT AGG A	60°C	Pannetier et al. 1993
Vβ10	ATC AAG TCT GTA GAG CCG GAG GA	60°C	Pannetier et al. 1993
Vβ13	AGG CCT AAA GGA ACT AAC TCC CAC	60°C	Pannetier et al. 1993
Vβ14	ACG ACC AAT TCA TCC TAA GCA C	55°C	Pannetier et al. 1993
Vβ15	CCC ATC AGT CAT CCC AAC TTA TCC	56°C	Pannetier et al. 1993
Vβ16	CAC TCT GAA AAT CCA ACC CAC	56°C	Pannetier et al. 1993
Vβ18	CAG CCG GCC AAA CCT AAC ATT CTC	56°C	Pannetier et al. 1993
Vβ20	TCT GCA GCC TGG GAA TCA GAA	56°C	Pannetier et al. 1993
C_n	CTT GGG TGG AGT CAC ATT TCT	variable	Abu-Hadid et al. 1996
β-actin A	TAA AAC GCA GCT CAG TAA CAG TCC G	54-61°C	Klein et al. 1998
β-actin S	TGG AAT CCT GTG GCA TCC ATG AAA C	54-61°C	Klein et al. 1998

Table 3.2 PCR-primer sequences and their annealing temperatures. All Vβ-primers are sense primers used in conjunction with the antisense primer C_n which binds in the constant region gene of the TCR, TCR-Cβ. The size of the amplified TCR-Vβ chain products is variable, depending on the TCR-Dβ (diversity region) and TCR-Jβ (joining region) usage by individual TCRs, while the β-actin product is 349 bp. All primers where designed for the murine system. A: antisense; S: sense.

3.3.6.2 Inverse PCR (iPCR)

1.0 mg double-stranded circularised cDNA is mixed with 5 ml 10x PCR buffer II, 1.5 ml 25 mM $MgCl_2$ solution, 400 µM dNTP, 250 pmol C_n-primer, and 250 pmol BCS-primer. H_2O-DEPC is added to a total volume of 49.5 ml. After a hot start of 10 minutes at 95°C, 0.5 ml Platinum Taq DNA polymerase (= 2.5 units) are added, and the PCR reaction is carried out with 40 cycles of 95°C (30 seconds), 53°C (30 seconds) and 72°C (60 seconds). The reaction is terminated by incubating the probes for 10 minutes at 72°C.

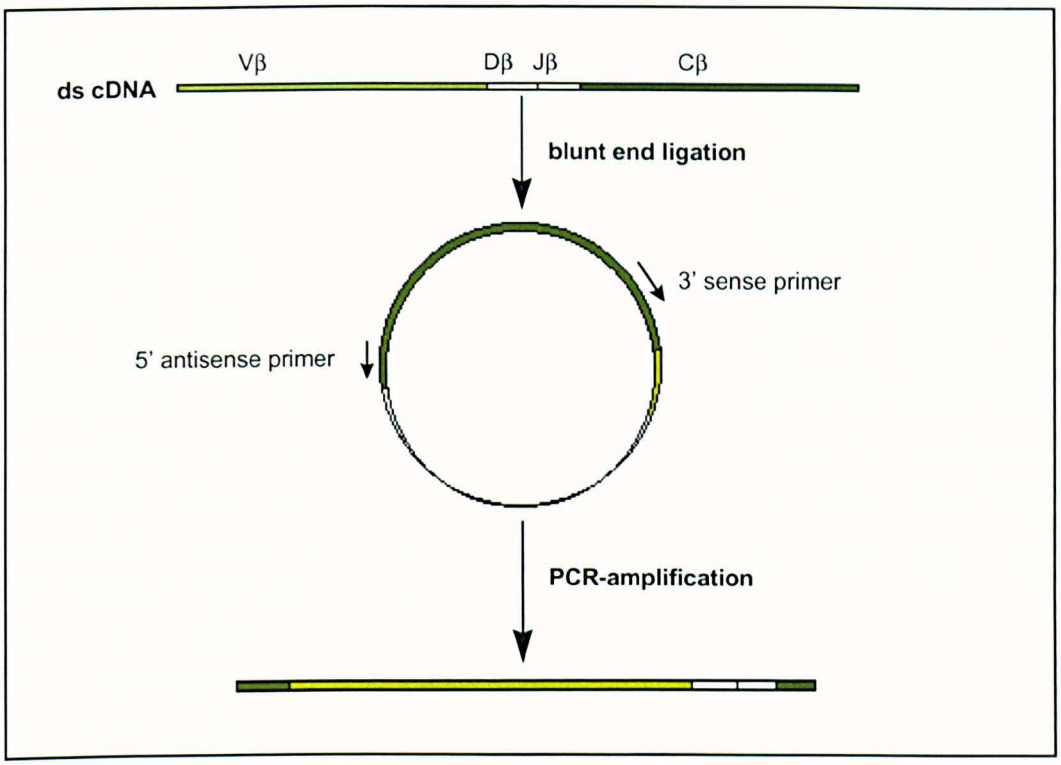

Fig. 3.3 Schematic representation of the iPCR method. RNA is used as a template to produce double-stranded (ds) cDNA. T4 DNA ligase then catalyses blunt end ligation. The resulting circular ds-cDNA is used as the substrate for PCR amplification. This method allows the amplification of unknown sequences, as primers lie in regions flanking the sequence(s) of interest, as well as the amplification of multiple sequences in a single PCR reaction. In this case, the primers were chosen to lie within the constant domain of the TCR-β chain (TCR-Cβ).

Reaction products are separated on a 1% agarose gel, southern blotted onto a nylon membrane and made visible by hybridisation with radioactively labelled TCR-Vβ chain specific probes.

Adapted from Weber-Arden et al. 1996.

The sense primer BCS (5'-TGG CCA GAG AGC TCA CCC-3') was chosen to lie towards the 3'-end of exon 1 of the TCR-Cβ region. Its binding efficiency and optimal annealing temperature were tested in conventional PCR in conjunction with the antisense primer UTA (5'-CTA TGC GTG ACT AGT AGG-3'), the recognition sequence of which is located in the untranslated region. The antisense primer C_n (see Table 3.2) anneals towards the 5'-end of the TCR-Cβ region, and was tested against the TCR-Vβ8 sense primer BV8 (5'-TAC TGG TAT CGG CAG GAC-3') in conventional PCR.

3.3.7 Gel electrophoresis

TAE-buffer

ddH_2O with	
Tris	0.48 % (w/v)
glacial acetic acid	0.12 % (v/v)
EDTA	1 mM
pH 7.5 - 8.0	

TAE buffer containing 0.8 % agarose (w/v) for pCMVβ digests, 1 % agarose (w/v) for iPCR probes, or 2 % agarose (w/v) for conventional PCR probes is brought to the boil by heating it in a microwave until the agarose is completely dissolved. Before pouring the gel, 1 µl ethidium bromide (10 mg/ml) per 30 ml agarose is added. The gel is left to polymerise.
Results from enzyme restriction experiments, or RNA- and PCR-probes, as well as molecular weight markers are mixed with 6x loading buffer and loaded into the pockets. Where RedTaq DNA polymerase was used for PCR amplification reactions, addition of loading buffer is not required, as the DNA polymerase mix already contains a loading dye.
Size fractionation is carried out at 100 V for 35' in an electrophoresis chamber, and results are documented by photography, using an ultraviolet (UV) lamp (254 nm) to visualise DNA-bound ethidium bromide.

3.3.8 DNA-extraction from an agarose gel

QIAquick Gel Extraction Kit

Buffers:	QG	- removes residual agarose
	PE	- ethanol containing buffer

All centrifugation steps are carried out for 1 minute at 10,000 x *g*.

The protocol proposed by the manufacturer is followed. Briefly, the DNA is visualised using a UV-lamp (366 nm) and the DNA-fragment of interest (max. weight = 400 mg) is excised from the agarose gel by use of a scalpel. For 2 % agarose gels, 3 volumes of buffer QG are added to one volume of gel. During a 10 minute incubation period at 50°C the probes are vortexed every 2-3 minutes. It is mandatory that the solution has changed colour to yellow (≤ pH 7.5) before adding one volume of isopropanol. If instead the solution is orange or violet, 10 µl 3M sodium acetate (pH 5.0) are added before continuing with the protocol. After isopropanol has been added, the sample is applied to a QIAquick spin column placed in a 2.0 ml collection tube and centrifuged. The flow-through is discarded and 500 µl buffer QG are given onto the filter membrane of the spin column before centrifuging. The flow-through is again removed and 750 µl PE buffer are given onto the filter

membrane. After soaking for 5 minutes, the sample is again centrifuged. The flow-through is discarded and the QIAquick spin column centrifuged anew before placing it into a clean 1.5 ml Eppendorf tube. For DNA elution, 30 µl ddH_2O are pipetted onto the membrane. After 1 minute, the sample is centrifuged and the column discarded.

3.3.9 Southern blot and hybridisation

3.3.9.1 Southern blot

Denaturation buffer

ddH_2O with	
NaOH	0.5 M
NaCl	1.5 M

iPCR products are separated by gel electrophoresis as described in section 3.3.7. Under UV-light (366 nm), nicks are cut into the gel to indicate locations of DNA-size markers, before incubating the gel under gentle shaking for 45 minutes in denaturation buffer. Hybridisation transfer membrane as well as 3 sheets of gel-blotting paper (3 MM Whatman paper) are cut to an appropriate size and soaked in dH_2O for at least 5 minutes. 2 extra sheets of gel blotting paper are left dry.
The agarose gel is inverted and placed on a glass plate. The transfer membrane, the 3 soaked blotting papers, the 2 dry blotting papers, and a 5 cm stack of paper towels are subsequently layered onto the gel. The pile is wrapped air-tight with cling-film and weighed down with a weight placed onto another glass plate.
DNA transfer from the gel to the membrane takes at least 1 hour. When the transfer is completed, markings are noted on the membrane before removing the gel. The DNA is then fixed to the membrane by UV-crosslinking using a Stratalinker.

3.3.9.2 Radioactive 5'-end labelling of oligonucleotides

10x reaction buffer

ddH_2O with	
Tris-HCl, pH 7.6	500 mM
$MgCl_2$	100 mM
DTT	50 mM
spermidine	1 mM
EDTA	1 mM

20 pmol oligonucleotides are admixed with 4 µl 10x reaction buffer, 100 µCi [γ-^{32}P]-ATP, and 10 U T4 polynucleotide kinase. The mixture is filled up to a total volume of 40 µl with H_2O-DEPC and

incubated at 37°C for 45 minutes. The reaction is terminated by incubating the sample for 10 minutes at 70°C.

STE buffer

ddH_2O with	
Tris-HCl (pH 7.5)	20 mM
NaCl	100 mM
EDTA	10 mM

A NucTrap® probe purification column is prewet with 70 µl STE buffer. 30 µl 1x STE are given to the radioactively labelled oligonucleotides before loading the sample onto the column. The probe is slowly forced through the column into a 1.5 ml collection tube using the plunger provided with the probe purification column. 70 µl STE are loaded onto the column and flushed into the same collection tube.
In order to test the success of [γ-^{32}P]-ATP incorporation, 1 µl of the probe is given onto a 1 cm^2 3 MM Whatman paper which is inserted into a pony vial. Radioactivity is determined by a Liquid Scintillation Analyser running a γ-^{32}P program.

3.3.9.3 Hybridisation

Church hybridisation buffer

ddH_2O with	
SDS	7 % (v/v)
BSA	1 % (w/v)
$NaHPO_4$	1 M
EDTA	1 mM

Church washing buffer

ddH_2O with	
SDS	1 % (v/v)
$NaHPO_4$	40 mM
EDTA	1 mM

The Southern blot (3.3.9.1) is incubated in 15 ml Church hybridisation buffer for 15 minutes at 65°C. The buffer is discarded and replaced by 10 ml Church hybridisation buffer containing [γ-^{32}P]-ATP labelled oligonucleotides. After incubating the blot with the probe o/n at 65°C under rotation, the membrane is washed 3x for 10 minutes in 100 ml pre-warmed (65°C) Church washing buffer.
The membrane is briefly dried on the work bench before fastening it onto blotting paper with sticky tape, wrapping it in cling film, and exposing a BioMax MS-1 roentgen film at -70°C for varying time

spans in a film exposure cassette containing a BioMax MS intensifying screen. The film is developed in a Cuvix 160 roentgen film developing machine.

3.3.9.4 Stripping radioactive probes off southern blots

Stripping buffer

ddH_2O with	
NaCl	1.5 M
SDS	0.01 % (v/v)

In order to remove DNA-bound [γ-^{32}P]-ATP labelled oligonucleotides from a southern blot, the membrane is incubated under rotation in 100 ml stripping buffer for 3 hours at 70°C. Subsequently, it is dried on blotting paper, and can be reused for another hybridisation experiment.

3.4 Immunobiological methods

3.4.1 Fluorescence-activated cell sorter (FACS)

3.4.1.1 Staining of cell surface molecules with monoclonal antibodies

FACS buffer

PBS with	
FCS	1 % (v/v)
sodium azide	0.01 % (v/v)

Cells are added to FACS-tubes, and all incubation steps are carried out at a concentration of 1 x 10^6 cells per 100 µl. Cell surface Fc-R are blocked by incubating the cells for 15 minutes at 4°C with 1 % NMS (3.2.3). The cells are washed once with cold FACS buffer before incubating them for 15 minutes at 4°C with fluorescently-conjugated antibodies (Abs). After washing the cells three times with 500 µl cold FACS buffer, they are taken up in 200-400 µl FACS buffer. Where unconjugated primary Abs are used, a second Ab-incubation step with a secondary fluorescently-conjugated Ab is required. In the case of biotinylated primary Abs, fluorescently-conjugated streptavidin is used.
10,000 - 100,000 events are counted on a FACScan flow cytometer and analysed using the CELLQuest Software. Unstained cells serve as autofluorescence controls.

3.4.1.2 Tetramer-staining

For tetramer-staining, cells are given to a 1.5 ml Eppendorf tube. Before incubation with H-2L^d-TPHPARIGL-PE tetramers for 1/2 hour at 37°C, cells are incubated with FITC-labelled anti-CD8 mAb (monoclonal Ab) following the protocol described in 3.4.1.1. This is necessary in order to prevent non-specific, CD8-mediated binding of the tetramer (communication of the NIAID, Bethesda, USA) which would result in overestimation of H-2L^d-TPHPARIGL-reactive CD8$^+$ T-cells. After the tetramer-staining procedure, the cells are washed twice with fresh FACS buffer (3.4.1.1). Shortly before FACScan analysis, propidium iodide (PI) is added to the probe in order to exclude dead cells from the evaluation of the results (see 3.4.1.4).

3.4.1.3 Intracellular staining with FDG

FDG-stock solution

FDG	20 mM
DMSO	10 % (v/v)
ethanol p.a.	10 % (v/v)
ddH_2O	80 % (v/v)

Fluorescein di-β-D-galactopyranoside (FDG) is used in order to detect β-gal expressing cells by FACS analysis. The non-fluorescent FDG is sequentially hydrolysed by β-gal, first to fluorescein monogalactoside (FMG), and then to the highly fluorescent fluorescein.

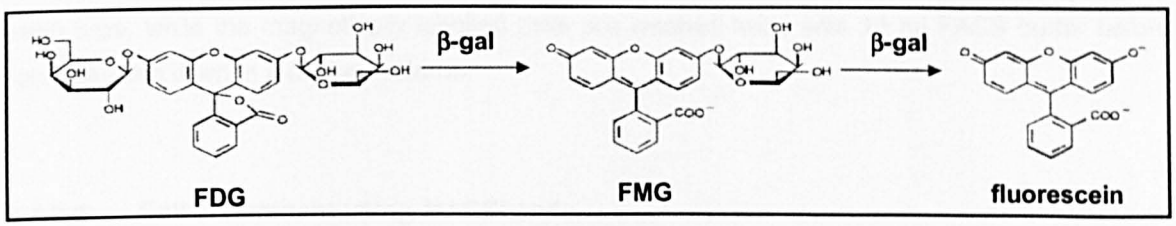

Fig. 3.4 FDG hydrolysis by β-galactosidase. A two-step hydrolysis of FDG by the bacterial β-galactosidase enzyme yields the green fluorescing protein fluorescein.

In a 2 ml Eppendorf tube, 1 x 10^7 cells are taken up in 100 µl FACS buffer (3.4.1.1) and incubated in a waterbath at 37°C for 10 minutes. 100 µl of a 2 µM FDG solution (diluted in ddH_2O) is also pre-warmed to 37°C before adding it to the cells, and incubating the mixture for another minute at 37°C. FDG enters the cells during this incubation step by way of hypotonic shock. The tube is filled up with ice-cold FACS buffer and put on ice for 10 minutes before washing the cells twice with fresh FACS buffer.

3.4.1.4 Detection of dead cells according to propidium iodide uptake

Propidium iodide (PI) staining allows the differentiation of dead from viable cells by FACS analysis, as dead cells exhibit holes in their membranes through which the PI can enter and bind to DNA. As a result, dead cells fluoresce intensely in the third channel (FI-3 = deep red) when analysed by flow cytometry.
After staining the cells with fluorescently labelled Abs as described in 3.4.1.1, PI is added to obtain a final concentration of 1 µg/ml, and the cells are allowed to incubate for one minute. The cells can then directly be analysed by FACS without having to wash off surplus PI.

3.4.2 Isolating specific immune cell populations via cell surface markers

3.4.2.1 Cell enrichment using Dynabeads

An estimate is made of the number of target cells and a 7-fold number of Ab-coupled Dynabeads is transferred to a clean 1.5 ml test tube. The beads are washed by placing the tube in an MPC-E-1 magnet stand for 2 minutes, pipetting off the fluid, and removing the tube from the magnet stand before resuspending the beads in 500 µl FACS buffer (3.4.1.1).
Cell surface Fc-R are blocked by incubating the cells for 15 minutes at 4°C with 1 % NMS (3.2.3). The cells are washed once with cold FACS buffer. The cell sample is then admixed with the beads in a 15 ml test tube and the mixture is diluted with FACS buffer to obtain a concentration of 1 x 10^7 beads/ml. Incubation occurs on a rotation device for 20 minutes at 4°C. The tube is then placed on an MPC-L magnet stand. After 2 minutes, the unbound cells (negative fraction) are transferred to a fresh tube, while the magnetically labelled cells are washed twice with 10 ml FACS buffer before resuspending them in a desired volume.

3.4.2.2 Cell enrichment using MACSbeads

MACS buffer

PBS with	
BSA	0.5 % (w/v)
EDTA	2 mM
pH 7.2	

Cell surface Fc-R are blocked by incubating the cells for 15 minutes at 4°C with 1 % NMS (3.2.3). The cells are washed once with cold FACS buffer (3.4.1.1), pelleted by centrifugation and taken up in 90 µl FACS buffer per 1 x 10^7 cells. Ab-conjugated MACS MicroBeads are given to the cell suspension at a concentration of 10 µl per 1 x 10^7 cells (= 10 beads/cell). The sample is mixed well

and incubated for 15 minutes at 4°C. 10 ml FACS buffer are given onto the cell suspension, the cells are pelleted by centrifugation and resuspended in cold MACS buffer at 50 µl per 1 x 10^7 cells. An MS^+ or LS^+ column (see Table 3.3 below) is placed in the magnetic field of a MACS separator and a 15 ml collection tube is placed underneath. The column is then pre-wet with an appropriate volume of MACS buffer, and the cell suspension is applied. This is allowed to pass through completely before washing the column three times with MACS buffer. The column is then removed from the magnetic field and placed onto a clean collection tube. In order to retrieve the labelled cells from the column, an appropriate volume of MACS buffer is pipetted onto the column and flushed through using the plunger provided with the separation columns.
All centrifugation steps are carried out for 5 minutes at 300 x *g*.

	MS^+ column	**LS^+ column**
max. no. of cells retained	1 x 10^7 labelled cells	1 x 10^8 labelled cells
MACS Separator	OctoMACS Separation Unit	Midi MACS Separation Unit
washing volume	500 µl	3.0 ml
elution volume	1.0 ml	5.0 ml

Table 3.3 Technical data for MS^+ and LS^+ separation columns.

3.4.2.3 Purification of cells using a FACSvantage

Cells are stained with fluorescently labelled Abs as described in 3.4.1.1. Using a FACSvantage cell sorter, cell populations defined by the expression of several specific cell surface molecules are isolated and sorted into a clean collection tube.
This method allows not the enrichment, but the purification even of rare cell types.

3.4.3 ELISA

OptEIA Sets for various cytokines (see 2.8); TMB microwell peroxidase substrate system

Coating Buffer

ddH_2O with	
sodium bicarbonate	8.4 % (w/v)
sodium carbonate	3.58 % (w/v)
pH 9.5	

Washing buffer

PBS with	
Tween 20	0.05 %

The manufacturer's protocols are followed for the detection of cytokines in the supernatants of short term cultures obtained as described in 3.1.6. Briefly, 96-well microtiter plates are coated o/n with in coating buffer diluted capture Ab at 4°C and washed three times. The plates are blocked with 100 µl assay diluent per well. After an incubation of one hour at r/t the plates are washed again. Standards and samples are applied at 100 µl/well and incubated for 2 hours at r/t. The plates are washed three times and incubated for one hour at r/t with 100 µl/well detector solution containing both a biotinylated detection Ab and horseradish peroxidase (HRP)-conjugated avidin. All unbound working detector is thoroughly removed by washing 5 times. TMB substrate solution is applied at 100 µl/well, and colour development allowed to take place in the dark. The colour reaction is terminated by adding 50 µl 2 N H_2SO_4 to each well and optical density is measured at 450 nm on an ELISA reader.

A standard curve is prepared for each cytokine measurement. Linear regression of the standard curve allows the calculation of cytokine content in the culture supernatants using the GraphPad Prism software.

3.5 *In vitro* assays with live cells

3.5.1 ^{51}Cr-release assay

Effector cells

d3 iPEC are produced as described in 3.1.5.5, washed twice in pre-warmed complete RPMI and diluted to a concentration of 2.5 x 10^6 viable effector cells, as determined by trypan blue exclusion (3.1.3). From this cell suspension, 200 µl are plated out in a round-bottomed 96-well plate, and a 1:2 serial dilution is carried out. With a constant target cell number (5 x 10^3, see below) this will give effector to target cell ratios (E:T ratios) of 50:1, 25:1, 12.5:1, and 6.25:1. All samples are produced in triplicates.

Target cells

Tumour cell lines should be in the exponential growth phase, i.e. at ~5 x 10^5 cells/ml culture. 2 x 10^6 target cells are pelleted in a 5.0 ml round-bottomed tube, taken up in 200 µl pre-warmed complete RPMI, and incubated with 200 µCi $Na_2{}^{51}CrO_4$ for 90 minutes at 37°C. In order to prevent sedimentation of the cells during this labelling step, which would result in unequal labelling and decreased viability, the samples are resuspended by shaking every 30 minutes. Labelled target cells are washed 3 times in pre-warmed complete RPMI and taken up in 1 ml medium. The samples are diluted to a concentration of 5 x 10^4 viable target cells per ml, as determined by trypan blue exclusion (3.1.3). 100 µl of the cell suspensions are added to the effector cells.

Co-culture of effector and target cells

The plates are centrifuged for 3 minutes at 55 x *g* in order to provide optimal effector : target cell contact. The plates are wrapped in cling film to minimise loss of liquid due to evaporation, and incubated for 4 hours at 37°C.

To ensure that all cell-associated $Na_2{}^{51}CrO_4$ is in the pellet, the plates are centrifuged for 5 minutes at 230 x *g*. 100 µl of each supernatant are transferred to 6.5 x 38 mm polystyrene tubes. These are sealed with paraffin wax, and radioactivity of the probes is determined using an Automatic Gamma Counter.

50 µl of the target cell suspension is used as the maximum release control, while 100 µl supernatant from target cells incubated without effector cells is taken as the minimum release.

Specific lysis is determined by using the following formula:

$$\% \text{ specific release} = \frac{\text{experimental release - spontaneous release}}{\text{maximum release - spontaneous release}} \times 100$$

3.5.2 Enzyme-linked immunospot assay (ELISPOT)

Murine IFN-γ ELISPOT Kit; Alkaline Phosphatase Conjugate Substrate Kit

The ELISPOT assay is designed to enumerate cytokine producing cells in a single cell suspension. After cell stimulation, locally produced cytokines are captured by a specific mAb, and are then detected by a second, biotinylated Ab and a colour reaction. Coloured spots then indicate cytokine production by individual cells.

Blocking buffer			
PBS with			
BSA	5	% (w/v)	
Washing buffer			
PBS with			
Tween 20	0.1	% (v/v)	
Detection Ab working solution			
PBS with			
detection Ab	550	µl/ml	
BSA	1	% (w/v)	
Substrate solution			
ddH_2O with			
AP colour development buffer	4	% (v/v)	
AP colour reagent A	1	% (v/v)	contains nitroblue tetrazolium in aqueous dimethylformamide (DMF) and $MgCl_2$
AP colour reagent B	1	% (v/v)	contains 5-bromo-4-chloro-3-indolyl phosphate in DMF

A 96-well plate bottomed with 0.45 µm cellulose ester membranes is incubated at r/t for 10 minutes with 100 µl 70 % sterile ethanol per well. The plate is washed three times with 100 µl PBS per well, before dispensing 100 µl capture Ab (diluted 1:100 in PBS) into each well and incubating the covered plate o/n at 4°C.

After washing the plate as above, 100 µl blocking buffer are given to each well, the plate is covered again and incubated for 2 hours at 37°C. Subsequently, the wells are emptied thoroughly but not washed. Ag-pulsed (see 3.1.9.3) or control DCs are co-incubated with T-cells enriched via one of the methods described in 3.4.2 at a ratio of T-cells : DCs = 5 : 1 in a volume of 200 µl X-vivo 20 medium per well. All samples are set up in triplicates, as well as with 3 cell dilutions. As a positive control, T-cells are incubated with PHA (5 µg/ml), while negative controls include T-cells alone and DCs alone, as well as co-incubations containing DCs pulsed with an irrelevant Ag. The cells are co-

incubated for 24 hours at 37°C under standard tissue culture conditions (see 3.1.1). It is mandatory that the plate is not moved during this incubation step.

The cells are discarded and wells are washed three times with 100 µl washing buffer per well. During the last washing step, the washing buffer is left on the plate for 10 minutes before emptying the wells thoroughly. The plate is then incubated with 100 µl detection Ab working solution per well for 1 ½ hours at 37°C and another 1 ½ hours at r/t. After washing three times with PBS, the plate is incubated for 45 minutes at 37°C with 100 µl alkaline phosphatase (AP)-conjugated streptavidin per well. The plate is again washed three times with PBS and wells are thoroughly emptied before dispensing 100 µl substrate solution to each well. The colour reaction is allowed to take place in the dark. In order to terminate the reaction, the wells are rinsed three times with ddH_2O.

The protective plastic cover is removed from the cellulose-bottomed wells and the plate is dried while keeping it protected from direct light. The cellulose ester membranes are transferred onto adhesive plastic in order to evaluate the plate using an Axioplan 2 imaging microscope in combination with a 3 CCD video camera and the KS ELISPOT Software.

3.6 Histological methods

3.6.1 Preparation of cytospins

1×10^5 to 5×10^6 cells are taken up in 200-500 µl PBS and given into the funnel of a cytospin apparatus containing a filter mat and microscope slide. After a 5 minute centrifugation at 55 x *g* the microscope slide is removed from the cytospin apparatus and left to air-dry for 15 minutes before staining or freezing at -20°C for storage.

3.6.2 Determination of *lacZ* expression by X-gal staining

Fixing solution

PBS with	
formaldehyde	2.0 % (v/v)
glutaraldehyde	0.2 % (v/v)

X-gal stock solution

N,N-dimethylformamide with	
X-gal	4.0 % (w/v)

the solution is kept at -20°C, protected from light

X-gal staining solution

PBS with	
$K_3Fe(CN)_6$	5.0 mM
$K_4Fe(CN)_6 \times H_2O$	5.0 mM
$MgCl_2$	2.0 mM
Na-deoxycholate	0.01 % (v/v)
NP-40	0.02 % (v/v)
X-gal stock solution	2.50 % (v/v)

the solution is kept at 4°C, protected from light

In order to evaluate β-gal expression in *lacZ* transduced cell lines or *ex vivo* isolated single cell suspensions, cytospins are prepared as described in 3.6.1 and fixed by incubating them for 5 minutes under gentle shaking in fixing solution. After washing the slides for 10 minutes in PBS under gentle shaking, they are incubated o/n at 37°C in X-gal staining solution. The slides are washed thoroughly with PBS and the cytospins are covered with Kaiser's glycerol gelatine and a cover slip.

Upon hydrolysis by the β-gal enzyme, X-gal yields a localised, insoluble blue precipitate which can be detected by light microscopy.

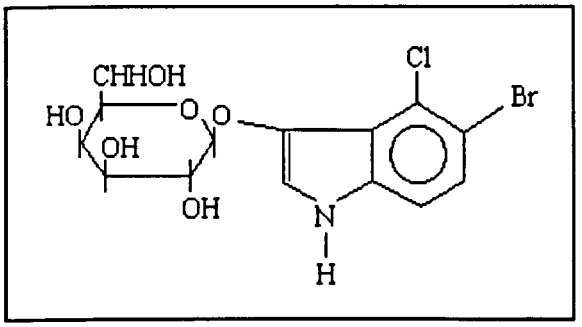

Fig. 3.5 Molecular structure of X-gal.

For macroscopic determination of metastatic load in the liver and spleen of tumour-bearing animals the organs are thoroughly washed in cold PBS and fixed during a 2 hour incubation in fixing solution at 4°C. The organs are rinsed three times with cold PBS and incubated o/n at 37°C in X-gal staining solution. After washing three times with PBS, the organs are stored at 4°C in fixing solution.

3.7 Statistics

Significance of differences between survival curves were compared using the Log-rank test.
The Student's t-test was used to calculate whether the difference between two means was significant or not.
Restricted Cubic Splines and the Wald Statistics were used for the primary kinetics of tetramer-binding cells after ear pinna priming with ESbL-Gal tumour cells. These latter calculations were kindly carried out by Dr. A. Benner.

Results

4.1 Characterisation of ESbL-Gal: a metastatic tumour line transfected with a foreign gene

The tumour cell line used in this study, ESbL-Gal, is the bacterial β-gal transduced variant of the DBA/2 mouse derived T-lymphoma ESb 289. To test for the stability of β-gal expression *in vivo*, tumour lines were established from *ex vivo* isolated tumour cells. Dormant tumour cells are known to persist for prolonged periods of time in syngeneic DBA/2 mice, mainly in the bone marrow and lymph nodes (Müller et al. 1998). The ESbL-Gal-BM variant was isolated from such bone marrow residing dormant tumour cells by growth of bone marrow cells from ESbL-Gal-immunised mice in minimal nutrient medium. Occasionally, the persistence of dormant tumour cells has been observed to result in the outgrowth of tumour nodules following a tumour challenge (Schirrmacher, in press). This is probably due to a recruitment of tumour-reactive T-cells from the site of tumour dormancy to the site of tumour challenge. ESbL-Gal-ET (ear tumour), -ST (spleen tumour). And -TT (throat tumour) are cell lines isolated from such solid tumour nodules.

Analysis of β-gal activity by X-gal and FDG staining revealed that β-gal, although highly immunogenic, appears to be stably expressed *in vivo*, as all ESbL-Gal variants tested (ESbL-Gal-ST and -TT not shown) had comparable β-gal expression levels to the parental ESbL-Gal (Fig. 4.1). Similar expression was also found in the unrelated DBA/2-derived mastocytoma P815-Gal, while the non-transfected ESbL cells served as a negative control.

The ESbL-Gal tumour is thus a useful tool for the study of Ag-specific T-cell responses, as the main imunogenic Ag (β-gal) is not lost during *in vivo* malignant progression.

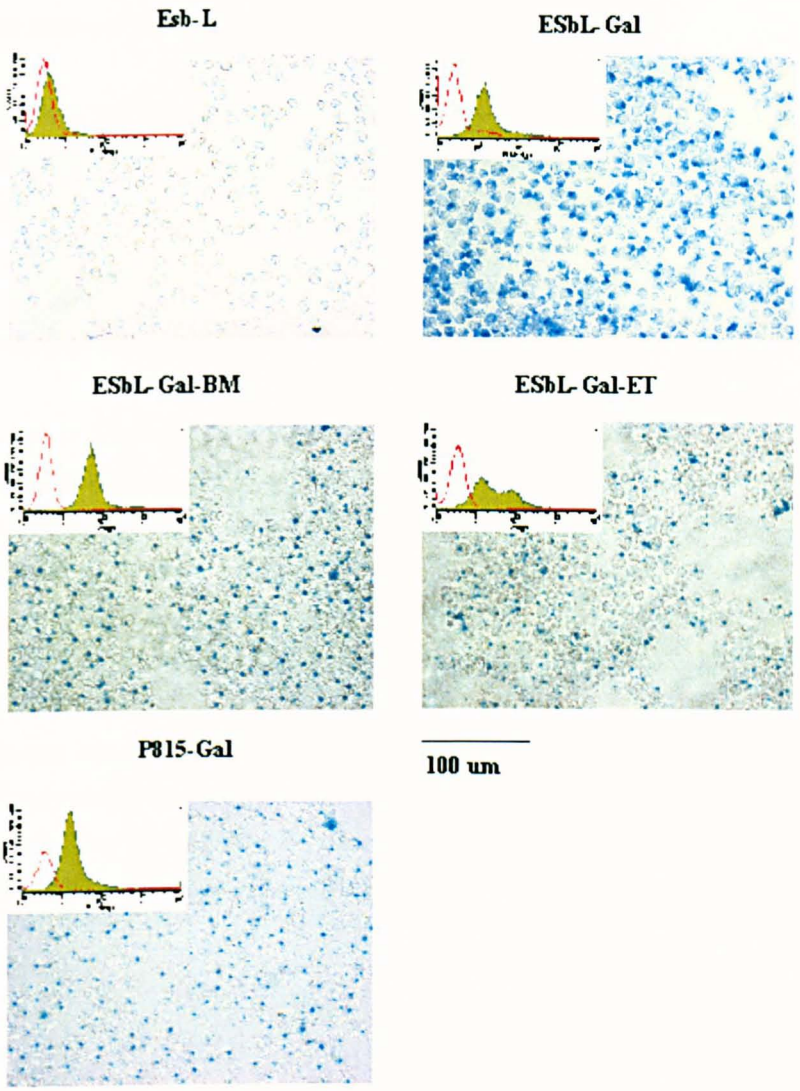

Fig. 4.1 β-gal expression by ESbL-Gal, *in vivo* variants thereof, and P815-Gal. Cultured tumour cells were tested for β-gal expression by X-gal staining (blue precipitate), as well as by FDG-staining in combination with flow cytometry (insets). Green histograms represent FDG-stained cells, red lines represent the autofluorescence. Parental ESb-L served as a negative control.

4.1.1 Cell surface expression of molecules on the parental ESbL-Gal tumour cell line and its bone marrow derived variant ESbL-Gal-BM

To better characterise the tumour cell line used in the present study, ESbL-Gal as well as a bone marrow derived variant thereof, ESbL-Gal-BM, were analysed for the cell surface expression of leukocyte lineage markers and molecules involved in Ag-presentation and cell adhesion.

4.1.1.1 Leukocyte lineage markers

ESbL-Gal cells are of T-lymphocyte origin (T-lymphoma). It has been proposed that the parental ESb, which is a spontaneous *in vivo* variant of the methylcholanthrene induced Eb, arose through fusion of an Eb tumour cell with a host macrophage. ESbL-Gal cells have only very low expression of the T-cell marker CD3 (Fig. 4.2, mean fluorescence/peak channel: 93.35/7) and detectable surface expression of Thy1.2 only on a subset of cells (8.4 %). The B-cell markers CD19 (17.25/17) and B220 (182.90/117) were found to be expressed on ESbL-Gal, while the macrophage marker F4/80 could not be detected.

Interestingly, the cell line established from dormant ESbL-Gal of the bone marrow, ESbL-Gal-BM, appear "naked" concerning cell surface expression of lymphocyte lineage markers. Whether this is due to *in vivo* selection of negative clones, a result of active down-regulation, or an altered phenotype due to further mutations is not known.

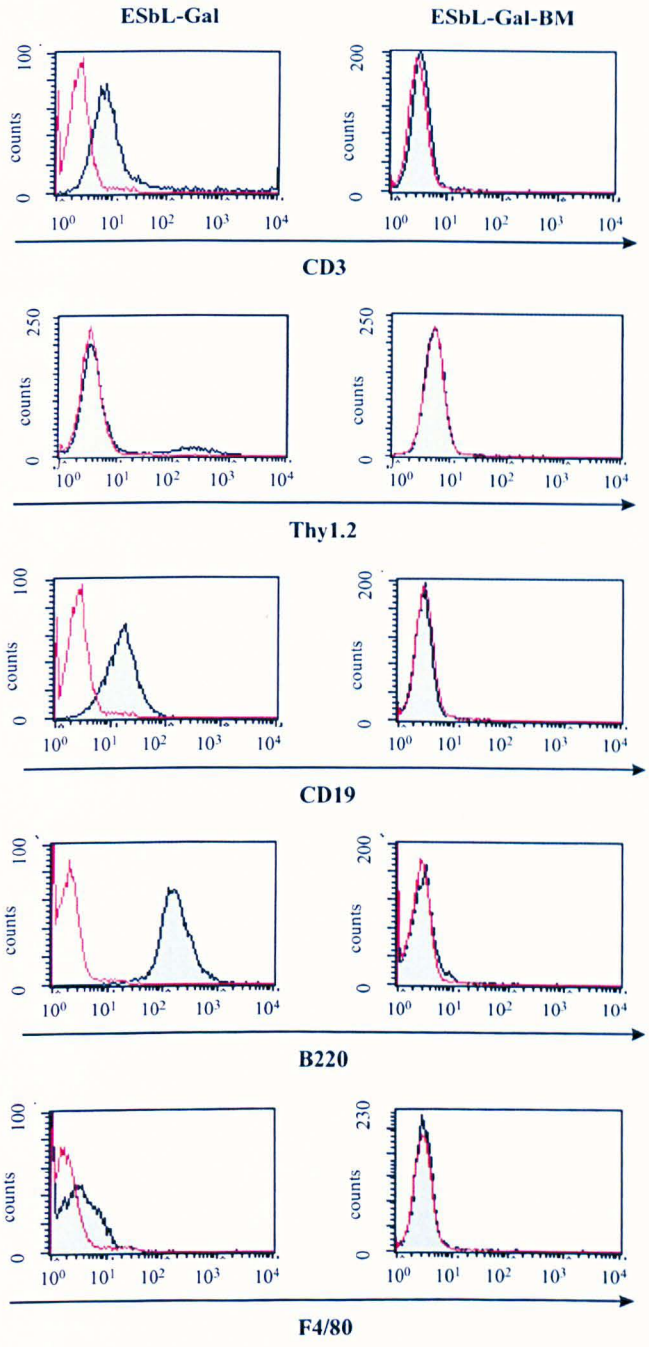

Fig. 4.2 Leukocyte lineage marker expression on ESbL-Gal and ESbL-Gal-BM. Cells were taken from cultures during the exponential growth phase and incubated with FITC or R-PE conjugated mAb to the lineage markers CD3 (clone 145-2C11), Thy1.2 (clone 53-2.1), CD19 (clone 6D5), B220 (clone RA3-6B2), or F4/80 (clone F4/80). Stained (---) and unstained (---) cells were analysed by flow cytometry.

4.1.1.2 Major histocompatibility antigens

ESb tumour cells have previously been shown to express the MHC class I molecules H-2D^d and H-2L^d, as well as the class II molecule I-A^d (Graf et al. 1985). Consistent with these results, ESbL-Gal expressed all three histocompatibility antigens although I-A^d expression was very low (Fig. 4.3, mean fluorescence/peak channel: 138.68/34 for H-2D^d, 76.02/58 for H-2L^d, 7.93/6 for I-A^d). ESbL-Gal-BM, on the other hand, were found to be negative for I-A^d. Surprisingly, this bone marrow-derived variant expressed higher levels of the MHC class I molecule H-2D^d (489.24/453) than the parental ESbL-Gal. Whether this represents an up-regulation of class I expression or a selection of tumour cells with high expression levels is not clear. Unfortunately, no conclusive results were obtained for H-2L^d expression on ESbL-Gal-BM.

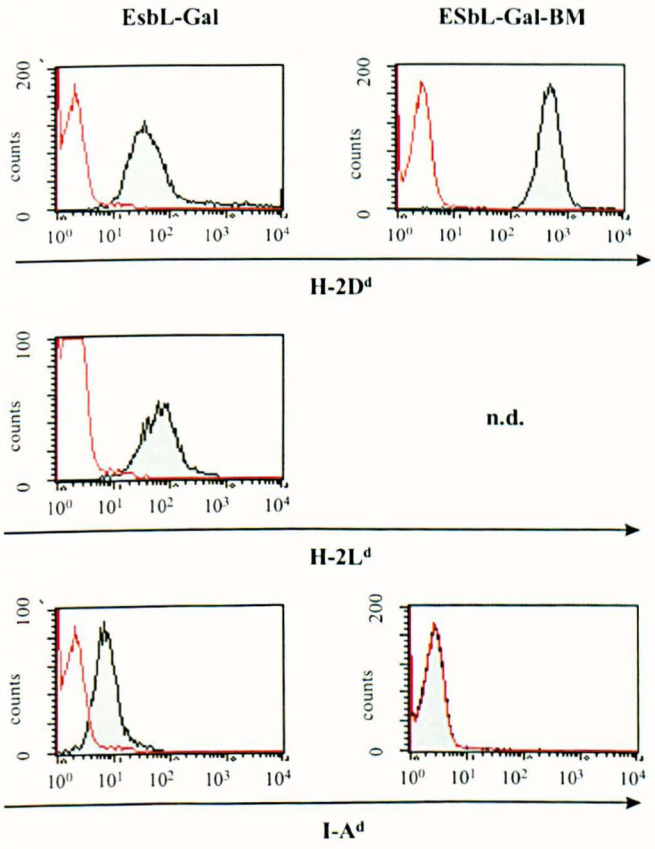

Fig. 4.3 Expression of major histocompatibility antigens on ESbL-Gal and ESbL-Gal-BM T-lymphoma cells. Cells were taken from cultures during the exponential growth phase and incubated with mAb to the major histocompatibility antigens H-2D^d (clone 34-2-12), H-2L^d (clone 19.191), or I-A^d (clone AMS-32.1). Where unconjugated mAbs were used, binding was revealed by incubation with a secondary R-PE-labelled donkey anti-rat IgG Ab. Other mAbs were either labelled with R-PE. Stained (---) and unstained (---) cells were analysed by flow cytometry. n.d.: not done.

4.1.1.3 Adhesion molecules

Adhesion molecules play an important role in the metastatic process as well as in the homing of disseminating tumour cells. Selected adhesion molecules were, therefore, analysed and found to be differentially expressed on the surface of the highly metastatic parental ESbL-Gal and its variant derived of bone marrow resident dormant tumour cells, ESbL-Gal-BM.

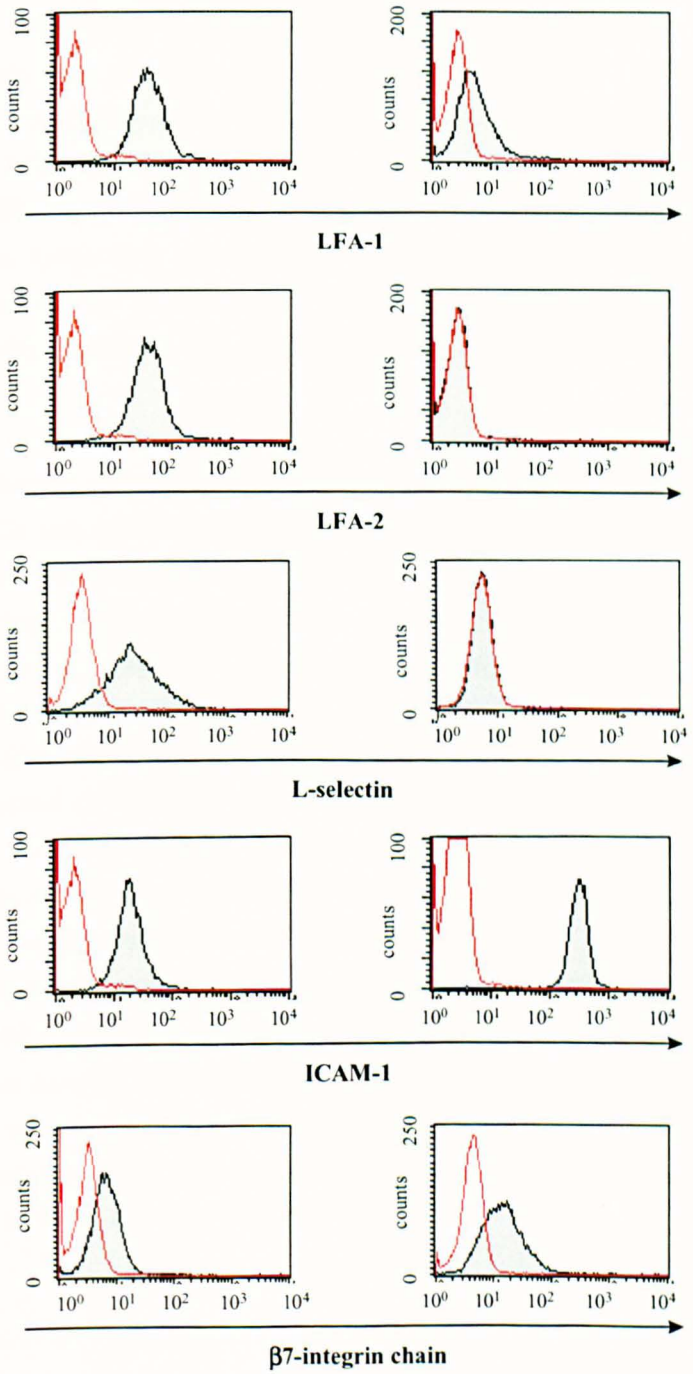

Fig. 4.4 Expression of selected adhesion molecules on ESbL-Gal and ESbL-Gal-BM. (continued on next page)

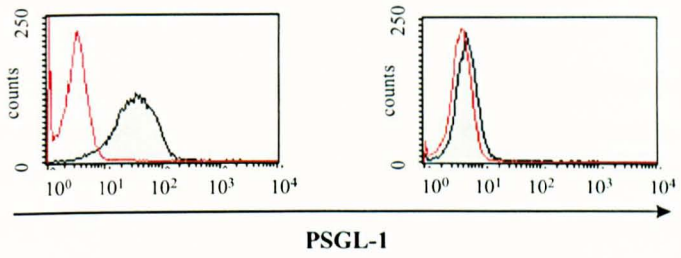

Fig. 4.4 Expression of selected adhesion molecules on ESbL-Gal and ESbL-Gal-BM. (this and previous page) Cells were taken from cultures during the exponential growth phase and incubated with mAbs to the adhesion molecules LFA-1 (clone Tib 213), LFA-2 (clone RM2-5), L-selectin (clone Mel-14), ICAM-1 (clone YN.1/1.7), β7-integrin chain (clone FIB 27), or PSGL-1 (clone 2PH-1). Where unconjugated mAbs were used, binding was revealed by incubation with a secondary R-PE-labelled donkey anti-rat IgG Ab. Other mAbs were either directly labelled with FITC or R-PE. Stained (---) and unstained (---) cells were analysed by flow cytometry.

The leukocyte adhesion molecule LFA-1 (CD11a) preferentially interacts with ICAM-1, which is expressed on APCs and activated endothelium, mediating cell-cell and cell-matrix interactions. It was found to be expressed on ESbL-Gal tumour cells (Fig. 4.4, mean fluorescence/peak channel: 41.56/32), confirming previous reports (Rocha et al. 1996, Rocha et al. 1997), whereas no expression was detected on the bone marrow variant (6.50/5).

LFA-2 (CD2) is an adhesion molecule present on a variety of haematopoietic cells, that binds to CD58, which is widely expressed on haematopoietic and non-haematopoietic cells. LFA-2 was found to be expressed on ESbL-Gal (41.72/32) but not on ESbL-Gal-BM (2.88/2). Similarly, the leukocyte selectin, L-selectin (CD62L), was expressed on the parental ESbL-Gal (37.01/23) but not on the bone marrow derived ESbL-Gal-BM (5.77/5).

ICAM-1, which is widely expressed on haematopoietic and non-haematopoietic cells, binds to LFA-1, and is important in mediating cell adhesion as well as enhancing Ag-specific T-cell activation. Increased levels of this adhesion molecule were detected on ESbL-Gal-BM (283.48/268) as compared to the parental ESbL-Gal (20.13/18). Expression levels of the β_7-integrin chain were also slightly more elevated on ESbL-Gal-BM (19.12/16) than on ESbL-Gal tumour cells (7.93/5). Likewise, the P-selectin glycoprotein ligand, PSGL-1 (CD162), was detected on ESbL-Gal cells (40.21/31) but not on ESbL-Gal-BM (6.21/5).

4.1.2 *In vivo* dissemination

The dissemination of ear pinna injected ESbL-Gal tumour cells was followed by FDG staining. To this end, bone marrow, spleen, and draining lymph node cells were loaded with FDG by osmotic shock and analysed by flow cytometry. β-gal$^+$ tumour cells could be distinguished by the green fluorescence resulting from cleavage of the FDG substrate by the β-gal enzyme. The results are illustrated in Fig. 4.5.

The frequency of tumour cells in the draining lymph node was below 0.2 % at all time points tested, although it is possible that a higher number would be present at earlier time points (within the first 24 hours of priming). Similar three-phasic kinetics were found in the bone marrow and spleen, with a first peak accumulation on day 5 post tumour injection (9.9 % in the bone marrow, 5.9 % in the spleen), a rapid decline thereafter to 0.5 % in the bone marrow and 1.8 % in the spleen on day 7, and a second increase in tumour cell numbers to 3.0 % in the bone marrow and 5.8 % in the spleen on day 14. Later time points were not analysed, but tumour cell levels are assumed to level off or possibly even decrease slightly, as ear pinna inoculated animals remain clinically healthy and the frequency of dormant tumour cells in the bone marrow is in the range of 10-100/10^6 total cells (Müller et al. 1998).

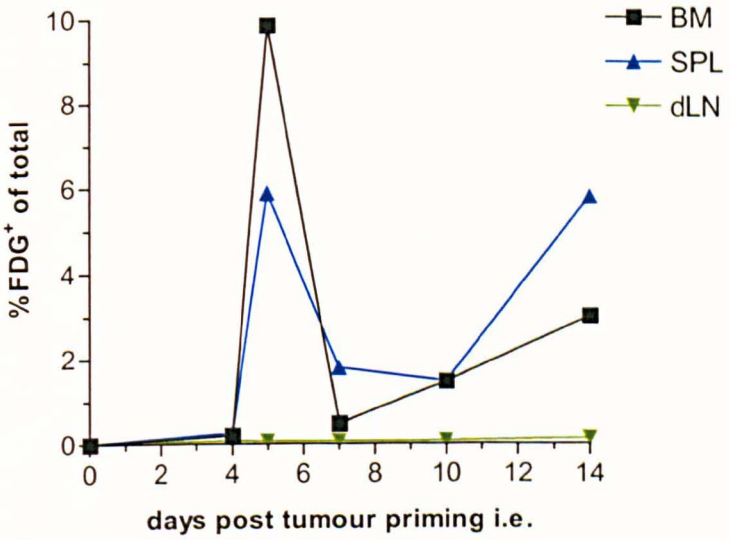

Fig. 4.5 Tumour cell dissemination after ear pinna inoculation. 5 x 10^4 ESbL-Gal cells were injected i.e. into the pinnae of both ears of syngeneic DBA/2 mice. The migration kinetics of ESbL-Gal were followed in the bone marrow (BM, ■), spleen (SPL, ▲), and draining lymph nodes (dLN, ▼) by FDG staining. Each data point represents a measurement of pooled organs from 3 animals.

4.2 Primary β-gal specific CD8$^+$ T-cell response *in vivo* after i.e. priming of syngeneic DBA/2 mice

The primary CD8$^+$ T-cell response to the immunodominant peptide of β-galactosidase (β-gal$^{876\text{-}884}$: TPHPARIGL) after ear pinna injection of ESbL-Gal was monitored in the bone marrow, spleen, and draining lymph nodes of the ear using peptide/MHC tetrameric complexes in combination with flow cytometry. The response was more pronounced in the bone marrow than in the draining lymph nodes of the ear (*superfiscia cervicalis*) or in the spleen (Fig. 4.6). The frequency of tetramer-binding cells among live CD8$^+$ T-cells in the bone marrow peaked on day 10 (5.6 %, background: 0.6 %), declining thereafter to 2.1 % by day 14. However, the decline was not down to zero, and memory T-cells were found to persist in the bone marrow for long periods of time (see 4.7.1). Similar but less pronounced kinetics were found in the spleen, where the highest frequency of tetramer binding cells was also found on day 10 (1.0 %, background: 0.3 %). This was significantly lower ($p = 0.0087$) than that detected in the bone marrow at the same time point. In the draining lymph nodes the highest frequency was measured 7 days after tumour inoculation (0.8 %, background: 0.5 %), but, statistically, this was not significantly different from any of the other time points. Overall, the kinetics of β-gal$^{876\text{-}884}$ specific CD8$^+$ T-cells in the bone marrow differed significantly from those in both the spleen and draining lymph nodes ($p = 0.0162$).

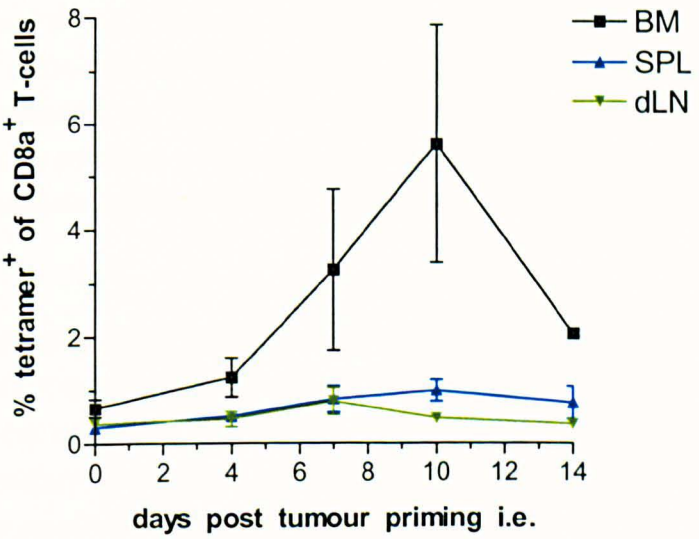

Fig. 4.6 Primary T-cell response to a tumour cell-associated Ag *in vivo*. 5 x 10^4 ESbL-Gal were injected i.e. into both ears of syngeneic DBA/2 mice. The primary MHC class I (L^d) restricted CD8$^+$ T-cell response to the immunodominant peptide of β-gal was analysed by MHC/peptide tetramer staining. Shown are means and standard deviations of tetramer binding, live CD8$^+$ T-cells from the bone marrow (BM, ■), spleen (SPL, ▲), and draining lymph nodes (dLN, ▼). The means are from 3 independent experiments with 3 mice per time point and experiment. Bars indicate standard error mean (SEM); where no bars are shown, SEM was < 0.1 %.

It has previously been reported that the bone marrow can induce primary responses under conditions of disrupted lymphocyte traffic (Tripp et al. 1997). Here I demonstrate for the first time, that this also occurs under normal physiological conditions.

4.3 Secondary anti-tumour T-cell response in the peritoneal cavity

4.3.1 Immune cell populations present in d3 iPEC

To determine the effect of intraperitoneal restimulation in ESbL-Gal-immune DBA/2 mice on the relative proportions of the different immune cell populations, d3 iPEC and PEC from naïve DBA/2 mice were incubated with cell type specific Abs and analysed by flow cytometry.

	average yield / animal
naïve PEC	$3.0 \times 10^6 \pm 0.5 \times 10^6$
ESbL-Gal-immune d3 iPEC	$1.6 \times 10^7 \pm 0.8 \times 10^7$

Table 4.1 Average cell yield from the peritoneal cavity of naïve vs. ESbL-Gal-primed DBA/2 mice after i.p. restimulation. DBA/2 mice were inoculated with 5×10^4 ESbL-Gal i.e. 7 days before restimulating intraperitoneally with 1×10^7 irradiation-inactivated (100 Gy) ESbL-Gal. ESbL-Gal-immune d3 iPEC were isolated 3 days later by peritoneal lavage. Naïve PEC were obtained by injection of 1 ml cold PBS into the peritoneum of naïve DBA/2, 1 day before isolation of the PEC.

In d3 iPEC, total cell numbers were increased by a factor of 5.3 in relation to PEC from naïve DBA/2 mice (Table 4.1). It is likely that this increase was not only due to proliferation of the cells already present within the peritoneum (see 4.3.3), but also due to an influx of primed T-cells and non-specific inflammatory cells caused by a pro-inflammatory environment (see 4.3.3), which was provoked by the presence of irradiated tumour cells.

In naïve mice, the peritoneal cavity hosts mainly B-cells. Fig. 4.7 C shows the immune cell populations present within naïve PEC (nPEC). 78.4 % of total nPEC were B-cells, while 9.8 % were macrophages, 5.7 % DCs and 4.9 % NK-cells. T-cells were represented by 5.8 % $CD4^+$ and only 0.5 % $CD8^+$ cells ($CD4^+$: $CD8^+$ T-cell ratio = 11.6 : 1).

In contrast, anti-ESbL-Gal d3 iPEC (Fig. 4.7 A) consisted of 18.6 % T-cells with a $CD4^+$: $CD8^+$ T-cell ratio of 1 : 1.5. Professional Ag-presenting cells (APCs) were represented by 9.9 % DCs, 34.7 % macrophages and 31.4 % B-cells. NK-cells constituted only a minor population of 2.6 %. Of the 7.4 % $CD8^+$ T-cells, 33.9 % bound to tetrameric complexes of the MHC class I molecule H2-L^d and the immunodominant β-gal peptide TPHPARIGL (aa 876-884, Fig. 4.7 B, background: 0.7 % (Fig. 4.7 D)), making up 2.5 % of the total d3 iPEC.

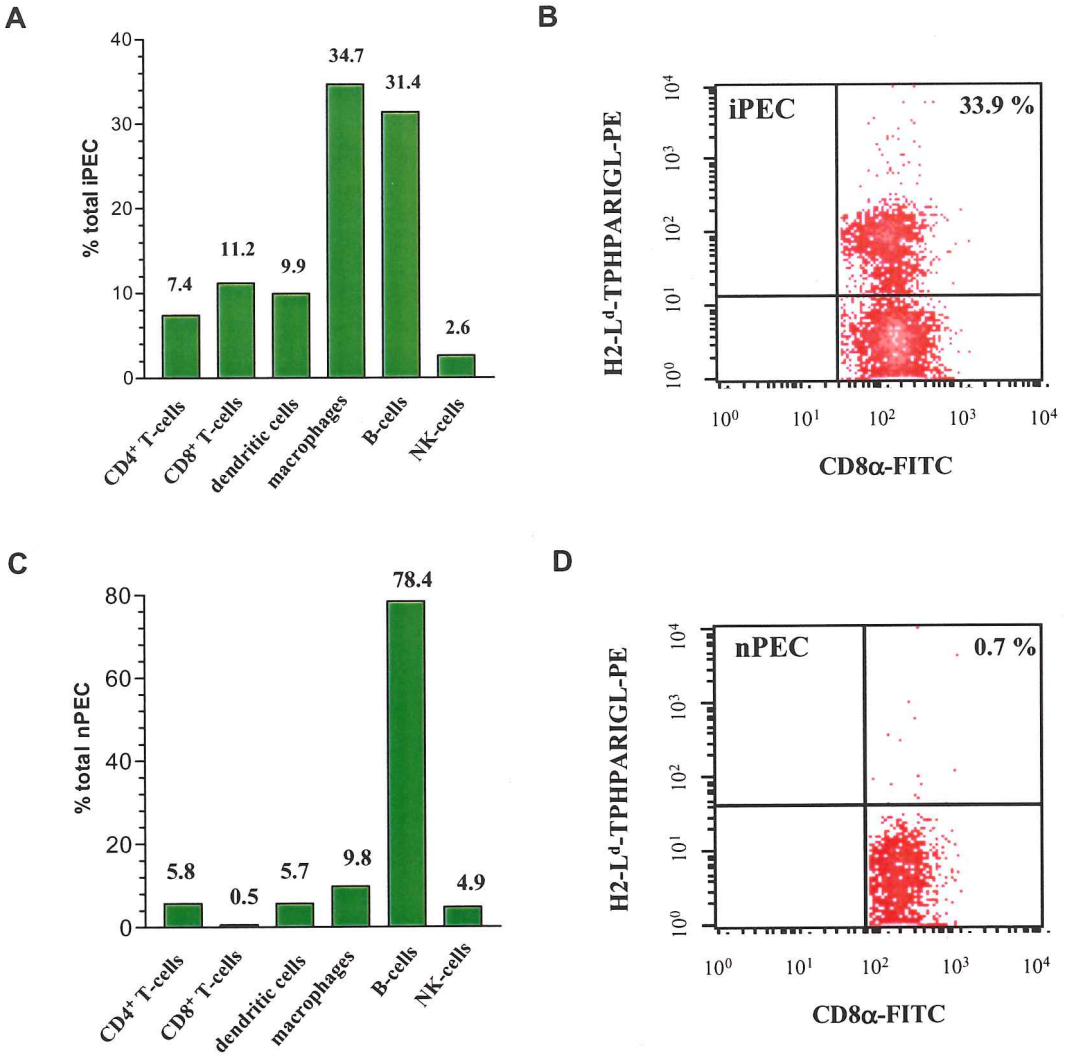

Fig. 4.7 Immune cell populations within ESbL-Gal-stimulated d3 iPEC vs. naïve PEC. Naïve DBA/2 mice were injected a sub-tumorigenic dose of 5 x 10^4 ESbL-Gal cells i.e. and 7 days later challenged with 1 x 10^7 irradiation-inactivated (100 Gy) ESbL-Gal i.p.. 3 days after the second tumour cell inoculation, d3 iPEC were harvested and analysed by 2-colour FACS staining to determine the proportions of the different immune cell populations (A). Enriched T-cells were tested for reactivity to the β-gal$^{876-884}$ peptide with PE-conjugated H2-L^d-TPHPARIGL tetramers. Live cells (PI$^-$) were gated on the CD8$^+$ fraction (B). PEC from naïve animals (nPEC) served as a control (C, D).

4.3.2 Cytotoxicity of d3 iPEC

In order to test for CD8$^+$ T-cell mediated cytotoxic activity of d3 iPEC, a 4 hour ^{51}Cr-release assay was performed against ESbL-Gal, ESb and P815-Gal target cells. P815-Gal are a *lacZ*$^+$ variant of the DBA/2-derived murine mastocytoma P815 and are commonly known as P13.1.

The ESbL-Gal and ESb cell lines share a common, as yet unidentified, H-2K^d (MHC class I) restricted TAA which is only weakly immunogenic in DBA/2 mice (Bosslet et al. 1979). The immunogenicity of ESbL-Gal is markedly increased by expression of the bacterial *lacZ* gene encoding β-gal (Krüger et al. 1994b).

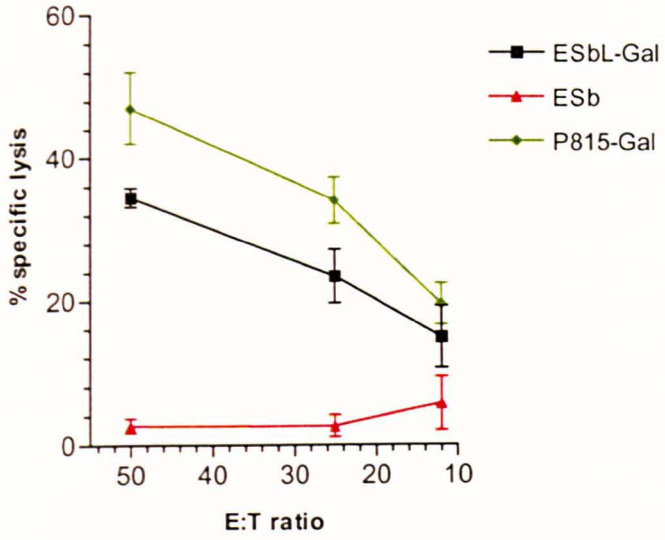

Fig. 4.8 Ear pinna inoculation of ESbL-Gal in combination with i.p. restimulation leads to a secondary β-gal specific CTL-response *in situ*. Naïve DBA/2 mice were injected a sub-tumorigenic dose of 5 x 10^4 ESbL-Gal i.e. and 7 days later challenged with 1 x 10^7 irradiation-inactivated (100 Gy) ESbL-Gal i.p.. 3 days after the second tumour cell inoculation, d3 iPEC were harvested and tested for their anti-ESbL-Gal cytotoxic activity (■) in a 4h ^{51}Cr-release assay. Specificity of the reaction was tested by including the following target cell lines: ESb 289, which expresses the same tumour Ag as ESbL-Gal, but is β-gal negative (▲); P815-Gal, an ESbL-Gal-unrelated, *lacZ*$^+$ mastocytoma (◆).
All samples were measured in triplicates, and spontaneous release was always below 15 %. Illustrated is one representative experiment of 8.

The intraperitoneal secondary immune response after i.p. challenge of ESb-immunised mice with peak CTL-activity on day 3 has previously been established (Schirrmacher et al. 1991). Here, the secondary CTL-response to β-gal could be demonstrated for the first time, and appears to be more dominant than the response to the ESb-derived TAA.

As shown in Fig. 4.8, CD8$^+$ T-cell mediated cytotoxicity of ESbL-Gal-stimulated d3 iPEC was mainly directed against the β-gal protein, specific lysis being significantly higher ($p = 0.0011$) against the *lacZ*$^+$ ESbL-Gal (34.5 %) than against the *lacZ*$^-$ ESb (2.7 %) (values are given for E:T ratio = 50:1). The higher specific kill observed against P815-Gal (46.9 %) was not due to a more elevated β-gal expression in these cells as compared to ESbL-Gal. In fact, as illustrated in Fig. 4.1, β-gal expression is similar in both cell lines. The increased sensitivity of P815-Gal to d3 iPEC mediated cytotoxicity may be due to a higher sensitivity to CTL-lysis and to some NK-mediated lysis, as P815-

Gal are NK-sensitive (Donskov et al. 1996), while ESb, and by inference also ESbL-Gal are not (**Schirrmacher** 1981). Although reproducible, the difference between the specific lysis of ESbL-Gal and P815-Gal was not significant at any of the E:T ratios tested ($p = 0.0605$ at E:T = 50:1).

4.3.3 Recruitment of β-gal specific CD8$^+$ T-cells to the peritoneal cavity

As mentioned in 4.3.1, the peritoneal cavity of naïve DBA/2 mice contains only few CD8$^+$ T-cells (0.5 %, see Fig. 4.7 A). In the present experiment the origin of T-cells, in particular the β-gal$^{876\text{-}884}$ specific CD8$^+$ T-cells, found within d3 anti-ESbL-Gal iPEC was investigated. To this end, the frequencies of tetramer-binding cells within the CD8$^+$ T-cell populations of spleen, bone marrow, regional lymph nodes of the ear, and of peripheral blood were measured. Organs from animals having received only the primary ear pinna inoculation (Fig. 4.9 gr. I) were compared with those from i.e. primed and i.p. re-stimulated animals (gr. II), as well as with those of naïve animals having received only the intraperitoneal challenge (gr. III).

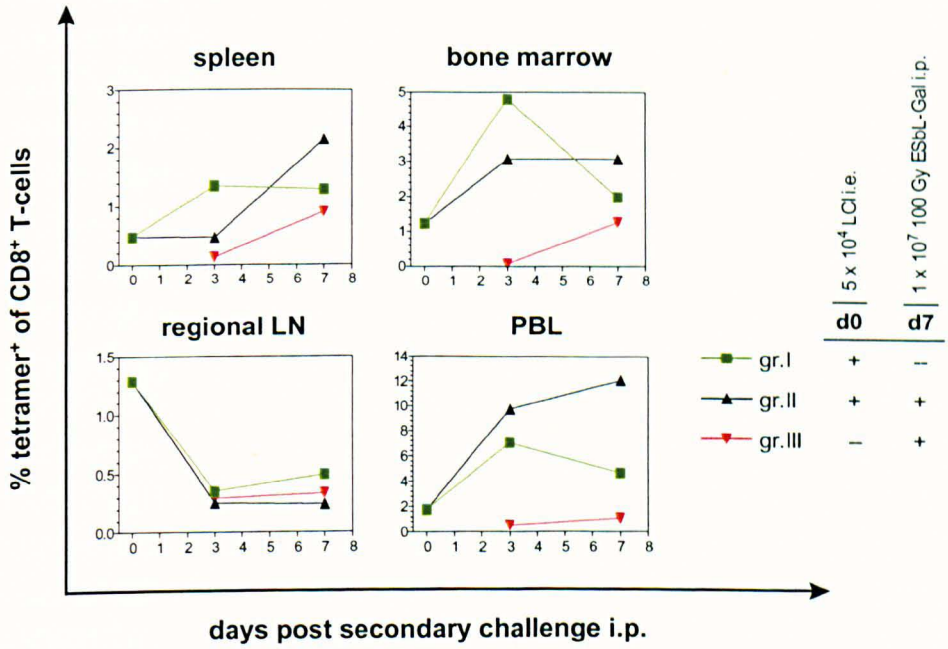

Fig. 4.9 Recruitment of Ag-specific T-cells after a secondary intraperitoneal challenge. DBA/2 mice were primed with 5 x 10^4 ESbL-Gal i.e. and restimulated 7 days later with 1 x 10^7 radiation-inactivated (100 Gy) ESbL-Gal cells i.p. (gr. II, ▲). Gr. I animals (■) were not restimulated, while gr. III mice (▼) received only the intraperitoneal challenge. 3 mice per time point and group were sacrificed. Spleens, bone marrow, regional lymph nodes of the ear, and blood from each group were pooled and the percentage of tetramer-binding cells within the CD8$^+$ T-cell compartment determined by FACS analysis.
Shown are the results of a single experiment.

The results show that β-gal$^{876-884}$ specific CD8$^+$ T-cells of the regional lymph nodes were not affected by the i.p. challenge, the frequency of tetramer-binding cells decreasing to the same extent in non-re-stimulated (gr. I, 0.35 % on d3) as in restimulated primed mice (gr. II, 0.25 % on d3). Recruitment was most likely from the spleen and bone marrow, where lower percentages of tetramer-binding cells were measured after a secondary tumour challenge i.p., and probably occurred via the blood stream where increased frequencies were recorded after i.p. challenge of ESbL-Gal immune mice as compared to the frequencies in non-rechallenged animals.
Intraperitoneal injection of 1 x 10^7 irradiated (100 Gy) ESbL-Gal cells yielded a measurable specific T-cell response in naïve DBA/2 mice (gr. III), but later and at a lower level than in tumour primed mice (gr. I).

4.3.4 Cytokine profile of iPEC and cytokine kinetics within the peritoneal cavity

In order to further analyse the mechanisms involved in the secondary *in situ* anti-ESbL-Gal response, 24h culture supernatants of iPEC isolated 1-12 days post restimulation of ESbL-Gal-immunised DBA/2 were tested for cytokine content. The results are shown in Fig. 4.10.
Bioactive IL-12 (p70) is a heterodimer composed of two disulfide-linked subunits, p35 and p40, neither of which alone display any significant activity (Chizzonite et al. 1998). IL-12 is an early response Th1-promoting cytokine produced by B-cells, activated macrophages, and DCs (Zitvogel et al. 1995), which stimulates proliferation, IFN-γ production, and cytotoxicity of both activated T-cells and NK-cells (Trinchieri 1995). Consistently, IL-12 was produced only at early time points of the secondary immune response within the peritoneum, at levels of 118.4 pg/2 x 10^6 cells on d1 and decreasing to 8.4 pg/2 x 10^6 cells on d3. By d4 no IL-12 could be detected.

Tumour necrosis factor-α (TNF-α) is produced by macrophages and T-cells, and activates the vascular endothelium, thus increasing vascular permeability. This leads to increased fluid drainage and cellular motility across the endothelium. Day 1 iPEC produced high levels of TNF-α (475.4 pg/2 x 10^6 cells), thus allowing the influx of immune cells into the peritoneal cavity upon stimulation with irradiated tumour cells. Recruitment of immune cells to the site of tumour vaccination occurs in a short period of time (1-2 days), and TNF-a secretion levels decrease dramatically thereafter. The kinetics paralleled that of IL-12.

Although DC, monocytes and macrophages can secrete some IFN-γ, the main producers are inflammatory CD4$^+$ T-cells, CD8$^+$ T-cells and NK-cells. IFN-γ primarily activates macrophages, but also affects T-cells by increasing the expression of MHC class I and class II molecules. Its capacity to stimulate the cytolytic activity of NK-cells has also been reported (de Maeyer et al. 1998). Thus, IFN-γ is a cytokine that recruits macrophages to sites of infection or inflammation to act both as effector cells, through the production and secretion of reactive oxygen species, and APCs. Highest production of IFN-γ by iPEC was found on d1 (5241.2 pg/2 x 10^6 cells), decreasing thereafter to 137.7 pg/2 x 10^6 cells on d3 and 50.3 pg/2 x 10^6 cells on d6. There was still secretion of IFN-γ on

d11 and d12, which might represent background levels produced constitutively by peritoneal macrophages, and thus indicate a return to cellular homeostasis.

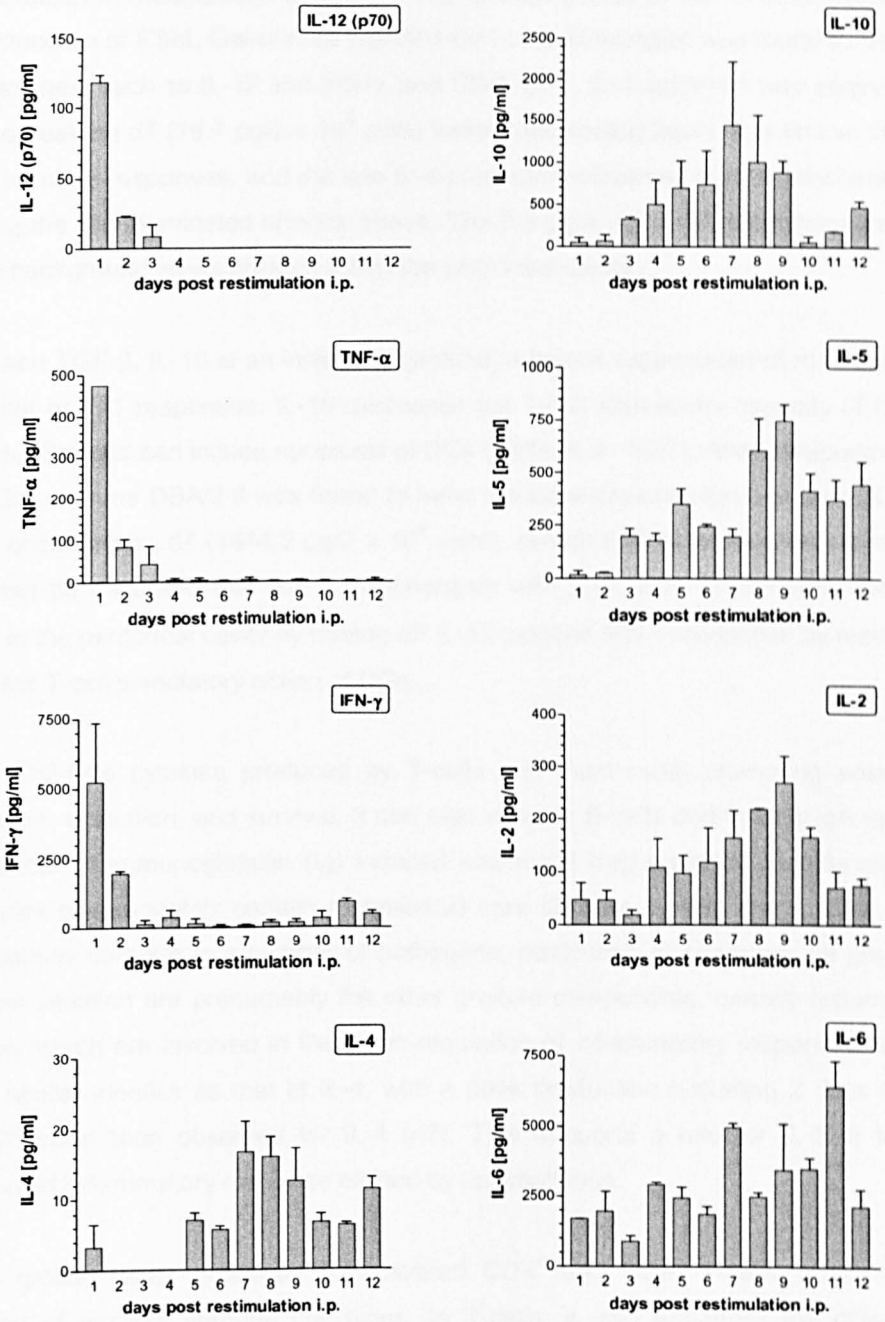

Fig. 4.10 Cytokine production by iPEC. DBA/2 mice were primed with 5 x 10^4 ESbL-Gal i.e. 7 days before restimulating with 1 x 10^7 radiation inactivated (100 Gy) ESbL-Gal i.p.. iPEC were isolated 1-12 days post restimulation and cultured for 24 hours in a round-bottomed 96-well plate at 2.0 x 10^6 iPEC/ml. Supernatants were collected and cytokine content measured in duplicates by ELISA. Minimum detection limits were at 4 pg/ml for IL-2, IL-4, IL-5, IL-6, IL-10, and TNF-α, and at 15 pg/ml for IL-12 and IFN-γ.

Shown are the results from two independent experiments.

The type 2 cytokine IL-4 is produced by $CD4^+$ T-helper cells, mast cells, eosinophils and basophils, and is involved in B-cell activation. Other effects of IL-4 include T-cell proliferation and survival, as well as inhibition of macrophage-activation. The effector phase of the immune response observed in the peritoneum of ESbL-Gal-primed DBA/2 after i.p. re-stimulation was found to be dominated by type 1 cytokines, such as IL-12 and IFN-γ, and $CD8^+$ CTL. IL-4 secretion was beginning on d5 and reaching a peak on d7 (16.7 pg/2 x 10^6 cells) before decreasing again. It is known that IL-4 inhibits Th1 type immune responses, and the late IL-4 production observed here is presumably involved in terminating the Th1 dominated effector phase. The 3.3 pg IL-4/2 x 10^6 cells measured on d1 might represent background levels present within the peritoneal cavity.

Like IL-4 and TGF-β, IL-10 is an inhibitory cytokine, a potent suppressant of macrophage functions and inhibitor of Th1 responses. IL-10 decreases the T-cell stimulatory capacity of DCs as well as IL-12 production and can induce apoptosis of DCs (Cella et al. 1997). After intraperitoneal challenge of ESbL-Gal immune DBA/2 it was found to have similar expression kinetics as IL-4, with maximal secretion occurring on d7 (1444.2 pg/2 x 10^6 cells), except that its production started earlier (d3). Thus, it can be assumed that IL-10, in synergism with IL-4, acts to terminate the inflammatory response in the peritoneal cavity by turning off IL-12 induced IFN-γ production by macrophages, and inhibiting the T-cell stimulatory action of DCs.

IL-5 is a Th2-type cytokine produced by T-cells and mast cells, promoting eosinophil growth, differentiation, activation, and survival. It can also activate B-cells and induce IgA synthesis. It is a potent inducer of immunoglobulin (Ig) induced eosinophil degranulation (Sanderson et al. 1998). The granules of eosinophils contain a crystalloid core of basic protein which, when released from the cell, causes damage to a number of pathogens, particularly to parasites. Of greater interest in the present situation are presumably the other granule components, namely histaminase and aryl sulphatase, which are involved in the down-regulation of inflammatory responses. IL-5 production exhibited similar kinetics as that of IL-4, with a peak production occurring 2 days later (d9 750.1 pg/2 x 10^6 cells) than observed for IL-4 (d7). This supports a role for IL-5 in terminating the intraperitoneal inflammatory response elicited by i.p. challenge.

IL-2 is a growth factor produced by activated $CD4^+$ and $CD8^+$ T-cells, which stimulates the proliferation of multiple immune cell types. In T-cells, it also enhances the differentiation, and cytotoxic activity of CTL. It can also stimulate other IL-2 receptor positive cells, such as NK-cells. IL-2 is generally considered a T-cell differentiation factor, but which type of T-cells are activated by IL-2 seems to depend on other co-secreted cytokines (Thorpe 1996). IL-2 production by iPEC correlated more with Th2 than Th1 type cytokine expression, with secretion peaking on d9 (271.0 pg/2 x 10^6 cells). It has been reported that activated T-cells show increased responses to IL-2 if IL-4 is also present (Thorpe et al. 1996). This indicates that in the present model system, IL-2 induces the expansion of Th2 type cells.

IL-6 exhibits complex kinetics. It is produced by a wide range of cell types, including Th2 type T-cells, activated B-cells, mast cells, fibroblasts, and, most importantly, macrophages, one of its

effects being induction of B-cell growth and differentiation. Along with IL-1 and TNF-α it is referred to as an 'endogenous pyrogen' because it causes fever and is derived from endogenous sources. Elevated temperatures are beneficial to host defence, as they protect host cells from deleterious effects of TNF-α. Although IL-4 and IL-10 have been reported to inhibit IL-6 production by monocytes and macrophages (Richards 1998), the expression pattern of IL-6 on later time points after i.p. re-stimulation is similar to that of IL-4 and IL-10, except that the increase occurs later and is less dramatic. IL-6 plays a major part in the homeostatic response to inflammation by inducing the release of all positive liver-derived acute-phase proteins (e.g. C-reactive protein, α_1-antitrypsin, α_1-antichymotrypsin), and inhibiting the release of negative acute-phase proteins by hepatocytes (e.g. albumin, transferrin). Many of the positive acute-phase proteins have anti-inflammatory properties, which could explain the relatively elevated IL-6 levels at later time points of the peritoneal immune response.

4.3.5 TCR-Vβ repertoire analysis

Prevalence of a limited set of TCR in an immune response might reflect selection of TCR binding a given peptide/MHC combination particularly well (Döffinger et al. 1997). In order to test whether T-cell clones expressing specific TCR-Vβ chains are selected during immune responses to ESbL-Gal, d3 iPEC were gained by the standard protocol (see 3.1.5.5) and compared with d3 iPEC from P815 (β-gal negative) immunised DBA/2 mice. $CD4^+$ and $CD8^+$ T-cells were purified by FACS sorting and analysed for expression of various Vβ-chains by PCR. Total thymocytes served as positive controls. The analysis included three Vβ-chains (Vβ5.1, Vβ5.2, Vβ8.1), which have been reported to be clonally eliminated in DBA/2 mice due to the presence of endogenous proviruses. The results are illustrated in Fig. 4.11.

All TCR-Vβ chains investigated, including those clonally eliminated in peripheral T-cell populations, could be detected in thymus preparations, although for Vβ13, only an extremely faint band was visible after gel electrophoresis of the PCR-products. Polyclonal T-cell responses were found in both $CD4^+$ and $CD8^+$ T-cell compartments, after stimulation with ESbL-Gal or P815. Five of the Vβ-chains analysed, namely Vβ1, Vβ8.3, Vβ10, Vβ15, and Vβ20, were found to be represented in all T-cell populations investigated. The $CD4^+$ T-cell fractions from animals immunised with ESbL-Gal or P815 tumour cells were very similar, and differed only in that $V\beta4^+$ clones were well represented in the response to P815, but not in the ESbL-Gal induced response. The $CD8^+$ T-cell fractions from the two animal groups were more dissimilar in their Vβ-chain involvement, markedly in that $V\beta4^+$ clones were more important in the ESbL-Gal reactive group, while the P815 reactive cells generally involved a greater variety of Vβ-chains with an important involvement of Vβ8.2.

It has previously been put forward that the Vβ5-chains are expressed in DBA/2 mice (Schirrmacher et al. 1992), and indeed, some Vβ5.1 and Vβ5.2 transcripts could be detected, albeit at very low levels. Whether these are also translated to form part of a functional TCR remains to be elucidated by another method, such as flow cytometry. The same applies to the Vβ8.1 transcripts detected in T-cells from P815 immunised DBA/2 mice.

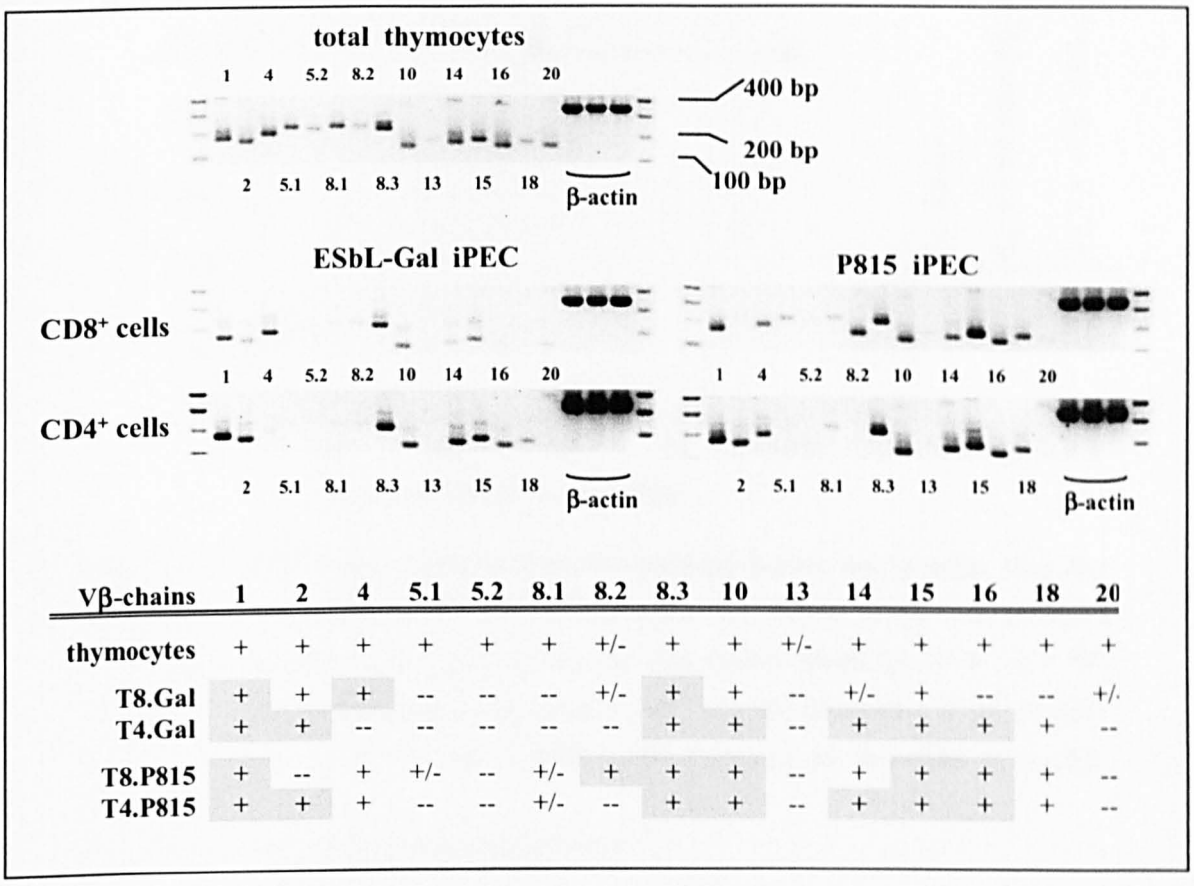

Vβ-chains	1	2	4	5.1	5.2	8.1	8.2	8.3	10	13	14	15	16	18	20
thymocytes	+	+	+	+	+	+	+/-	+	+	+/-	+	+	+	+	+
T8.Gal	+	+	+	--	--	--	+/-	+	+	--	+/-	+	--	--	+/-
T4.Gal	+	+	--	--	--	--	--	+	+	--	+	+	+	+	--
T8.P815	+	--	+	+/-	--	+/-	+	+	+	--	+	+	+	+	--
T4.P815	+	+	+	--	--	+/-	--	+	+	--	+	+	+	+	--

Fig. 4.11 TCR-Vβ repertoire of CD8⁺ vs. CD4⁺ T-cells in d3 iPEC. DBA/2 were primed i.e. and re-stimulated i.p. either with ESbL-Gal (left) or P815 (right). $CD8^+$ and $CD4^+$ T-cells were purified from d3 iPEC by FACS sorting using a FACSvantage machine. TCR-Vβ chain expression was analysed by RT-PCR, using C_n (anneals in TCR-C region) as a counter-primer for Vβ-specific primers. Thymocytes served as a positive control. The results obtained are summarised in the table. T8.Gal, T4.Gal: $CD8^+$ and $CD4^+$ T-cells, respectively, from ESbL-Gal immunised mice. T8.P815, T4. P815: $CD8^+$ and $CD4^+$ T-cells, respectively, from P815 immunised mice. --, not detected; +/-, weakly expressed; +, involvement; ▒, strong involvement.

4.4 Therapeutic potential of secondary activated anti-β-gal effector cells

An experimental system was needed to analyse the fate of memory T-cells *in vivo*. As described in the introduction (1.3.2), a syngeneic ADI system had previously been established, where an immunotransfer of DBA/2-derived d3 iPEC to ESb tumour bearing DBA/2 mice resulted in long-term survival (Schirrmacher et al. 1994b, Schirrmacher 1995b). This protocol of graft versus leukaemia (GvL) ADI was altered to include T-cell deficient Balb/c nu/nu mice as recipients of tumour and immune cells.

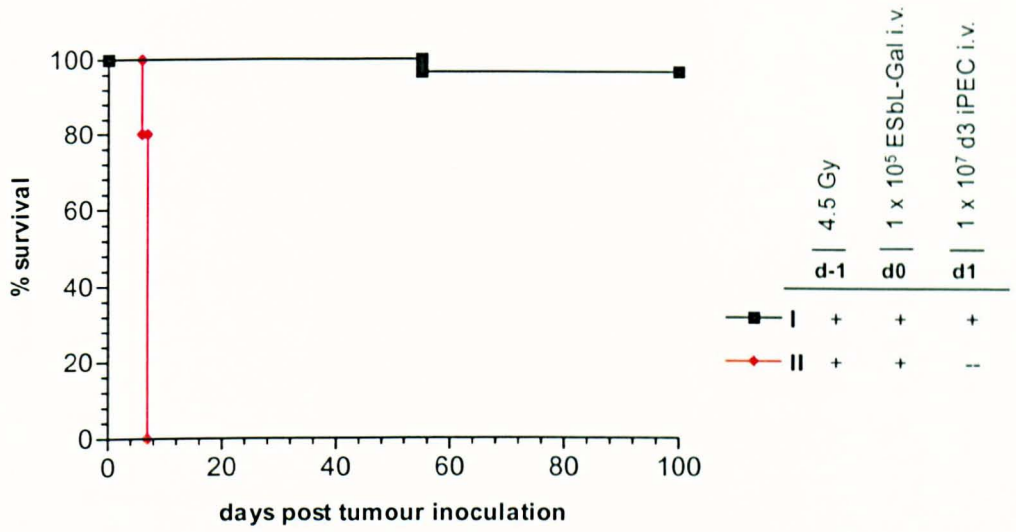

Fig. 4.12 ADI of pre-irradiated ESbL-Gal-bearing Balb/c nu/nu mice. One day before tumour inoculation with 1 x 10^5 ESbL-Gal i.v., Balb/c nu/nu mice received whole-body γ-irradiation at a dose of 4.5 Gy. The control group (gr. II, ◆ , n = 10) received no further treatment, while group I (■ , n = 30) received 1 x 10^7 d3 anti-ESbL-Gal iPEC i.v. on d1. Day 3 iPEC were produced as described in 3.1.5.5. $p < 0.0001$.
Illustrated is one representative experiment of 7.

Fig. 4.12 illustrates the survival of ADI-treated (gr. I) or -untreated (gr. II) Balb/c nu/nu mice after ESbL-Gal tumour injection i.v.. ESbL-Gal is a highly aggressive T-lymphoma, which kills its hosts within 8-10 days if it remains untreated. The DBA/2-derived anti-ESbL-Gal d3 iPEC, which could be shown to exert anti-β-gal specific killing activity *in vitro* (4.3.2), proved to be highly effective also *in vivo*, prolonging survival of tumour-bearing Balb/c nu/nu mice.
The altered ADI-protocol thus resulted in a very high therapeutic success, with ADI-treated animals surviving for over one year (see Fig. 4.13 in section 4.4.1). It, therefore, provides optimal conditions for the study of the protective effects and long-term fate of the tumour reactive T-cells.

4.4.1 Pre-irradiation of therapy recipients improves survival

The effects of sub-lethal γ-irradiation (4.5 Gy in mice) on the organism and the immune system are multiple (Schirrmacher et al. 1994a). Primary B- and T-lymphocyte responses are suppressed, but the phagocytic activity of the reticuloendothelial system, including macrophages, is not affected. Secondary lymphoid tissues, such as the spleen and lymph nodes, are depleted of radio-sensitive leukocytes, providing additional space and improved take of transferred cells. Preceding a cellular transfer to immuno-competent animals, whole-body γ-irradiation can eliminate the problem of host versus graft (HvG) reactions, in which mature host T-cells attack the grafted cells.

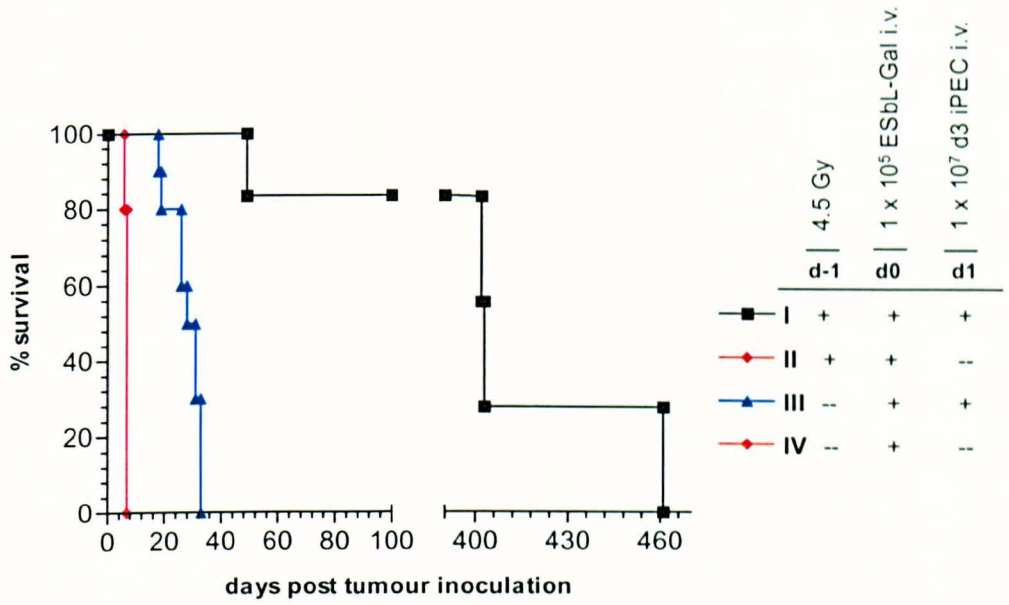

Fig. 4.13 Pre-irradiation of ADI recipients is necessary for achieving a complete therapeutic effect. 4.5 Gy γ-irradiated (gr. I, ■ , n = 10) or non-irradiated (gr. III, ▲ , n = 10) tumour bearing Balb/c nu/nu mice were treated with 1 x 10^7 d3 iPEC. Negative controls were either whole-body γ-irradiated (gr. II, ◆ , n = 10) or not (gr. IV, ◆ , n = 10) and received no ADI.
Illustrated is a single experiment.

In the present system, which involves a cellular transfer to immunocompromised (athymic) mice, ADI was most effective in conjunction with whole-body irradiation of 4.5 Gy (Fig. 4.13 gr. I). Such treatment resulted in long-term survival of ESbL-Gal tumour bearing Balb/c nu/nu mice, with most animals surviving for over 1 year. Although the immunotransfer alone resulted in a significant ($p < 0.0001$) increase in survival compared to control animals (gr. IV), non-irradiated ADI-recipients died within 1 month after tumour injection (gr. III). The life expectancy of non-irradiated ADI-recipients was significantly lower ($p < 0.0001$) than that of irradiated ADI-recipients (gr. I). Control animals having received 1 x 10^5 ESbL-Gal i.v. but no ADI died within 8 days after tumour injection, no matter whether they received whole-body irradiation (gr. II) or not (gr. IV).
The ADI-model including whole-body γ-irradiation and immunotransfer of 1 x 10^7 ESbL-Gal reactive d3 iPEC will hereafter be referred to as 'standard therapy'. The therapy scheme is illustrated in Fig. 4.14.

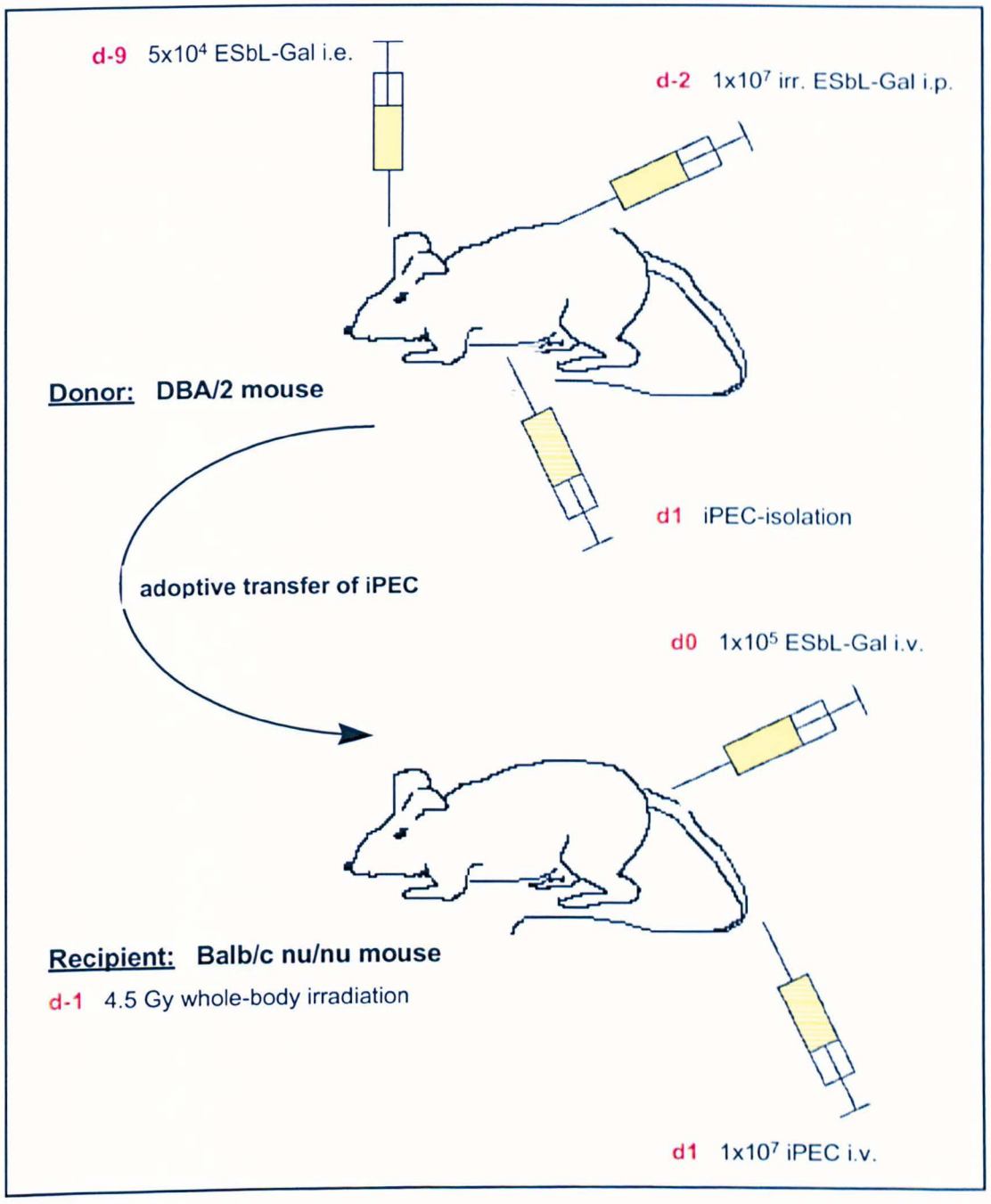

Fig. 4.14 Schematic representation of the standard therapy protocol. Naïve DBA/2 mice were injected a sub-tumorigenic dose of 5 x 10^4 ESbL-Gal i.e. (day -9) and 7 days later challenged with 1 x 10^7 irradiation-inactivated (100 Gy) ESbL-Gal i.p. (day -2). 3 days after the second tumour cell inoculation (day 1), d3 iPEC were harvested and adoptively transferred to ESbL-Gal tumour-bearing Balb/c nu/nu mice by i.v. injection. These had been whole-body irradiated (day -1) one day before tumour inoculation with 1 x 10^5 ESbL-Gal i.v. (day 0).

In order to investigate the effect of this model of ADI *in situ*, the experiment described above was repeated with all four groups. Livers and spleens (target organs of ESbL-Gal metastases) were isolated at different time points after tumour injection and incubated with X-gal staining solution in

order to reveal metastatic tumour nodules according to β-gal positivity. Fig. 4.15 A shows X-gal stained organ fragments. Organs from animals having received standard therapy (gr. I) did not reveal any macroscopically detectable metastases at any time point examined. The same was true for non-irradiated ADI-recipients (gr. III). Control animals, on the other hand, exhibited a high metastatic load in both liver and spleen, no matter whether the animals had been pre-irradiated (gr. II) or not (gr. IV).

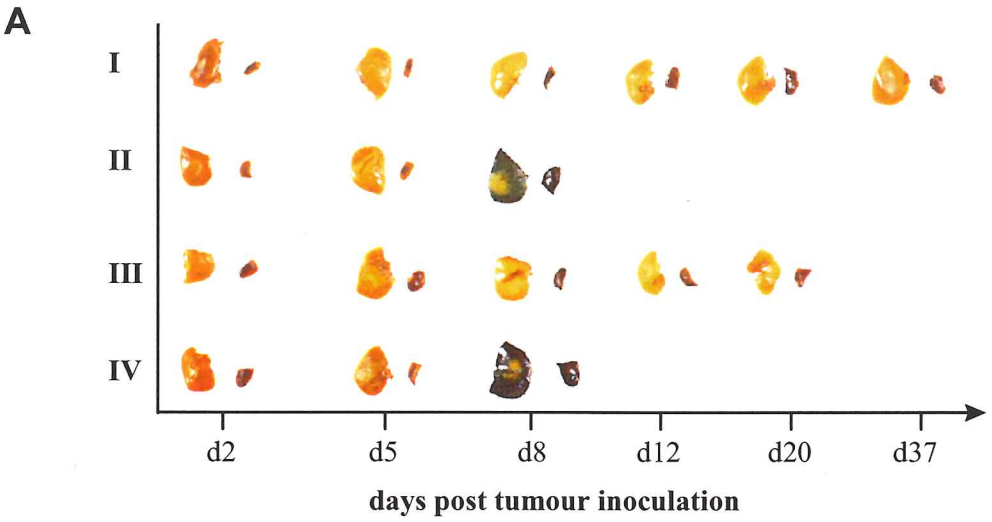

Fig. 4.15 Cellular transfer in combination with whole-body irradiation results in prevention of malignant outgrowth in internal organs and the periphery. Gr. I-IV were treated as described for Fig. 4.13. (A) X-gal staining of liver and spleen fragments revealed no micrometastases within organs of ADI treated mice (gr. I and III) at any time point, while control animals (gr. II and IV) exhibit a high metastatic load on d8. (B) Although internal organs of non-irradiated ADI-recipients remained clear of micrometastases, multiple rapidly growing tumour nodules appeared in the periphery on d28 (below), while irradiated ADI-recipients remained healthy (above).

Fig. 4.15 B shows one gr. I and gr. III animal, respectively, 28 days after tumour inoculation. The non-irradiated gr. III animal exhibited multiple fast growing tumour nodules, presumably located in peripheral lymph nodes, while the pre-irradiated gr. I animal suffered no externally visible tumour growth and remained clinically healthy throughout the observation period (over one year).
d3 iPEC transfer to ESbL-Gal-bearing Balb/c nu/nu thus appeared to be sufficient for eradicating liver and spleen metastases, as no micrometastases were evident macroscopically after X-gal staining even at late time points (d20). Although internal organs seemed to be free of tumour cells in both groups of ADI-treated animals, whole-body irradiation was necessary to prevent outgrowth of tumours in the periphery.

4.4.2 MHC-compatible T-cell deficient recipients provide an optimal model system

Two different strains of T-cell deficient nude mice were compared as d3 iPEC recipients, namely Balb/c nu/nu and CD1 Swiss nu/nu mice. Like the donor mice (DBA/2), Balb/c nu/nu mice are back-crossed and express the MHC class I allele H-2^d, whereas CD1 Swiss nu/nu mice are outbred, exhibiting genetic variance at the MHC-locus. Thus, the former were used as MHC-identical and the latter as MHC-unidentical ADI-recipients.
In both cases (Fig. 4.16 A), ADI without pre-irradiation of the therapy-recipients conferred significantly higher ($p < 0.0001$) survival times to ESbL-Gal-bearing mice than no treatment (gr. II). The overall therapy efficiency was significantly higher ($p < 0.0001$) in MHC-compatible Balb/c nu/nu mice than in MHC-unmatched CD1 Swiss nu/nu. While Balb/c nu/nu mice died between d18 to d33 having a median survival of 29.5 days, CD1 Swiss nu/nu died already from d9 to d20 and had a median survival of 16 days.
As the liver is a target of metastasis in the ESbL-Gal tumour model, a parallel ADI-experiment was set up in which 1-3 animals per group were killed at various time points in order to follow the metastatic load of the isolated livers by whole-organ X-gal staining. In Balb/c nu/nu mice, the livers remained clear of macroscopically visible metastases throughout the experiment (Fig. 4.16 B). There was, however, tumour growth at peripheral sites (see 4.4.1). In contrast, some CD1 Swiss nu/nu mice produced liver metastases as early as d8 post tumour inoculation, while on d12 (= 11 days after immune cell transfer) no metastases were detectable by whole-organ X-gal staining. On d15, the livers stained blue all over, exhibiting a distinct mosaic-like pattern. The same pattern of metastasis has been found in immunocompetent DBA/2 mice 23 to 30 days after intradermal inoculation of ESbL-Gal (Krüger et al. 1994b).
The results clearly show the superiority of H-2 matched Balb/c nu/nu (i.e. MHC-compatible) as ADI-recipients in the present therapy model. This also holds true for a protocol which does not include pre-irradiation of the treated animals.

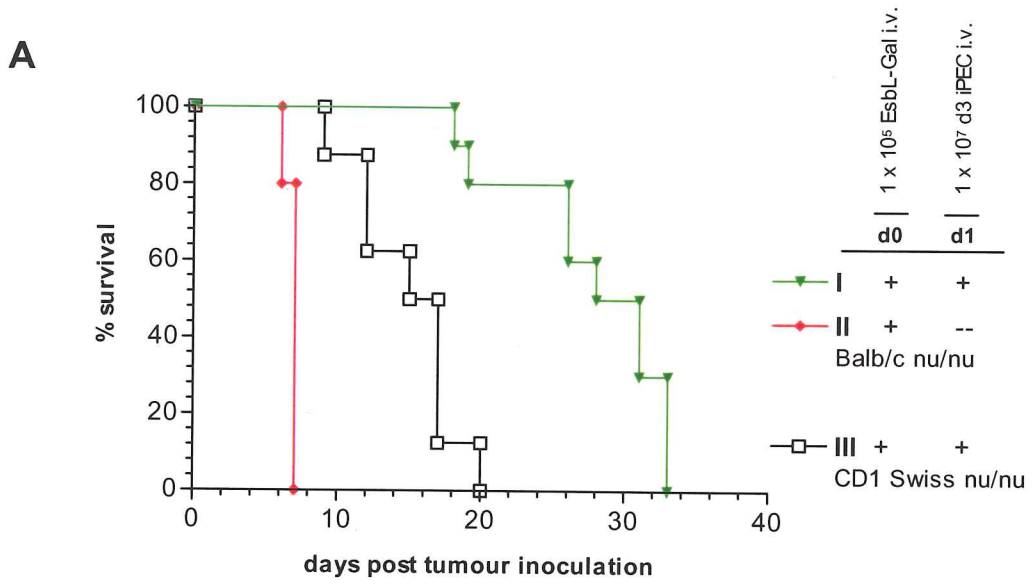

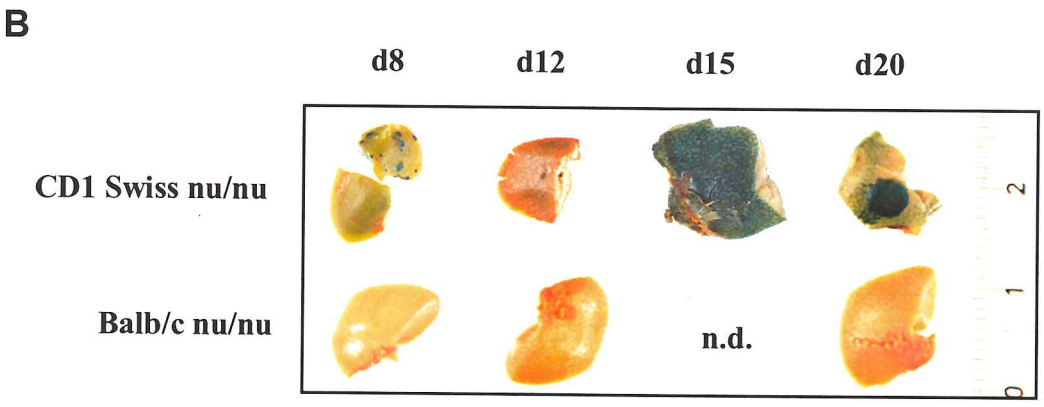

Fig. 4.16 Importance of MHC-matched recipients for the success of anti-tumour ADI. ESbL-Gal tumour bearing mice either received ADI consisting of 1 x 10^7 d3 iPEC from DBA/2 (gr. I, ▼ , n = 10), or remained without treatment (gr. II, ◆ , n = 10). For both groups, MHC-matched recipients (Balb/c nu/nu, H-2^d) were used. The outbred strain CD1 Swiss nu/nu was used as a non-MHC matched ADI-recipient (gr. III, □ , n = 8). (A) Survival graph. Shown is one single experiment. (B) Whole-organ X-gal staining of liver fragments from gr. I and gr. III isolated at various time-points after treatment.

Shown are representative organs from 1-3 mice per time point.

4.4.3 Requirement of both $CD4^+$ and $CD8^+$ T-cells for a complete therapeutic effect

T-lymphocytes are the main mediators and effectors of anti-tumour immunity. $CD4^+$ T-cells play an important role during the initiation phase of an immune response, although they can also exert effects later on (Pardoll et al. 1998). $CD8^+$ T-cells, on the other hand, are the main lymphocyte population exerting Ag-specific cytotoxicity and destroying tumour cells directly *in situ*.

Surman and colleagues described the $CD4^+$ T-cell mediated control of $CD8^+$ T-cell reactivity to a model tumour Ag (Surman et al. 2000). They used a Th1-type $CD4^+$ T-cell clone specific for β-gal to activate CTLs *in situ* in tumour bearing mice. It has previously been reported that the afferent phase of the anti-ESb tumour immune response is dependent on both $CD4^+$ and $CD8^+$ T-cells (Schirrmacher et al. 1994a), while the effector phase is mainly dependent on $CD8^+$ T-cell mediated cytotoxicity (Schirrmacher et al. 1991, Schirrmacher et al. 1994a). In order to analyse to what extent these two T-cell populations are responsible for the therapeutic success of ADI treatment, ESbL-Gal-bearing Balb/c nu/nu mice received a cellular transfer of $CD4^+$ or $CD8^+$ cell depleted ESbL-Gal-immune d3 iPEC.

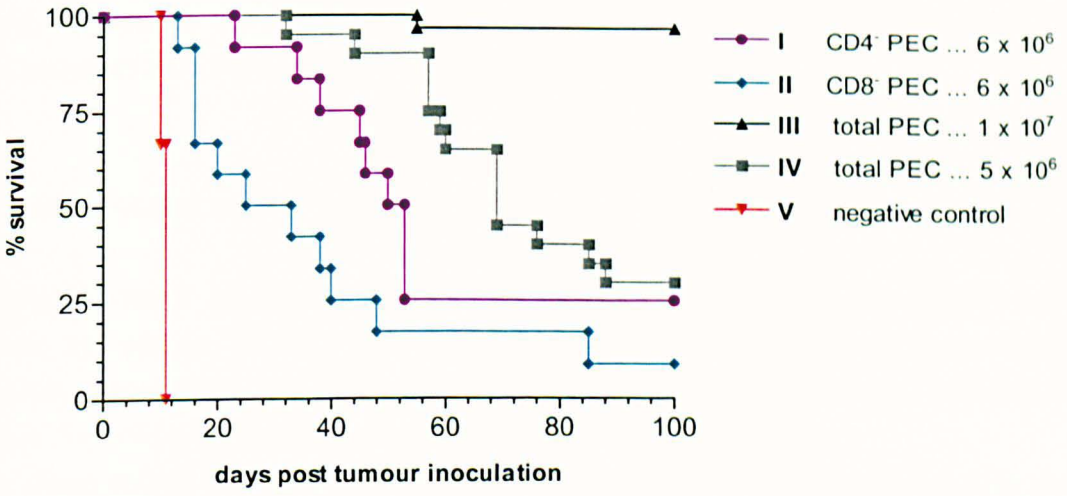

Fig. 4.17 Both $CD4^+$ and $CD8^+$ T-cells are required for optimal anti-tumour protection. Balb/c nu/nu mice received whole-body γ-irradiation at a dosis of 4.5 Gy one day prior to tumour inoculation of 1 x 10^5 ESbL-Gal i.v. . On d1, gr. I animals (● , n = 12) received 6 x 10^6 $CD4^+$ cell depleted d3 iPEC, while gr. II animals (◆ , n = 12) received 6 x 10^6 $CD8^+$ cell depleted d3 iPEC. Both treatments resulted in reduced survival of ESbL-Gal-bearing Balb/c nu/nu mice compared to animals having received the full dosis (1 x 10^7 cells) of total d3 iPEC (gr. III, ▲ , n = 30). Gr. IV (5 x 10^6 iPEC, ■ , n = 20) shows that this decreased survival is not solely due to the lower iPEC numbers applied. Negative control animals (gr. V, ▼ , n = 3) received no ADI. Represented is one experiment of two.

CD4-depleted iPEC (Fig. 4.17, gr. I, 6 x 10^6 iPEC) conferred decreased survival in comparison to undepleted iPEC (gr. III and IV), though the difference to half-dose standard therapy (gr. IV, 5 x 10^6 iPEC) was not significant ($p = 0.0918$). ADI with CD8-depleted iPEC resulted in an even lower survival rate, which proved significantly different than that of animals having received half-dose standard therapy ($p = 0.0058$). The median survival time of animals having received CD8-depleted iPEC (gr. II) was 29 days, while that of CD4-depleted iPEC recipients (gr. I) was 51.5 days. In spite of this, the two groups were not significantly different ($p = 0.2131$). The fact that gr. IV animals having received 5 x 10^6 total iPEC had a better median survival (69 days) demonstrates that the decreased survival of gr. I and gr. II animals in comparison with those having received the full therapy (gr. III: 1 x 10^7 total iPEC) was not only due to the lower cell numbers applied (6 x 10^6).
The results clearly support previous data, demonstrating that the induction of optimal systemic anti-tumour immunity involves both $CD4^+$ and $CD8^+$ T-cells specific for tumour-associated Ag (Schirrmacher et al. 1992; Hung et al. 1998).

4.5 Long-term immunological memory

One of the most important features of adaptive immune response is its ability to provide protective immunity, for instance against re-infection with the same pathogen, or, in the case of cancer, against outgrowth of dormant tumour cells or minimal residual disease.

4.5.1 Anti-ESbL-Gal long-term protection

To determine whether the present anti-ESbL-Gal therapy model results in long-lasting immune protection, i.e. whether or not it yields anti-ESbL-Gal specific immunological T-cell memory, successfully treated Balb/c nu/nu mice received an intravenous tumour challenge of live ESbL-Gal more than 2 months after their first exposure to ESbL-Gal.
Tumour doses as high as 5 x 10^7 cells were successfully rejected (Fig. 4.18 gr. I) and 66 % of the animals survived for over 8 months. Although untreated memory animals (gr. II) had a better survival than tumour-challenged mice, this difference was not significant ($p = 0.0999$).
The cells involved in long-term immune protection are memory cells by definition, as tumour challenge was done over 2 months after the initial effector phase had subsided. This experiment illustrates that the therapy model used produces long-lived memory T-cells which can rapidly be activated to expand and eliminate high doses of ESbL-Gal tumour cells. It was, therefore, concluded that this model provides a suitable system for studying features of T-cell memory.

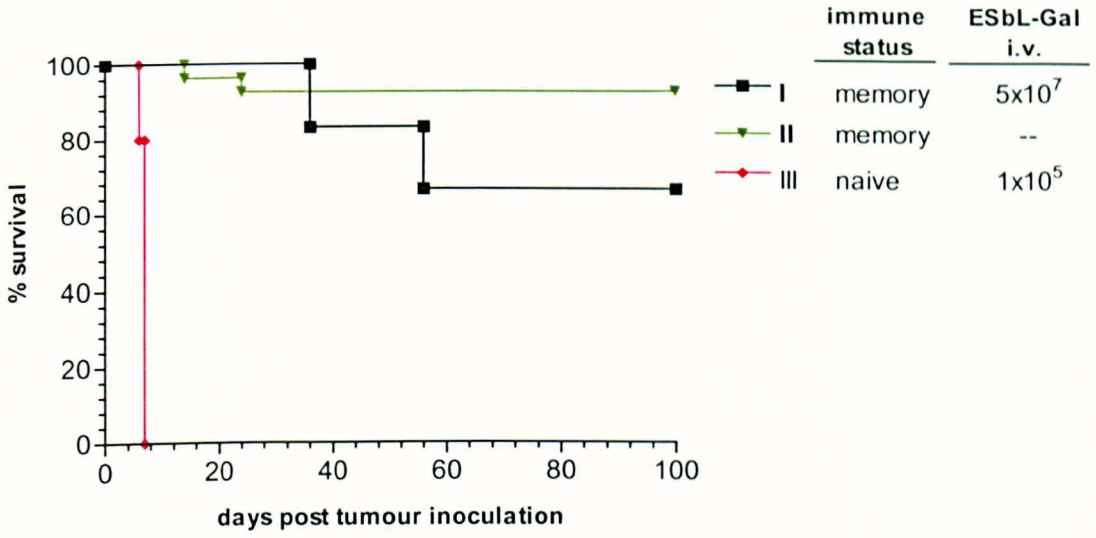

Fig. 4.18 Anti-ESbL-Gal long-term protection. Balb/c nu/nu mice having survived anti-ESbL-Gal ADI for over 2 months received a tumour challenge of 5 x 10^7 ESbL-Gal i.v. (gr. I, ■ , n = 6). Animals from the same ADI experiment obtaining no second tumour injection served as positive controls (gr. II, ▼ , n = 27), while naïve Balb/c nu/nu mice receiving 1 x 10^5 ESbL-Gal i.v. served as negative controls (gr. III, ◆ , n = 10).
The graph shows one of two experiments.

4.5.2 Radiation-resistance of memory T-cells

Biologic functions of naïve T-cells requiring proliferation and differentiation are adversely affected by γ-irradiation, while effector functions of T-cells activated before administration of irradiation are not suppressed (Igietseme et al. 1995). It has previously been reported that immunological memory, similar to an immunological effector phase, is resistant to 5 Gy γ-irradiation (Müller et al. 1998). If memory T-cells were as radiation-sensitive as naive T-cells, whole-body irradiation of memory animals should result in the destruction of memory cells via radiation induced apoptosis. Thus, administration of irradiation prior to a secondary tumour challenge would as a consequence prevent the tumour cells from being attacked by T-cells (destroyed T-cell memory) and would, therefore, markedly reduce survival.

The results of the experiment shown in Fig. 4.19 support previous reports that memory T-cells are radio-resistant. The survival of memory animals, which were irradiated (gr. II) was not significantly different ($p = 0.3408$) from that of non-irradiated (gr. I) memory animals after high dose tumour challenge (5 x 10^7 ESbL-Gal i.v.). The reduction seen was, nevertheless, reproducible.

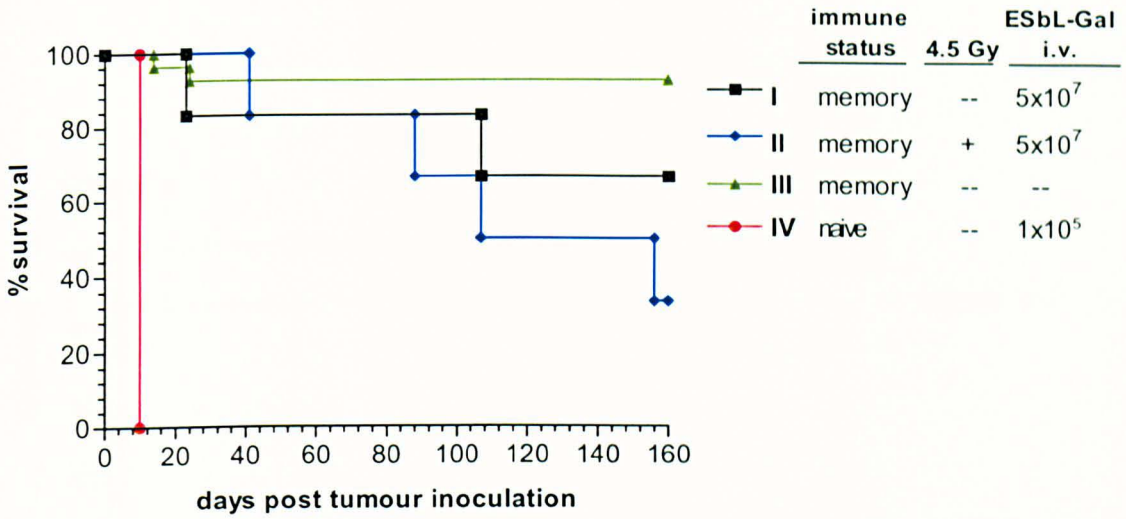

Fig. 4.19 Anti-ESbL-Gal specific memory T-cells are long-lived and radio-resistant. 2 months post ADI, Balb/c nu/nu mice received a tumour challenge of 5 x 10^7 ESbL-Gal i.v., either without (gr. I, ■ , n = 6) or with prior whole-body γ-irradiation of 4.5 Gy (gr. II, ◆ , n = 6). Positive control animals remained without tumour challenge (gr. III, ▲ , n = 10), while naïve Balb/c nu/nu inoculated with 1 x 10^5 ESbL-Gal i.v. served as negative controls (gr. IV, ● , n = 5).
Shown is one representative experiment of two.

4.6 Longevity and therapeutic potential of memory T-cells after multiple transfers

In order to determine whether donor T-cells retain their tumour-reactivity *in vivo*, Balb/c nu/nu mice having received standard therapy (4.4.1) were restimulated intraperitoneally one month after ADI transfer. mPEC (memory PEC) were isolated 3 days after i.p. challenge and transferred to secondary ESbL-Gal tumour-bearing Balb/c nu/nu (Fig. 4.20, gr. I).

The presence of ESbL-Gal tumour reactive memory immune cells was demonstrated in ADI-treated Balb/c nu/nu mice. These cells could be attracted to the peritoneum by i.p. stimulation with 1 x 10^7 irradiated (100 Gy) ESbL-Gal for transfer into a secondary tumour-bearing Balb/c nu/nu host (gr. I). 66 % of the secondary hosts survived for 5 months. Negative control animals received whole-body γ-irradiation and tumour cells but no immune cell transfer (gr. II). Their survival was significantly lower than that of animals having received mPEC ($p < 0.0001$). Balb/c nu/nu mice treated by standard therapy were used as positive controls (gr. III). The difference in survival between gr. I and gr. III animals was found to be statistically significant ($p = 0.0343$).

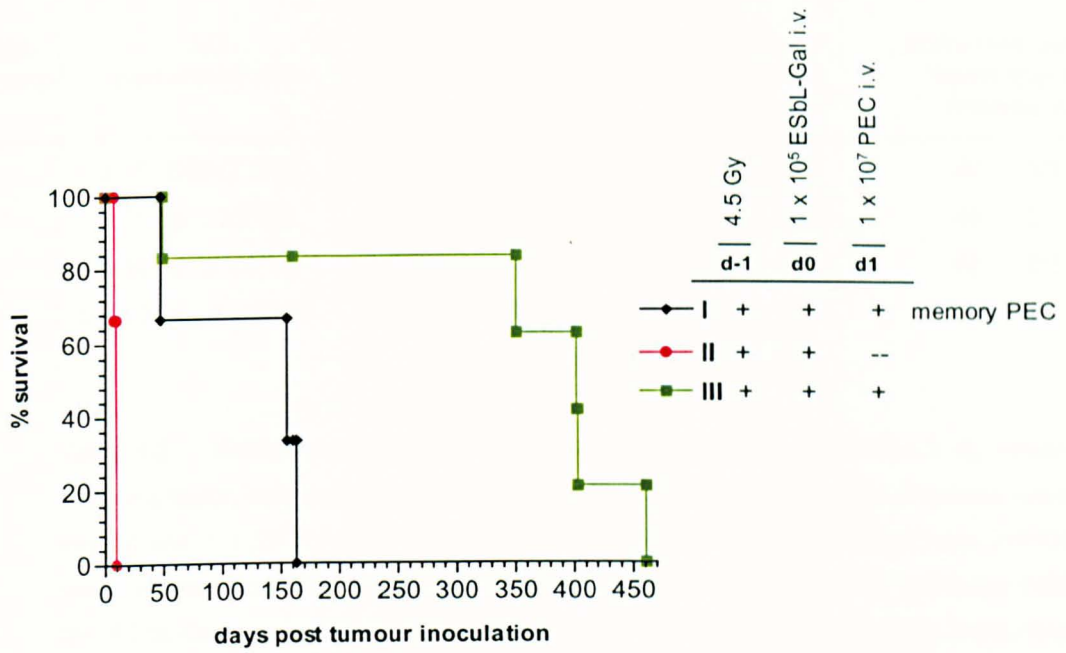

Fig. 4.20 ADI by transfer of memory cells to tumour bearing Balb/c nu/nu mice. Tumour bearing Balb/c nu/nu mice received 1 x 10^7 mPEC isolated from ADI-treated memory Balb/c nu/nu mice (3.7 months post ADI) (gr. I, ◆ , n = 11). Negative control animals received no treatment (gr. II, ■ , n = 10), while positive controls received 1 x 10^7 d3 iPEC isolated from DBA/2 mice (gr. III, ● , n = 3). All animals were whole-body irradiated with a dosis of 4.5 Gy 1 day prior to receiving a tumour inoculation of 1 x 10^5 ESbL-Gal i.v. .
Illustrated is one of two experiments.

Memory cells can thus be attracted to the peritoneal cavity by antigenic stimulation from where they can be recovered for further *in vivo* and *in vitro* experiments.

One way of monitoring the division rate of cells is by telomere analysis, as the length of telomere restriction fragments (TRF) is reduced at every cell division. Telomeres are the terminal repeat sequences (5'-TTAGGG-3') of chromosomes which are necessary for correct replication during cell division, as well as for prevention of chromosome loss (Harley et al. 1995, Artandi et al. 2000). However, telomere analysis is not very practicable in the murine system (Lansdorp 1995).

To determine how often ESbL-Gal-stimulated immune cells can be expanded *in vivo* before exhaustion and loss of function, the standard ADI-protocol was extended to include multiple transfers of immune cells from one host to another.

As illustrated in Table 4.2, Ag-specific memory T-cells retained their reactivity and protective capacities for a long period of time (test duration: 8 months), even when repeatedly stimulated to proliferate and expand. Gr. III and IV animals reveal a marked increase in survival (compared to untreated controls) with half the dose of PEC (5 x 10^6) than that which is normally administered for ADI, and nevertheless, protective immunity was transferred.

expt. group	ADI performed with	nu/nu host	duration of PEC within host	deaths: day and frequency[1)]	untreated control: death day and frequency[1)]
I	1 x 10^7 DBA/2 iPEC	1°	33 days	-- 0/21	d9 5/5
II	1 x 10^7 gr. I mPEC	2°	43 days	-- 0/19	d8 2/2
III	5 x 10^6 gr. II mPEC	3°	41 days	d40 1/10	d9 2/2
IV	5 x 10^6 gr. III mPEC	4°	145 days	d39 1/3 d78 1/3 d145 1/3	d10 2/2

Table 4.2 Multiple transfer of memory cells. All animals received 4.5 Gy whole-body irradiation before being inoculated with 1 x 10^5 ESbL-Gal i.v. . Gr. I animals were treated with 1 x 10^7 d3 iPEC obtained from ESbL-Gal-immunised DBA/2 mice. mPEC were isolated from ADI-treated Balb/c nu/nu mice by injecting 1 x 10^7 irradiated (100 Gy) ESbL-Gal i.p., 3 days before mPEC-isolation. These were used to cure ESbL-Gal-bearing Balb/c nu/nu mice (gr. II) following the standard ADI protocol. This procedure was repeated 3 times, leaving the immune cells within one host for a minimum of one month (see time spans indicated) before re-isolation and transfer to the next host. Total duration of the experiment: 8 months.
Shown are the results from a single experiment. [1)] frequency indicates the number of dead animals from the total number of animals per group.

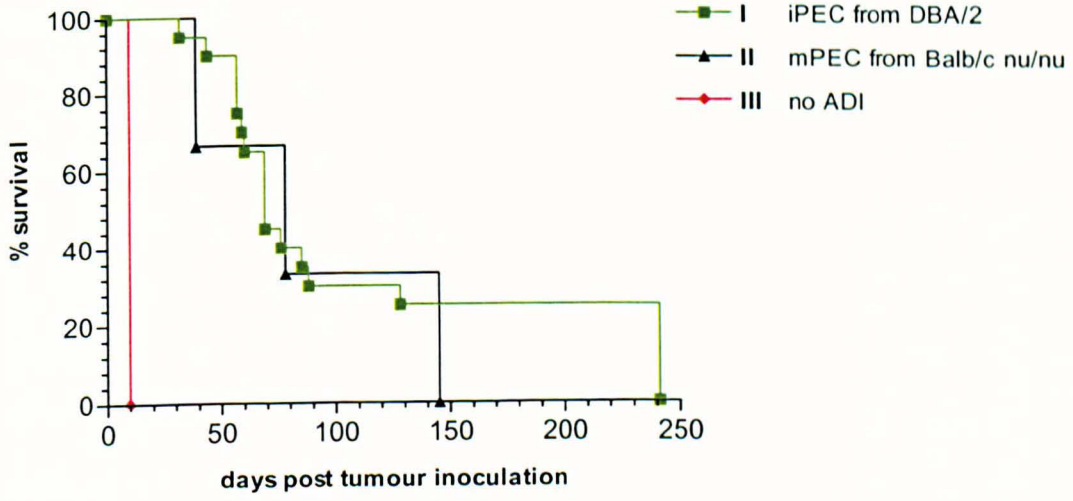

Fig. 4.21 mPEC from Balb/c nu/nu are as potent as iPEC isolated from DBA/2 mice in a GvL ADI transfer. Whole-body irradiated (4.5 Gy) ESbL-Gal tumour bearing Balb/c nu/nu received 5 x 10^6 iPEC from DBA/2 (gr. I, ■ , n = 20), 5 x 10^6 mPEC from the quaternary host (see Table 4.2) (gr. II, ▲ , n = 3), or no treatment (gr. III, ◆ , n = 2). Shown is a single experiment.

To test whether mPEC were equally potent as DBA/2-derived iPEC, the survival of quaternary host animals (table 4.2 gr. IV = Fig. 4.21 gr. II) was compared to that of tumour-bearing Balb/c nu/nu mice having received half-dose standard therapy (Fig. 4.21 gr. I). Both groups were treated with 5 x 10^6 ESbL-Gal reactive PEC. In both cases, the low dose of 5 x 10^6 PEC was insufficient for providing long-term survival of ESbL-Gal-bearing Balb/c nu/nu mice. Survival curves for the two groups are virtually identical, and the differences not statistically significant ($p = 0.6464$).

4.7 Persistence of Ag in the long-term maintenance of tumour specific memory T-cells

4.7.1 Distribution of memory T-cells throughout the body as visualised by tetramer staining

The efforts in T-cell memory research are mainly focused on elaborating their requirements for long-term survival and maintenance of Ag-reactivity. Whether compartments exist *in vivo* where memory T-cells preferentially localise has hardly been investigated.

In order to address this question, single cell suspensions were prepared from spleen, bone marrow, peripheral lymph nodes, and peripheral blood from Balb/c nu/nu mice having received ESbL-Gal tumour cells as well as ADI 6.4 months before. The frequency of β-gal$^{876\text{-}884}$/MHC tetramer binding cells within the CD8$^+$ compartment was determined by flow cytometry, and the results are illustrated in Fig. 4.22. The highest frequency of tetramer binding cells among CD8$^+$ cells was detected in the bone marrow (26.3 %), while the spleen hosted only 3.4 % and peripheral lymph nodes only 0.7 % tetramer binding cells. Of the blood circulating CD8$^+$ cells, 4.2 % bound the tetrameric complexes. Organs from naïve aged Balb/c nu/nu mice served as negative controls, where the frequency of tetramer binding cells ranged from 0 % in the bone marrow to 0.5 % in peripheral lymph nodes. Memory T-cells thus appear to accumulate in the bone marrow, indicating that this microenvironment might be of major importance in the maintenance of such long-term surviving cells.

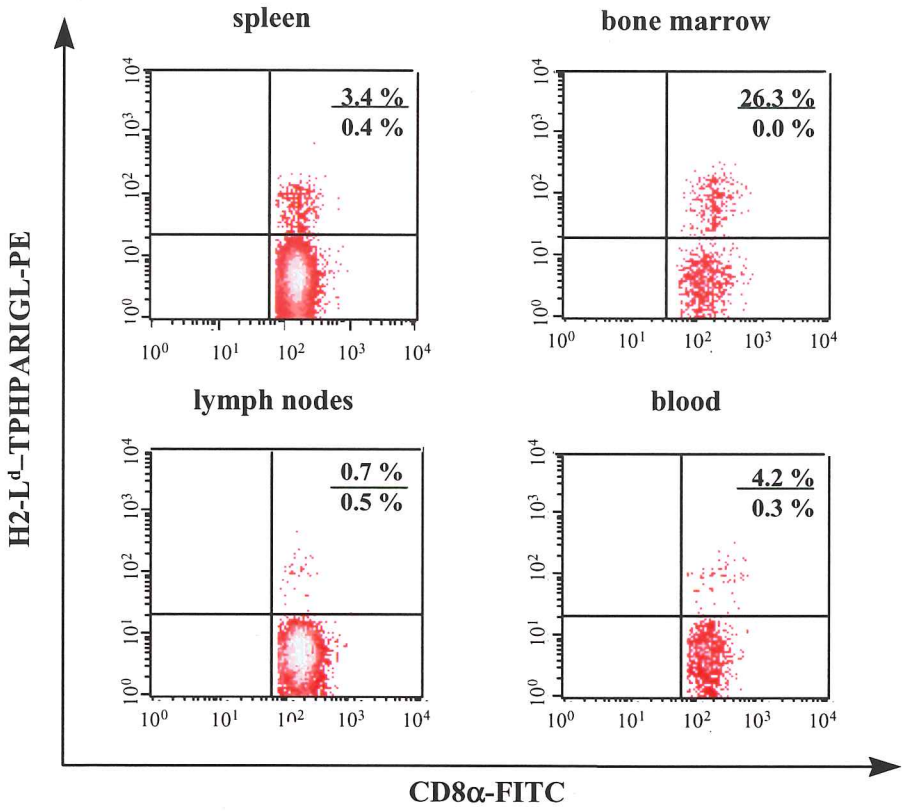

Fig. 4.22 The frequency of β-gal$^{876-884}$ specific cells among CD8$^+$ memory T-cells is highest in the bone marrow as compared to spleen, lymph nodes and blood. Spleen, bone marrow, lymph nodes and blood were isolated from memory Balb/c nu/nu mice (6.4 months post ADI) and analysed for the presence of live (PI$^-$) CD8$^+$ T-cells specific for the immunodominant β-gal peptide (aa 876-884) by tetramer staining and FACS analysis. % above the bars indicates the frequency of tetramer binding cells of live CD8$^+$ cells within organs of experimental animals, while % below the bar indicates that within organs from aged naïve Balb/c nu/nu mice.
Illustrated are the data from one of two experiments.

4.7.2 Dormant ESbL-Gal appear to be required for the maintenance of anti-ESbL-Gal memory

Tumour cells persist at a low level in the bone marrow of EblacZ ear pinna inoculated and thereby primed DBA/2 mice (Khazaie et al. 1994). Such dormant tumour cells were shown to be proliferating but prevented from outgrowth by active host control involving CD8$^+$ T-cells (Müller et al. 1998). As a consequence, the bone marrow resident tumour cell population is kept at a more or less stable size of 1-100/10^6 cells. This is also true for the present model of anti-ESbL-Gal memory in Balb/c nu/nu mice. It would, therefore, appear that Ag is constantly present, thus enabling Ag-specific maintenance of memory T-cells.

Whether or not the presence of Ag is required for supporting the survival of memory T-cells was tested in the following experiment by transferring anti-ESbL-Gal specific mPEC to naïve, whole-body irradiated Balb/c nu/nu mice. This procedure has been termed "parking experiment", as Ag-specific memory T-cells are "parked" in a host that is negative for the specific Ag (here, the ESbL-Gal associated β-gal). From here, T-cells can be re-isolated, using the standardised intraperitoneal challenge with irradiated target cells expressing the Ag of interest, in order to test for the presence (via peptide/MHC tetramer staining) and functionality (via tests such as ^{51}Cr-release assay) of Ag-specific cells.

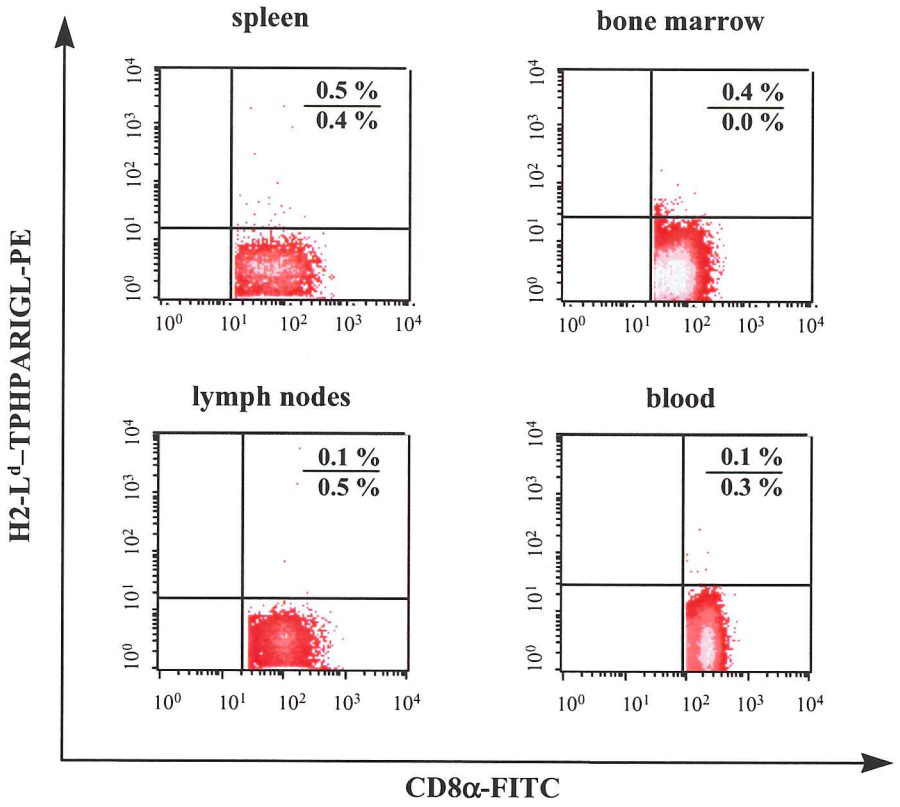

Fig. 4.23 Persistence of Ag is required for the maintenance of β-gal$^{876-884}$ specific CD8$^+$ memory T-cells. 5 months post transfer of immune cells to naïve, 4.5 Gy whole-body γ-irradiated Balb/c nu/nu mice, spleen, bone marrow, peripheral lymph nodes, and blood were isolated and analysed for the presence of live (PI$^-$) CD8$^+$ T-cells specific for the immunodominant β-gal peptide (aa 876-884) by tetramer staining and FACS analysis. % above the bars indicates the frequency of tetramer binding cells of live CD8$^+$ cells within organs of experimental animals, while % below the bar indicates that within organs from aged naïve Balb/c nu/nu mice.
Illustrated are the data from one of two experiments.

5 months after initiation of the parking experiment, single cell suspensions were prepared from spleen, bone marrow, peripheral lymph nodes and peripheral blood, and stained for CD8-

expression and tetramer-binding. The frequency of tetramer binding cells within the live $CD8^+$ population was extremely low (≤ 0.5 %, Fig. 4.23), and tetramer binding was mainly unspecific (no tight $tetramer^+$ populations, compare with Fig. 4.22). Organs from naïve aged Balb/c nu/nu mice served as negative controls, where the frequency of tetramer binding cells was in the same range (0.0 - 0.5 %) as in the organs from animals in the parking experiment (0.1 - 0.5 %).
It is, therefore, concluded that in the present model Ag-persistence is necessary for the maintenance of Ag-specific memory T-cell numbers.

4.8 Anti-β-gal DNA-vaccination

In the ADI experiments described so far, d3 iPEC were generated in DBA/2 mice by anti-tumour immunisation in the ear pinna, followed by i.p. restimulation with irradiated ESbL-Gal tumour cells. In this situation, the CTL present within the d3 iPEC will be reactive against a panel of tumour Ags, including the endogenous ESb TAA and the bacterial β-gal expressed by this T-lymphoma cell line. DNA-vaccination allows to restrict the immunisation against a single protein Ag, such as β-gal, or even against single peptide epitopes. This would facilitate the *ex vivo* analysis of memory T-cells, especially for elaboration of their functional properties.
The following experiments using DNA-vaccination were designed to determine whether iPEC reactivity against the β-gal protein is sufficient to prevent rapid death due to liver metastasis in tumour-inoculated Balb/c nu/nu mice after ADI, and whether DNA-vaccination results in the development of long-term T-cell memory.

4.8.1 Induction of delayed type hypersensitivity (DTH)-reactivity following DNA or cellular vaccination

Delayed type hypersensitivity (DTH) reactions can be induced by a large variety of Ags and appear to depend upon a special subset of $CD4^+$ T-lymphocytes which secrete inflammatory cytokines. The inflammatory reaction following an Ag-specific challenge of immunised individuals can typically be observed to start 6 - 12 hours after Ag-administration, peaking between 24 - 72 hours, and decreasing again thereafter. The stronger the DTH response, as determined by the degree of redness and swelling at the site of Ag-challenge, the stronger the T-cell response (de Weck 1998).
Here, a DTH test was used to analyse T-cell activation following either DNA or cellular ear pinna vaccination. To this end, DBA/2 mice received either one or two ear pinna injections (with a 2 week interval) of either pCMVβ DNA (coding for β-gal) or ESbL-Gal tumour cells. 5 days after immunisation, the animals were challenged with ESbL-Gal lysate in the contralateral ear pinna, and the DTH reaction was evaluated two days later as previously described (Schirrmacher et al. 1994c). The results are illustrated in Fig. 4.24.

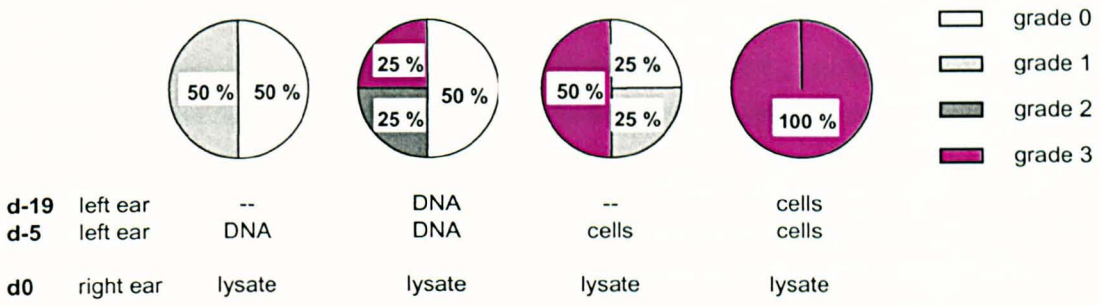

Fig. 4.24 DTH-reaction following DNA or cellular vaccination in the ear pinna.
DBA/2 mice were primed in the left ear pinna as indicated and challenged 5 days after the last stimulus in the contralateral ear pinna with 50 µl ESbL-Gal lysate (from a cell suspension of 2 x 10^6 cells/ml). 48 hours after the lysate injection, DTH reaction was evaluated using an established grading system. grade 0: no erythema and no swelling (□); grade 1: erythema without swelling (■); grade 2: erythema with swelling of <0.5 mm (■); grade 3: erythema with swelling of >0.5 mm (■). %: percentage animals per group with the indicated DTH-grade; DNA: 50 µg pCMVβ plasmid DNA; cells: 5 x 10^4 ESbL-Gal.
Shown are the results of a single experiment with 4 animals per group.

After two DNA-injections administered with an interval of 2 weeks, the reaction was stronger in responding animals (grade 2-3) than after a single injection (grade 1), though in both cases half the animals still had no measurable DTH-reaction (grade 0) following ear pinna challenge with ESbL-Gal lysate. After a single cellular vaccination, the DTH-response ranged from grade 1-3, while in ESbL-Gal double immunised animals, the intensity of swelling ranged from 0.5 to 2.5 mm (grade 3). In all groups, erythema and swelling declined after 72 hours.

The results indicate that, under the present conditions, cellular priming results in a stronger T-cell response than does DNA-vaccination, though with both types of stimuli, two injections were more efficient than one in the induction of Ag-reactive $CD4^+$ T-cells. In the case of the tumour primed animals, the priming and DTH stimuli contained more than one common Ag (the Esb-derived TAA and β-gal), while in DNA-primed animals there was only one common Ag (β-gal). This might, at least partially, explain the more elevated responses observed in ESbL-Gal primed mice.

The experiment will have to be repeated with more animals per group to determine the significance of the present preliminary data. Additionally, the DTH-stimulus should be chosen to have only one common Ag with both pCMVβ and ESbL-Gal, in order to provide more comparable conditions for the cellular and DNA-vaccination.

4.8.2 DNA-vaccination is less efficient than cellular vaccination in the induction of CTLs

It is known that bacterial DNA can circumvent the need for $CD4^+$ T-cells in the activation of Ag-specific CTLs, as the recognition of unmethylated CpG motifs present in bacterial DNA by TLR9 on DCs can directly condition the DCs to provide the signals necessary for CTL-activation (Cho et al. 2000, Akira et al. 2001). As the results presented in the previous section (4.8.1) indicated a lower efficiency of a DNA-vaccine, as compared to a cellular stimulus, in the induction of Ag-specific $CD4^+$ T-cell responses, the efficiency of $CD8^+$ T-cell induction was now investigated.

To this end, animals received either a single ear pinna injection of 5 x 10^4 ESbL-Gal, or four pCMVβ injections administered in intervals of 1 week. Ag-reactive immune cells were recruited to the peritoneal cavity by intraperitoneal injection of radiation-inactivated ESbL-Gal and analysed for T-cell content by flow cytometry.

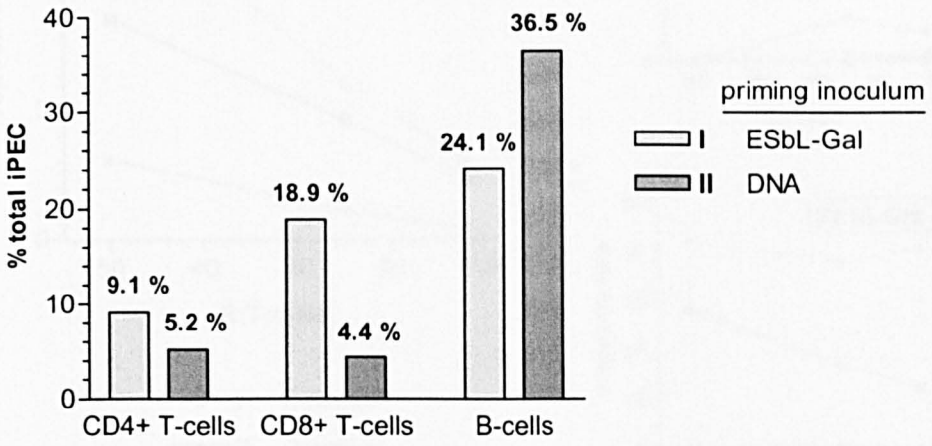

Fig. 4.25 T-cell and B-cell content in iPEC from DNA-vaccinated or ESbL-Gal immunised DBA/2 mice. DBA/2 mice were primed with either 5 x 10^4 ESbL-Gal (gr. I, ▫) or 50 µg pCMVβ i.e. (4x in weekly intervals, gr. II, ■) and restimulated with 1 x 10^7 irradiation-inactivated ESbL-Gal i.p. . iPEC were isolated 3 days later and analysed by 2-colour flow cytometry for the presence of $CD4^+$ and $CD8^+$ T-cells, and B-cells. Shown is one of two experiments.

While iPEC from ESbL-Gal immunised DBA/2 mice contained 9.1 % $CD4^+$ and 18.9 % $CD8^+$ T-cells (Fig. 4.25, gr. I), iPEC from DNA-vaccinated animals contained only 5.2 % $CD4^+$ and 4.4 % $CD8^+$ T-cells (gr. II). The ratio of $CD4^+$ to $CD8^+$ T-cells was also different in gr. II iPEC (1.2 : 1) and gr. I iPEC (1 : 2.1). In contrast to the low frequency of T-cells in DNA-vaccinated animals, the frequency of B-cells was higher in iPEC from these mice (36.5 %) than in iPEC from ESbL-Gal immunised mice (24.1 %). This might indicate a more important involvement of Ab-mediated immune responses following DNA-vaccination than following a cellular stimulus.

Taken together these data indicate that, under the present experimental conditions, vaccination with DNA coding for a protein Ag might not be sufficient to induce strong secondary CTL responses.

4.8.3 Generation of cytotoxic killer cells after DNA-vaccination

In order to test whether iPEC from DNA-primed DBA/2 mice, albeit their low $CD8^+$ T-cell content, are able to exert Ag-specific cytotoxicity, it was evaluated which vaccination regimen would be most suitable for the production of peritoneal CTL. To this end, DBA/2 mice were vaccinated with pCMVβ plasmid DNA in the ear pinna 1 week (Fig. 4.26 gr. III), 2 weeks (gr. II), or 3 weeks (gr. I) before i.p. re-stimulation with irradiation-inactivated P815-Gal. iPEC were isolated 3 days later and tested for *in vitro* cytotoxic activity against ESbL-Gal in a ^{51}Cr-release assay.

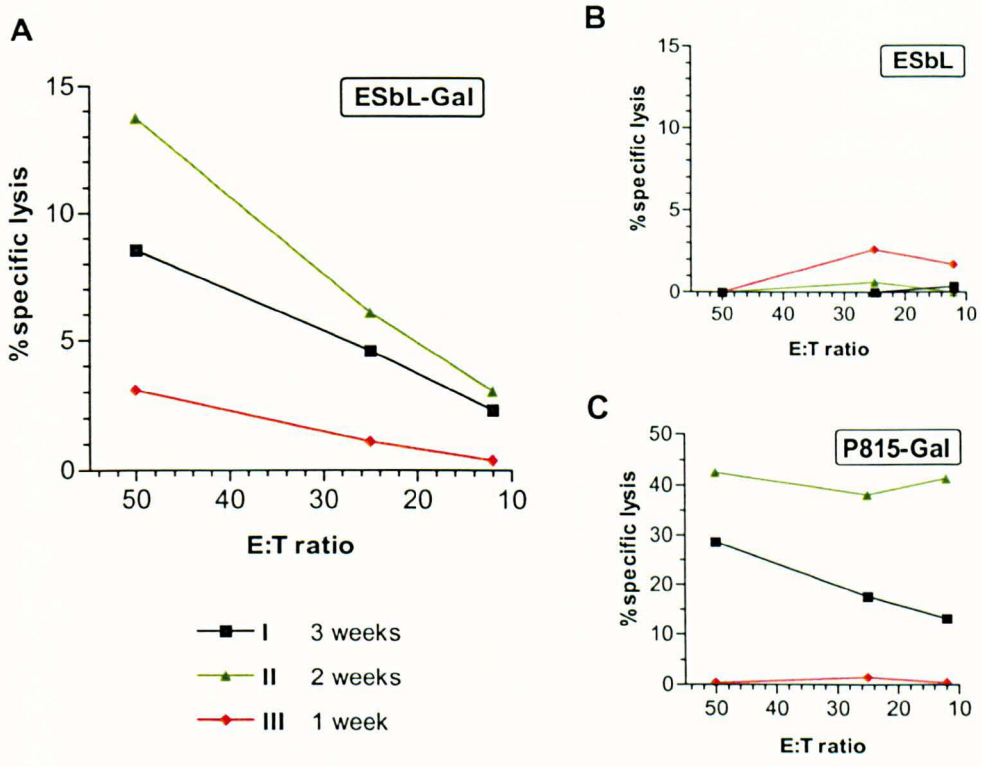

Fig. 4.26 ***In vitro*** **cytotoxicity of d3 iPEC from DNA-vaccinated animals.** Naïve DBA/2 mice were primed with 50 µg pCMVβ i.e. and restimulated with 1 x 10^7 irradiation-inactivated P815-Gal i.p. . gr. I (■) received the second injection 3 weeks, gr. II (▲) two weeks and gr. III (◆) one week after priming. iPEC were isolated 3 days after restimulation and tested for cytotoxic activity against ESbL-Gal (A), ESbL (B), or P815-Gal (C) in a 4h ^{51}Cr-release assay.

Highest specific lysis was achieved when DNA-vaccination occurred 2 weeks before i.p. restimulation (Fig. 4.26 A gr. II, 13.7 %). A time lapse of 3 weeks between the priming and restimulating inoculum yielded a lower reactivity against β-gal (Fig. 4.26 A gr. I, 8.5 %), whereas a time span of one week between the two inoculations was not sufficient to raise specific lysis levels above the unspecific ^{51}Cr-release from β-gal$^-$ target cells (Fig. 4.26 B, <5 %) (values are given for E:T = 50:1). These conclusions were also supported by the results obtained with the more sensitive target cell line P815-Gal. With ESbL-Gal as target cells the difference in specific kill between groups I and II was not significant ($p = 0.0584$), but the greater cytotoxic activity of gr. II iPEC was

statistically significant when using P815-Gal as targets (p = 0.0343) Only iPEC from gr. III animals (1 week between primary and secondary challenge) caused no release of ^{51}Cr from P815-Gal target cells upon co-culture.

Overall the results demonstrate that β-gal reactive iPEC can be obtained from DNA-primed animals. The time span between priming i.e. and re-stimulation i.p. needs to be longer (2 weeks) than in ESbL-Gal primed animals (1 week, Fig. 4.7, 4.3.2).

4.8.4 Anti-ESbL-Gal ADI with iPEC from DNA-vaccinated DBA/2 mice

The question arose whether anti-β-gal reactive iPEC from DNA-vaccinated were potent enough to yield long-term survival of LCI-bearing Balb/c nu/nu mice after adoptive transfer. To this end, DBA/2 mice were primed with β-gal coding pCMVβ plasmid DNA 2 weeks prior to receiving an intraperitoneal challenge with irradiation-inactivated P815-Gal tumour cells. iPEC were isolated 3 days later and transferred to ESbL-Gal tumour bearing Balb/c nu/nu mice.

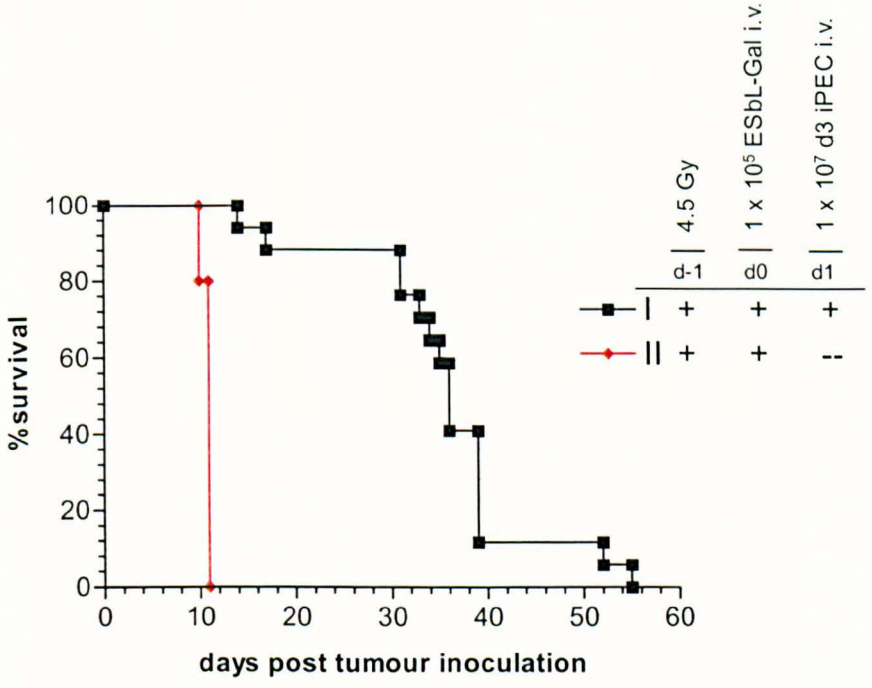

Fig. 4.27 Therapy of ESbL-Gal-bearing mice by ADI of anti-β-gal d3 iPEC. One day before tumour inoculation with 1 x 10^5 ESbL-Gal i.v., Balb/c nu/nu mice received whole-body γ-irradiation at a doses of 4.5 Gy. The control group (gr. II, ◆ , n = 5) received no further treatment, while the experimental group (gr. I, ■ , n = 17) received 1 x 10^7 d3 anti-β-gal iPEC i.v. on d1. d3 iPEC were isolated from DBA/2 primed with 50 µg pCMVβ two weeks before i.p. restimulation with 1 x 10^7 irradiation-inactivated P815-Gal.

Represented are the results of a single experiment.

In combination with whole-body irradiation, ADI of d3 iPEC from pCMVβ primed and P815-Gal restimulated DBA/2 mice (Fig. 4.27 gr. I) was significantly less efficient ($p < 0.0001$) than treatment with ESbL-Gal-primed and restimulated d3 iPEC (Fig. 4.12 in 4.4). Nevertheless, survival was significantly better ($p < 0.0001$) than in untreated controls (Fig. 4.27 gr. II), with treated animals having a median survival of 36 days, while untreated animals died on days 10-11 post tumour inoculation.

4.8.5 Long-term T-cell memory after DNA or cellular vaccination

Immunisation with naked DNA provides an enormous potential for developing new vaccines, but, as tumour vaccines are not only aimed at inducing protective anti-tumour immunity but also at producing long-term T-cell memory, vaccination protocols need to be designed that provide such long-lasting T-cell memory.

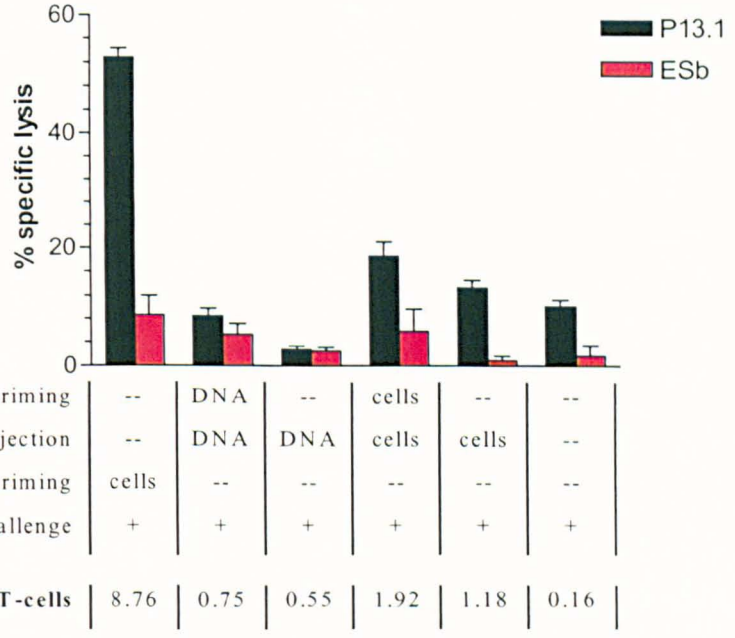

Fig. 4.28 Long-term CTL memory after DNA- vs. cellular vaccination. DBA/2 mice were primed as indicated and challenged i.p. with 1 x 10^7 irradiation-inactivated (100 Gy) ESbL-Gal. iPEC were isolated 3 days later and Ag-specific killing activity tested in a 4h ^{51}Cr-release assay. Standard ESbL-Gal-specific d3 iPEC were used as a positive control, while PEC from DBA/2 having received only the secondary i.p. challenge served as a negative control. i.e. priming/injection: either 50 µg pCMVβ plasmid DNA (DNA) or 5 x 10^4 ESbL-Gal i,e (cells). The values given are for E:T ratio of 50:1.

The results are from a single experiment.

Vaccination with the pCMVβ-plasmid can induce immunological memory directed against β-gal. DBA/2 mice which received a s.c. challenge with β-gal expressing tumour cells 3 weeks after DNA-vaccination i.e. rejected the tumour to variable degrees, depending on the aggressiveness of the tumour line used (Schirrmacher et al. 2000). Experiments using the T-lymphoma line ESb 289 demonstrated that a single i.e. injection is not sufficient to initiate long-lasting CTL memory, while i.e. immunisation followed by an intra-peritoneal challenge 9 days later resulted in the maintenance of tumour specific CTL over a period of at least two months (Schirrmacher 1999).

The preliminary data shown in Fig. 4.27 indicate that DNA-vaccination did not result in long-term surviving Ag-specific memory T-cells. Anti-P815-Gal cytotoxic activity of PEC from DNA-primed animals was below the negative control (10.2 %, i.p. challenge only). PEC from DBA/2 mice having received two ear pinna injections of ESbL-Gal exerted β-gal specific cytotoxic activity (18.7 %) which was significantly higher than that from negative control animals ($p = 0.0327$). The difference in kill by PEC from negative controls and mice having received a single injection of ESbL-Gal (13.2 %) was not significant ($p = 0.1428$). After a priming regimen with two cellular stimuli, Ag-specific memory T-cells survived over a long period of time (6 months) and retained their capability of exerting Ag-specific effector functions. In contrast, a single cellular injection or DNA-vaccination did not result in the maintenance of β-gal specific memory T-cells.

Discussion

5.1 Cell surface expression of molecules on the parental ESbL-Gal tumour cell line ad its bone marrow derived variant ESbL-Bal-BM

ESbL-Gal are a *lacZ*-transfected variant of the murine T-lymphoma ESb, expressing the bacterial enzyme β-galactosidase as an additional, highly immunogenic TAA. As the ESb-derived TAA could not be identified so far, β-gal provides an ideal model Ag for the analysis of primary and secondary tumour-specific immune responses, as well as the effect of Ag-removal on the memory T-cell pool. To this end, it was a prerequisite that β-gal expression is not lost during tumourigenic progression *in vivo*. Analysis of *ex vivo* isolated ESbL-Gal from bone marrow derived dormant tumour cells, ESbL-Gal-BM, and the immune escape variants ESbL-Gal-ET, -ST, and -TT obtained from solid tumour nodules revealed that β-gal is stably expressed *in vivo* (Fig. 4.1). Furthermore, many other tumour nodules were isolated, all of which consisted of β-gal$^+$ cells, as determined by whole-organ X-gal staining. The ESbL-Gal tumour thus represents a relevant model for the study of Ag-specific immune responses to cell-bound Ag.

As mentioned, ESbL-Gal is a variant of the ESb 289 T-lymphoma. The ESb tumour arose spontaneously *in vivo*, and, in contrast to the parental Eb-line, is highly metastatic. Early studies indicated that ESb might have evolved by fusion of an Eb tumour cell with a host macrophage, as experimental hybridomas of ESb cells with bone marrow-derived macrophage cultures resembled ESb and not Eb in respect to TAA expression, metastatic behaviour, and aggressiveness (Larizza et al. 1984). Intriguingly, the macrophage marker F4/80 could not be detected on ESbL-Gal, whereas these cells were found to express the B-cell specific markers CD19 and B220 (Fig. 4.2), suggesting that the *in vivo* fusion partner of Eb cells might also have been a B-cell. Furthermore, the macrophage cultures used for the fusion experiments were not purified, so that the presence of B-cells could not be excluded. In order to clarify the etiology of ESb cells, it would be instructive to repeat such fusion experiments using purified macrophages or B-cells.
Nevertheless, the expression of B-cell markers does not necessarily point toward a B-cell origin, as tumour cells can lose Ags specific for their tissue of origin while acquiring others during malignant progression. Additionally, the macrophage markers MOMA and Sn have been found to be expressed by ESbL-Gal tumour cells *in vitro*, albeit at a low level, suggesting a possible macrophage origin (Rocha et al. 1997).

Many tumours have been shown to have defective MHC biosynthesis pathways as a strategy of immune escape (Alimonti et al. 2000, Seliger et al. 2000). The dormant tumour cell derived ESbL-Gal-BM where found to be negative for MHC class II, whereas a low level expression was detected on the parental ESbL-Gal T-lymphoma cell line. Both ESbL-Gal and ESbL-Gal-BM expressed MHC

class I molecules on their surface, with expression levels being more elevated in the latter cell line (Fig. 4.3), indicating that they can present endogenously derived peptides, including those of the model tumour Ag β-gal. Thus, they could potentially stimulate tumour-reactive CTL directly. To what extent the high surface expression of MHC class I plays a role in the sensitivity of tumour cells to the host's immune system is unclear.

How dormant tumour cells protect themselves against elimination by the immune system remains to be determined. It has been shown that dormant tumour cells are prevented from expansion on a population level by $CD8^+$ T-cells, depletion of which results in the rapid outgrowth of tumour cells and death of the animals (Müller et al. 1998). The dormant tumour cells are thus under tight control of the host's immune system, without being completely eliminated.

Bosslet and colleagues have demonstrated a high frequency development of ESb tumour variants *in vivo*. Such variants had altered TAA expressions as compared to ESb, and this altered phenotype proved to be genetically transmitted and stable both *in vitro* and *in vivo* (Bosslet et al. 1982). ESbL-Gal-BM can thus be assumed to closely represent the phenotype of ESbL-Gal-derived dormant tumour cells, providing an optimal tool for the analysis of factors that could influence the persistence of tumour dormancy in immunocompetent hosts.

The highly metastatic ESbL-Gal expressed a variety of adhesion molecules, including LFA-1, LFA-2, L-selectin, ICAM-1, and PSGL-1, and minimally also the β_7-integrin chain (Fig. 4.4), which might be necessary for its metastatic phenotype. Injection of ESbL-Gal tumour bearing mice with mAbs to LFA-1 and ICAM-1 has been shown to prolong their survival, thus demonstrating an involvement of these two molecules in tumour progression (Rocha et al. 1996).

Bone marrow metastases of cancer patients could be shown, without exception, to express ICAM-1 (Putz et al. 1999), which could point towards an involvement of this molecule for homing and survival in the bone marrow. Consistently, ICAM-1 expression was found to be increased on ESbL-Gal-BM. In combination with the high expression of MHC class I on the dormant tumour cells, high expression levels of ICAM-1 could also indicate that these cells are able to activate tumour-specific CTL activity *in situ*, without the need for APC, thus being directly involved in the control and maintenance of a steady population size of dormant tumour cells within the bone marrow microenvironment.

L-selectin mediates the initial adhesion of lymphocytes to high endothelial venules of peripheral lymph nodes, an interaction required for the entry of blood circulating naïve T-cells into the lymph nodes. L-selectin expression on ESbL-Gal has previously been published (Rocha et al. 1997). Rapid loss of L-selectin expression following T-cell activation may be required for the detachment of leukocytes from the endothelium to allow their migration into tissues. Likewise, the fact that ESbL-Gal-BM proved to be negative for this adhesion molecule might be involved in the seeding of this tumour variant to the bone marrow.

β_7-chain integrins as well as PSGL-1 are involved in the migration and homing of leukocytes. The β_7-integrin chain forms a functional adhesion molecule in combination with either the α_4- or the α_E-

integrin chain, and expression of the latter appears to be restricted to intra-epithelial lymphocytes (Lefrançois et al. 1999). $\alpha_4\beta_7$ functions as a mucosal homing receptor and its ligands include the vascular cell adhesion molecule-1 (VCAM-1), fibronectin, and the mucosal addressin cell adhesion molecule-1 (MadCAM-1). $\alpha_4\beta_7$ expression on LB lymphoma cells could be shown to strongly suppress metastasis formation at a stage subsequent to infiltration of the target organs spleen, lymph nodes, liver, lung, and kidney. Only expansion in the bone marrow was not affected by $\alpha_4\beta_7$ integrin expression (Gosslar et al. 1996). A weak expression of the β_7-integrin chain was detected on ESbL-Gal tumour cells, which correlates with their ability to form metastases in the liver and spleen. Studies on human multiple myeloma peripheral blood B-cells implicated $\alpha_4\beta_7$ in the tumour cell adhesion to bone marrow fibroblasts (Masellis-Smith et al. 1997). Likewise, the slightly increased β_7-integrin expression on ESbL-Gal-BM might be involved in the retention of dormant tumour cells within the bone marrow.

PSGL-1 has been shown to mediate specific rolling of haematopoietic stem and progenitor cells (HSPC) on constitutively expressed P-selectin (platelet selectin) of bone marrow microvenules and sinusoids, and has, therefore, been proposed to be involved in the specific homing and extravasation to the bone marrow of HSPC following bone marrow transplantation (Greenberg et al. 2000). PSGL-1 could thus be involved in the homing of some ESbL-Gal cells to the bone marrow. In contrast to the parental line, ESbL-Gal-BM were found to be negative for this adhesion molecule. As adhesion via PSGL-1 has been shown to suppress the proliferation of HSPC (Lévesque et al. 1999), down-regulation of PSGL-1 on ESbL-Gal-BM might be a strategy to allow their proliferation within the bone marrow microenvironment. Again, whether this involves an actual down-regulation of PSGL-1 expression or a selection of PSGL-1 negative tumour cells is not clear.

ESbL-Gal-BM are more sensitive to CTL-mediated cytotoxicity *in vitro* than the parental ESbL-Gal (data not shown) but, nevertheless, persist for prolonged periods of time in the presence of tumour-reactive memory CTL (Müller et al. 1998). One explanation for these findings could be that adhesion molecules are more important for CTL-tumour cell interactions *in vivo* than *in vitro*. The expression of only few adhesion molecules on tumour cells could complicate CTL-tumour cell interactions *in situ*, thus allowing for the co-existence of CTL-sensitive tumour cells and tumour reactive killers in the bone marrow microenvironment, whereas the close cell-cell contact during cytotoxicity assays owing to the experimental conditions could circumvent the need for interaction via specific adhesion molecules.

In contrast to the parental ESbL-Gal, the bone marrow derived variant, ESbL-Gal-BM, appears to have a rather naked cell surface concerning not only adhesion molecules but also leukocyte markers. As an exception to this, MHC class I and ICAM-1 were highly expressed on these cells, both with elevated levels as compared to the parental ESbL-Gal. A general down-regulation of adhesion molecules required for rolling interactions with the vascular endothelium during migration and dissemination could indicate that dormant tumour cells are a non-migratory population. Selective up-regulation of ICAM-1 and $\alpha_4\beta_7$, might then be important for the retainment of these

cells within the bone marrow. Down-regulation of PSGL-1 might be involved in allowing bone marrow resident tumour cells to proliferate, as it has been shown that adhesion via PSGL-1 suppresses the proliferation of HSPC of the bone marrow (Lévesque et al. 1999).

5.2 *In vivo* dissemination of ESbL-Gal following ear pinna inoculation

ESbL-Gal have been shown to rapidly disseminate to the draining lymph node after ear pinna injection, and tumour cells were detected in the subcapsular space of the spleen as early as 15 minutes after inoculation (Schirrmacher et al. 1997). The tumour cells thus drained quickly from the injection site, via lymphatic fluid, into the lymph node where they could induce a primary anti-tumour T-cell response. Dissemination to the spleen, on the other hand, occurred via the blood circulation. Similar to the spleen, bone marrow is vascularised by blood vessels (Osmond 1994), suggesting that tumour cell dissemination to this microenvironment could be equally fast. Unfortunately, no data were obtained for early time points (less than 4 days) to test this hypothesis. Nevertheless, tumour cells could be detected in the bone marrow with a peak accumulation on day 5 after ear pinna injection (Fig. 4.5). Similar kinetics of tumour cell numbers where found in the spleen and bone marrow. As the bone marrow stroma contains macrophages that are specialised in phagocytosing incorrectly developed blood elements (Krstic 1994) as well as foreign material invading the bone marrow microenvironment, it is highly likely that these macrophages, similar to those in the spleen, are capable of internalising disseminated tumour cells or products thereof, providing the possibility of initiating a tumour-specific T-cell response directly *in situ*.

5.3 Bone marrow functions as a secondary lymphoid organ

The rapid dissemination of tumour cells after ear pinna inoculation not only to the draining lymph node but also to other lymphoid organs, such as the spleen and bone marrow, suggests that anti-tumour reactive T-cells might also be primed in these compartments.

The spleen is a secondary lymphoid organ where immune responses can be initiated. Consistently, phagocytic cells of the spleen have been shown to internalise ESbL-Gal cells already 3 hours after tumour injection. Tumour Ag can thus be processed and presented to $CD4^+$ T-cells via MHC class II and to $CD8^+$ T-cells via MHC class I, providing one of the necessary conditions for T-cell priming in the spleen (Schirrmacher et al. 1997).

The bone marrow, on the other hand, is classically known as a primary lymphoid organ where haematopoiesis and lymphopoiesis take place. To date, its potential role in secondary immune functions has been ignored.

Findings from our group demonstrate that bone marrow APC can take up soluble blood-borne Ag for presentation to T-cells both *in vitro* and *in situ* (Feuerer et al., submitted), thus indicating that the bone marrow is able to behave like a secondary lymphoid organ where primary T-cell responses can take place. Staining with peptide/MHC class I tetrameric complexes has now allowed the monitoring of Ag-specific T-cell kinetics directly *ex vivo* following priming, and revealed that the

highest frequency of tetramer binding cells within the $CD8^+$ population are present in the bone marrow, peaking 10 days after tumour inoculation (Fig. 4.6). It is unlikely that this is solely due to an influx of primed cells into the bone marrow from the spleen or lymph nodes, and indicates that T-cell responses to cellular antigenic material can be initiated in the bone marrow microenvironment, although, as also found in the spleen, with slower kinetics than in lymph nodes. These findings parallel previously published data demonstrating that the bone marrow supports the majority of all Ig-secreting cells which exhibit slower induction of Ig-production, but an overall longer lasting response than that observed in other lymphoid compartments (Benner et al. 1981).

Taken together, the data demonstrate the ability of bone marrow to function as a secondary lymphoid organ, and, together with its body distribution and size, suggests that the bone marrow can be considered of central importance also for the establishment of immune responses and systemic immune control.

5.4 Secondary anti-tumour T-cell response in the peritoneal cavity

Intraperitoneal challenge of tumour-primed DBA/2 mice with radiation-inactivated ESbL-Gal resulted in a 5.3-fold increase of immune cell numbers within the peritoneal cavity (Table 4.1). While the immune population of the naïve peritoneum mainly consisted of B-cells (78.4 %) and contained only low numbers of T-cells (5.8 % $CD4^+$ and 0.5 % $CD8^+$ T-cells), T-cell numbers increased dramatically after a secondary challenge at this site (Fig. 4.7). Most markedly, $CD8^+$ T-cell numbers exploded to 11.2 % on day 3 post challenge, with 33.9 % of these binding β-$gal^{876-884}$ peptide/MHC class I tetrameric complexes. Consistently, iPEC tested at this time point for *ex vivo* Ag-specific $CD8^+$ T-cell mediated killing activity exhibited a high β-gal specific lysis of target cells (34.5 % specific lysis of ESbL-Gal at an E:T ratio of 50:1, Fig. 4.8). Tumour-specific $CD8^+$ T-cells were most likely recruited from the spleen and bone marrow as exemplified by tetramer staining of β-$gal^{876-884}$ reactive cells (Fig. 4.9). Three days after the secondary stimulus, their frequency was demonstrated to be lower in these organs as compared to organs from animals having received only the primary ear pinna tumour inoculation.

Influx of immune cells into the peritoneal cavity was enabled by the production of high amounts of TNF-α early after tumour challenge, which is known to increase vascular permeability by activating the vascular endothelium. Overall, the early phase (days 1 to 3) of the secondary immune response within the peritoneum was dominated by type 1 cytokines, namely TNF-α, IL-12, and IFN-γ (Fig. 4.10). These pro-inflammatory molecules were involved in inducing the activation and maturation of tumour-reactive CTL. In contrast, during the late phase (days 4 to 12) of the immune response, type 2 as well as inhibitory cytokines were dominating, as illustrated for IL-4, IL-5, and IL-10, with IL-2 acting as a growth factor for Th2 type cells.

The secretion kinetics for IL-4 and IFN-γ correlated well, considering that these cytokines reciprocally inhibit each other's production, as well as the activation of the respective secreting cell populations. At time points when one was highly expressed the other was suppressed and *vice versa*.

Polyclonal T-cell responses were found in both $CD4^+$ and $CD8^+$ T-cell compartments, although the $CD8^+$ T-cell pool appeared to use a more restricted number of Vβ-chains (Fig. 4.11). Overall, the TCR-Vβ chain repertoire appeared rather similar to that of iPEC from animals challenged with an ESbL-Gal unrelated, β-gal negative tumour (P815). Whether specific Vβ-chains are better suited to recognise the immunodominant peptide of β-gal (aa 876-884, TPHPARIGL) than others and whether such T-cells preferentially accumulate during the memory phase remains to be elucidated.

5.5 ADI model in syngeneic nude mice

Athymic nude mice were chosen as recipients for the adoptive transfer of Ag-specific cells (Fig. 4.12) in order to be able to monitor the fate of tumour-reactive T-cells in an otherwise T-cell deficient environment. In this context it was of importance to use ADI recipients (Balb/c nu/nu mice: $H\text{-}2^d$) that were MHC compatible to the immune cell donors (DBA/2 mice: $H\text{-}2^d$) in order to obtain an optimal therapy outcome and long-term survivors in which long-term T-cell memory could be studied. Use of unmatched recipients (CD1 Swiss nu/nu: outbred) resulted in outgrowth of hepatic metastases and premature death of the animals (Fig. 4.16).

However, a characteristic mosaic-like pattern of metastases was observed in the livers of CD1 Swiss nu/nu mice 14 days post immune cell transfer (= 15 days after tumour inoculation). In the DBA/2 model, this mosaic-like pattern was exclusively detected at very late stages of the disease, with tumour cells preferentially localising to periportal regions of liver lobuli. Perivenous areas hosted only a low metastatic load (Krüger et al. 1994b). ESbL-Gal were demonstrated to have a 3-phasic growth characterised by an initial growth phase (d0 to d9), a plateau phase (d9 to d20), and a secondary expansion phase (d20 to d30) as determined by measurement of the tumour diameter after i.d. inoculation into DBA/2 mice (Krüger et al. 1994b). This might explain the present results of liver metastases (Fig. 4.16 B), where d12 (no visible metastatic expansion) would lie within the plateau phase of tumour growth. In the present model where tumour cells are applied intravenously, allowing for a rapid systemic spread, the secondary expansion phase appears to commence earlier than in the DBA/2 system, with the mosaic-like pattern of metastases appearing already on d15.

As an effect of HvG should be negligible in nude host mice, it is possible that GvH reactions are at least partially responsible for the diminished therapeutic efficiency (Fig. 4.16 B) and premature death (Fig. 4.16 A) of tumour-bearing ADI-recipients obtained when using CD1 Swiss nu/nu mice. Another reason could be that host APC are required for an optimal therapeutic outcome as demonstrated in an allogeneic immunotransfer system, where Sn^+ liver macrophages were shown to form tight clusters with donor $CD4^+$ and $CD8^+$ T-cells. Kupffer cell depletion by chlodronate-treatment resulted in loss of the therapeutic effect (Müerköster et al. 1999). Such interactions of host APC with donor T-cells requires donors and recipients to express identical MHC molecules.

Best therapeutic effect of ESbL-Gal tumour-bearing Balb/c nu/nu mice was achieved when adoptive transfer of ESbL-Gal reactive d3 iPEC was combined with a whole-body irradiation regimen

administered one day before tumour-inoculation and two days before ADI (Fig. 4.13). Although cellular treatment alone was sufficient to prevent macroscopically visible metastases in internal organs (liver and spleen, Fig. 4.15 A) as visualised by X-gal staining, tumour nodules were able to grow at peripheral sites (Fig. 4.15 B). In contrast, ADI in combination with pre-irradiation of the animals prevented tumour outgrowth at both internal and peripheral locations.
Here, the most important effect of pre-irradiating the ADI-recipients was probably the damage to vascular endothelial cells, as this improves the extravasation of immune cells, thus enabling their rapid migration and distribution throughout the body. Feurgard and colleagues (1999) found that ionising radiation alters the hepatic cholesterol metabolism and plasma lipoproteins. They suggested that lipoprotein modifications could result from an induced inflammatory state and may further contribute to vascular damage.

$CD4^+$ T-cells act as mediators of anti-tumour immunity, producing cytokines that induce the accumulation and activation of accessory cells such as tumoricidal macrophages, as well as the differentiation of NK-cells into lymphokine activated killer cells (LAK-cells) (Cohen et al. 2000). They can also activate DCs, enhancing their ability to stimulate naïve $CD8^+$ cytotoxic T-cells (Ridge et al. 1998). This explains why $CD4^+$ cell depletion of d3 iPEC prior to ADI reduced survival but did not have as severe effects as $CD8^+$ cell depletion, $CD4^+$ T-cells being mainly required during the initiation phase of both the primary (Schild et al. 1987) and secondary (Schirrmacher et al. 1994c) immune responses, in this case after ear pinna priming, as well as after restimulation of DBA/2 mice in the peritoneum (Fig. 4.17). $CD8^+$ T-cells, on the other hand, function during the effector phase after transfer to the ESbL-Gal-bearing Balb/c nu/nu. In the CD8 negative ADI group, the prolonged survival, as compared to untreated controls, was presumably due to eosinophils and the production of oxygen radicals, namely nitric oxide and superoxide, by tumoricidal macrophages, activated by $CD4^+$ T-cell secreted IFN-γ (Toes et al. 1999).

5.6 Characteristics of memory T-cells

The ADI model presented in this thesis is highly efficient in providing long-term survival of tumour-bearing nude mice (over 1 year), thus representing optimal conditions for the study of long-term memory T-cells *in vivo* and *ex vivo*.
High dose tumour challenge (by i.v. injection of 5×10^7 live tumour cells) of such long-term survivors (2 months) resulted in 33 % decreased survival over a time period of 5.3 months compared to untreated control mice from the same ADI experiment (Fig. 4.18), and in 66 % mortality if the challenge was preceded by whole-body irradiation (Fig. 4.19). Although the difference in survival rates did not prove statistically significant, it was reproducible. This could point towards the increasingly accepted view that there exist two distinct subsets of memory T-cells with different homing potentials and effector functions (Bell et al. 1998, Mackay 1999, Sallusto et al. 1999), one subset resembling activated effector cells ("memory primed") while the other being more similar to naïve T-cells ("memory revertant"), with the exception of an elevated precursor frequency (see Table 1.2 of the introduction). If this is so, it is conceivable that the effector-like memory T-cells

are radio-resistant, while the naïve-like memory T-cells, similar to naïve cells, are radio-sensitive, as it is known that naïve T-cells are radio-sensitive while activated T-cells are not (Schirrmacher et al. 1994a, Igietseme et al. 1995). I am not aware of any publications on the radio-sensitivity of the different memory T-cell pools.

In the case of whole-body irradiation prior to tumour challenge (Fig. 4.19 gr. II) the memory T-cell pool would then be depleted of the naïve-like memory cells, thus accounting for the slightly reduced survival as compared to the non-irradiated group (Fig. 4.19 gr. I).

Overall, immunological memory against ESbL-Gal proved to be long-lived and the immune cells could be demonstrated to retain their tumour reactivity, as ESbL-Gal inoculated Balb/c nu/nu mice having received standard therapy could reject a high dose tumour challenge of 5×10^7 cells with 66 % efficiency (over a time course of 5.3 months).

5.7 Recruitment of memory T-cells for multiple ADI transfers

ESbL-Gal specific memory T-cells retained their tumour reactivity for long periods of time, as mPEC isolated from tumour bearing Balb/c nu/nu mice having been treated according to the standard ADI protocol 3.7 months earlier could transfer tumour protection to secondary tumour-bearing Balb/c nu/nu hosts (Fig. 4.20). As the naïve peritoneal cavity contains only few $CD8^+$ T-cells (0.5 %, see 4.3.1), most T-cells obtained by the present method of peritoneal antigenic challenge of tumour immune animals will be primed with the Ag of choice, although some irrelevant T-cells will also be attracted due to bystander effects. Thus, when using Balb/c nu/nu mice as hosts for the monitoring of memory T-cells, the majority of T-cells present in the hosts should be Ag-primed, originating from anti-ESbL-Gal immunised DBA/2 mice. Nevertheless, in sites like the bone marrow, memory T-cells will represent only a very small percentage of total cells (of total bone marrow cells only ~2 % are T-cells), which means that laborious procedures would have to be applied in order to harvest even a few memory T-cells. The present protocol of T-cell reactivation in the peritoneal cavity allows for the enrichment of Ag-reactive T-cells as well as their recruitment to a site from where isolation is uncomplicated. The recent stimulation will result in the activation and expansion of Ag-specific cells, thus increasing their numbers. This activation also means, though, that this method is inappropriate for the isolation of cells in the memory state. If interested in analysing features of *ex vivo* memory T-cells, one would have to segregate these from the large number of irrelevant cells, e.g. from the bone marrow.

Advantage	Disadvantage
recruitment and enrichment of memory cells	memory cells are activated, i.e. isolated in an effector phase

Table 5.1 Advantage and disadvantage of isolating memory cells by antigenic stimulation in the peritoneal cavity.

It is known that normal somatic cells are unable to divide indefinitely and will die after a certain number of divisions. Telomeres are required for complete replication. They prevent chromosome loss during cell division. Nevertheless, telomere length decreases with every cell division. This eventually leads to truncated chromosome ends, to chromosome ends binding to each other, and to chromosome loss (Harley et al. 1995, Artandi et al. 2000).

Telomere length analysis thus allows the estimation of the number of cell divisions a cell has experienced. This tool could be exploited to monitor cell division rates of memory cells over a given time course. Unfortunately, detection of changes in telomere length is rather difficult in inbred mouse strains, as they have extremely long TRF (Prowse et al. 1995). *Mus musculus* species have unusually long telomeres among mice (>30 kb; wild-derived species *Mus spretus*: <25 kb (Prowse et al. 1995); humans: 5-15 kb (Rhyu et al. 1995)), and TRF length in a given murine tissue can differ between individuals of the same age (Kipling 1990, Prowse et al. 1995). Furthermore, inbred mice were shown to have sequences with homology to telomeric repeats at intra-chromosomal sites, making telomere analysis of murine tissues extremely problematic (Lansdorp 1995).

For this reason, longevity of memory T-cells had to be evaluated by an alternative approach. To this end, the tumour specific T-cells were recruited to the peritoneum as described and tested indirectly for their capacity to expand before exhaustion and loss of function in a multiple transfer experiment. The cells were transferred from one group of ESbL-Gal tumour bearing nude mice to the next, leaving them to "rest" for at least one month in every host. At every transfer, the cells could prevent premature death of the host animals and mPEC isolated from the tertiary host were shown to be as efficient as iPEC from DBA/2 mice in prolonging the survival of ESbL-Gal inoculated Balb/c nu/nu mice (Fig. 4.21).

Nevertheless, the number of tumour reactive cells appeared to decrease with every transfer. While the donor : recipient ratio from the 1° to 2° host was 1.1 : 1, for the 2° to 3° host transfer it was 3.8 : 1 (half the number of cells were transferred to half the number of mice), and for the 3° to 4° host transfer it was 3:1 (Table 4.2). This is probably a result of elimination of a memory T-cell fraction following over-stimulation, which results in prolonged proliferation and terminal differentiation of Ag-specific T-cells, and ultimately in their apoptosis (Sprent et al. 2001).

The memory T-cells produced in DBA/2 mice by ear pinna immunisation and intraperitoneal challenge with ESbL-Gal tumour cells were thus long-lived and retained their reactivity over a long period of time (8 months, including four T-cell expansion phases following i.p. challenge of the respective hosts). Repeated antigenic stimulation probably resulted in a reduction of the memory T-cell pool. This is consistent with data from other groups indicating that persistent antigenic stimulation results in terminal differentiation and exhaustion of the reactive T-cell population (Moskophidis et al. 1993).

5.8 Bone marrow is a central compartment for memory T-cells

It has previously been found that the frequency of $CD4^+$ T-cells with an activated or memory phenotype is four- to fivefold higher in the bone marrow as compared to the peripheral lymphatics

This is not only true for immunised mice, but also for untreated, conventionally housed animals, that are in contact with environmental Ags (Price et al. 1999), which gives one more reason to work with an immunotransfer system to T-cell deficient nude mice for the phenotypical analysis of memory T-cells. Like this, all T-cells present in the host with a memory phenotype will have developed in response to the Ag of choice and not due to unrelated, environmental stimuli.

So far, it could not be demonstrated in which organ(s) $CD8^+$ memory T-cells survive until reactivation, although it has been published that they occur at higher frequencies in the bone marrow as compared to peripheral blood, and that the bone marrow resident Ag-specific T-cells were superior to their blood circulating counterparts in Ag-specific cytotoxicity, cytokine production, and *in vivo* therapeutic potential (Feuerer et al. 2001). In the case of the present ADI model system, memory T-cells were known to be present in the bm, but it was not clear whether this is the only "memory compartment".

Using peptide/MHC class I tetrameric complexes it could now be demonstrated that the bone marrow is not the only, but by far the major, compartment for $CD8^+$ memory T-cells. The frequency of β-$gal^{876-884}$ specific cells within the $CD8^+$ T-cell pool in this organ was 7.7 x higher than in the spleen and 37.6 x higher than in the lymph nodes. A fraction of tetramer-binding cells were also detected in the blood, "patrolling" the circulation for β-gal^+ cells.

It is not known what makes the bone marrow microenvironment so attractive for memory CTLs, but the unique structural organisation could play a part. A fine network of arterioles and sinuses provides an optimal blood supply. The bone marrow stroma also produces vital growth factors, and stromal cell derived type I IFNs have been implicated in the long-term maintenance of memory T-cells (Akbar et al. 2000).

It would now be instructive to try *in situ* tetramer stainings of bone marrow plugs in order to determine which cells tetramer-binding cells interact with and whether they preferentially locate to defined sites within this organ. This would give further insights into the mechanisms and factors involved in the preferential localisation of memory T-cells to this anatomical site. An *in situ* tetramer (IST) staining technique has recently been set up, using spleens from TCR-transgenic mice. TCR-transgenic T-cells could also be detected in spleen sections after adoptive transfer to non-transgenic animals, and sensitivity of IST proved to be comparable to flow cytometry (Skinner et al. 2000).

5.9 The role of Ag-persistence in the maintenance of long-term memory T-cells

It has previously been found that $CD4^+$ and $CD8^+$ T-cell memory can persist in the absence of Ag, as well as in the absence of MHC (Goldrath et al. 1999), but most of the work has been done in viral systems where low level Ag may persist in specialised depots, as for example in follicular dendritic cells. In the present tumour model, the presence or absence of Ag does make a difference for long-term survival of $CD8^+$ memory T-cells. In a "parking experiment", tetramer-staining revealed the disappearance of β-$gal^{876-884}$ specific $CD8^+$ T-cells in bone marrow, spleen, lymph nodes and blood in the absence of Ag.

Many memory $CD8^+$ T-cells specific to one pathogen may disappear after infection with subsequent pathogens (Varga et al. 2001). One explanation for this phenomenon might be the fact that $CD8^+$ T-cells proliferate vigorously upon Ag-stimulation. This poses a high selective pressure on them once the infection has been cleared, as there will be a competition for space in the respective memory T-cell compartment which is controlled by homeostatic mechanisms. Recently activated memory cells may displace older ones from their protective niches. Even those memory T-cells that may have been rescued from apoptosis by stromal cell derived type I IFNs will slowly be replaced, or at least decimated, owing to competition with other, more recently activated, T-cells for survival factors (Akbar et al. 2000).

Homeostatic regulation limits the expansion of the T-cell pools as well as the size of lymphoid organs. Therefore, the memory T-cell pool increases only moderately in size with age. As a consequence, the $CD8^+$ T-cell memory pool would quickly fill to capacity if CTL memory for each pathogen that a host experiences were preserved at a similar frequency.

Antigenic stimulation of the memory T-cell pool will induce proliferation of specific T-cells, boosting the Ag-specific memory T-cell pool at the cost of other memory T-cells. It could be possible that low level Ag-persistence may ensure survival of respective memory cells, even if the dose were not sufficient for triggering proliferation and/or differentiation to effector cells. This might explain the great difference in the frequency of $\beta\text{-gal}^{876\text{-}884}$ specific $CD8^+$ memory T-cells in the presence (26.3 % in the BM) or absence of Ag (0.4 % in the BM). As mentioned in 4.3.2, the ESb derived tumour Ags expressed by ESbL-Gal are only weakly immunogenic. In contrast, the introduced β-gal is highly immunogenic, with TPHPARIGL (aa 876-884) being its immunodominant peptide. This might confer clonal dominance to $\beta\text{-gal}^{876\text{-}884}$ specific $CD8^+$ memory T-cells through Ag-driven selection. It is then conceivable, that such clonal dominance is lost following Ag-removal.

Although it has been published that memory T-cell survival is independent of TCR-signals and that these cells can persist over extended periods of time in the absence of Ag, it could be demonstrated that, following Ag-removal, the memory T-cell pool decreases in size, often falling below detection levels for tetramer staining. Nevertheless, Ag-specific T-cell numbers were found to increase again rapidly after rechallenge with Ag (Faint et al. 2001).

Whether in the present "parking experiment" the absence of Ag also resulted in the loss of Ag-reactivity or only in a drastic reduction in Ag-specific cells remains to be tested.

5.10 DNA-vaccination

Under the conditions used in the present study, a systemic β-gal specific T-cell response could be measured following dual ear pinna injection of pCMVβ DNA. Injection of a cell lysate from the β-gal positive ESbL-Gal tumour line into the contralateral ear pinna resulted in the induction of a weak DTH-response (Fig. 4.23). Stronger DTH-responses were obtained in animals having received cellular vaccination, which might indicate that the immune response induced by DNA-vaccination either develops more slowly or occurs at a more local level than immune responses following tumour cell inoculation. It is known that tumour cells disseminate rapidly to lymph nodes, spleen,

and possibly also to other organs after i.e. injection (Schirrmacher et al. 1997), which could allow for a systemic activation of tumour reactive immune cells (see also 4.2). Stimulation with pCMVβ, on the other hand, results in the uptake and expression of β-gal at the site of injection (Förg et al. 1998), thus generating a more local immune response, which could play a role in the development of weaker DTH-responses after Ag-stimulation at a location distant from the priming site.
The more elevated DTH-responses observed in ESbL-Gal primed mice as compared to DNA-vaccinated animals could also be due to the fact that in the former case, the priming and DTH stimuli contained more than one Ag in common, namely the Esb-derived TAA and β-gal, while in the latter situation there was only one Ag in common (β-gal).

Förg and colleagues were able to produce β-gal specific CTL by pCMVβ inoculation i.e. followed by a 5 day co-culture of splenocytes, isolated 9 days post DNA-vaccination, together with the H2-L^d restricted β-gal peptide TPHPARIGL (Förg et al. 1998). pCMVβ vaccination also resulted in the induction of a protective anti-tumour immunity, causing rejection of subsequently s.c. injected *lacZ*$^+$ tumours (Schirrmacher et al. 2000).
Here, β-gal reactive iPEC could be produced following ear pinna DNA-vaccination with pCMVβ by an intraperitoneal challenge with P815-Gal tumour cells. Such iPEC specifically lysed the β-gal positive tumour cell lines ESbL-Gal and P815-Gal (Fig. 4.25). iPEC isolated from pCMVβ primed and ESbL-Gal restimulated DBA/2 mice contained only few $CD8^+$ T-cells (Fig. 4.24, 4.4 %) compared to iPEC from ESbL-Gal primed and restimulated animals (18.9 %), which might account for the comparably lower cytotoxic activity of iPEC for DNA-vaccinated mice.
Nevertheless, such iPEC were able to significantly prolong the survival of ESbL-Gal inoculated Balb/c nu/nu after adoptive transfer (Fig. 4.26). Preliminary results indicated that DNA-vaccination (no Ag-persistence) is not sufficient for the maintenance of long-term surviving (6 months) memory CTL as determined by cytotoxicity of iPEC isolated after Ag-specific challenge (Fig. 4.27). This could indicate either that, at least in this system, maintenance of memory T-cells does require the persistence of Ag, or that the β-gal specific memory T-cells were displaced by other, more recently activated (by environmental stimuli), memory T-cells. Although studies have been published on the generation of B-cell memory (He et al. 2001), I am not aware of any publications on the induction of long-term T-cell memory following DNA-vaccination.

Conclusion

In this thesis, a novel model system for the study of anti-tumour T-cell memory was introduced, comprising an adoptive transfer of tumour reactive immune cells, including effector cells and APCs, to pre-irradiated, tumour-bearing, T-cell deficient hosts. The immune cell mixture used for the adoptive transfer was produced by injection of a subtumorigenic dose of the highly aggressive, β-gal transduced T-lymphoma ESbL-Gal into the ear pinna of syngeneic immunocompetent DBA/2 mice, followed by an intraperitoneal challenge with irradiation-inactivated tumour cells. This resulted in the recruitment of Ag-specific $CD8^+$ T-cells into the peritoneal cavity, most probably from the spleen and bone marrow, as revealed by peptide/MHC class I tetramer staining. The i.p. challenge caused a pro-inflammatory environment in the peritoneum which, during the early phases, was dominated by the type I cytokines TNF-α, IL-12, and IFN-γ. Production of the T-cell growth factor IL-2 occurred at later time points and appeared to be involved in the expansion of Th2 type cells which secreted the type 2 and inhibitory cytokines IL-4, IL-5, and IL-10. These seemed to played a role in the general down-regulation of the intraperitoneal immune response.

Three days after the challenge with ESbL-Gal, the number of immune cells in the peritoneal cavity had multiplied 5.3-fold, and contained increased numbers of T-cells. Most markedly, $CD8^+$ T-cells now represented 11.2 % of total iPEC (naïve PEC: 0.5 %), 33.9 % of which specifically recognised the immunodominant peptide of β-gal, as demonstrated by peptide/MHC tetramer staining. Consistently, $CD8^+$ CTL mediated cytotoxicity was directed against β-gal, and no specific lysis was detected against the ESb derived TAA. The TCR-Vβ repertoire of both $CD4^+$ and $CD8^+$ iPEC T-cells was polyclonal, although it appeared more restricted than that of iPEC generated against the unrelated DBA/2 derived mastocytoma P815. Whether this indicates that some TCR-Vβ chains are better suited for the recognition of β-gal derived peptides, and that, because of the high frequency of $CD8^+$ T-cells reactive to a single β-gal derived peptide, are thus enriched, remains to be investigated.

The immunisation protocol used could thus be shown to yield tumour-reactive $CD8^+$ CTL exerting a highly specific β-gal directed cytotoxicity. It would now be interesting to investigate which factors (chemokines) are involved in the recruitment of such Ag-specific CTL to the peritoneal cavity in response to the secondary i.p. stimulus.

Upon transfer to pre-irradiated, tumour-bearing, MHC-compatible Balb/c nu/nu mice, ESbL-Gal reactive iPEC conferred tumour protection and long-term survival. Pre-irradiation of the recipients proved to be a prerequisite for the prevention of metastases formation both in internal organs and at peripheral sites. A critical involvement of both $CD4^+$ and $CD8^+$ T-cells for optimal therapeutic success could be demonstrated.

Even after successful therapy, dormant tumour cells persist for extended periods of time in the host. Analyses of reisolated tumour cells both from solid tumour nodules and from bone marrow resident dormant tumour cells demonstrated that β-gal expression by ESbL-Gal was stable *in vivo*. Comparison of the parental ESbL-Gal with the bone marrow derived ESbL-Gal-BM variant revealed that, in contrast to its parental cell line, the latter possesses a rather naked cell surface concerning the expression of leukocyte lineage markers and adhesion molecules. Interestingly, H-2D^d (MHC class I), ICAM-1 and the β_7-integrin chain where found to be upregulated, with high expression levels of the former two molecules. This might explain the apparent contradiction between high sensitivity to iPEC mediated cytotoxicity *in vitro* and *in situ* co-existence with tumour-reactive memory CTLs in the bone marrow microenvironment. The adhesion molecule ICAM-1 and the β_7-integrin chain might also be involved in the retention of dormant tumour cells at this unique anatomical site. It would be interesting to further exploit this model system in order to elucidate the factors involved in tumour dormancy.

Following ADI, anti-tumour immunological memory proved to be long-lived and, at least partially, radiation-resistant. Memory T-cells could be demonstrated to retain their Ag-reactivity as well as their potential of exerting tumour protection in a multiple transfer study. The bone marrow could be identified as the major compartment for the long-term survival of Ag-specific memory T-cells, the frequency of tetramer-binding cells within the CD8$^+$ pool being much more elevated at this anatomical site as compared to the spleen and lymph nodes. However, a 'parking experiment' revealed that Ag-persistence in the form of dormant tumour cells appeared to be required for the maintenance of Ag-specific memory T-cell numbers. These data were supported by preliminary findings that DNA-vaccination (no Ag-persistence) does not result in the long-term persistence of CTL memory.

Analysis of bone marrow plugs from long-term survivors using the novel IST staining technique (Skinner et al. 2000) would be very instructive, as this promises to give insights into the cell-cell interactions and precise localisation of memory T-cells within the bone marrow microenvironment. Moreover, investigation of chemokine receptor expression on memory T-cells could further indicate why these cells appear to be predominantly attracted to this anatomical site.

Recently, type I IFNs have been proposed to be of central importance in the long-term maintenance of memory T-cells, as they could be demonstrated to prevent apoptosis of activated T-cells without simultaneously inducing their proliferation (Akbar et al. 2000). In collaboration with Dr. R. Zawatzky, type I IFN-receptor knockout mice are currently being backcrossed onto the DBA/2 background. This will provide a valuable research tool for determining the involvement of type I IFNs in T-cell memory directly *in vivo*. The use of ESbL-Gal reactive iPEC generated in such mice for the ADI transfer system presented in this thesis should reveal to what extent type I IFNs are responsible for the long-term survival of Ag-specific CTL and whether alternative mechanisms can also provide the necessary survival signals.

References

Abo T (2001) Extrathymic pathways of T-cell differentiation and immunomodulation. *Int. Immunopharmacol.* **1**: 1261-1273

Abu hadid MM, Fuji H, Hsu S, and Sood AK (1996) A one step PCR procedure for analysis of tumor specific T lymphocyte responses. *J. Immunol. Methods* **190**: 91-105

Ahmed R, and Gray D (1996) Immunological memory and protective immunity: understanding their relation. *Science* **272**: 54-60

Akbar AN, Lord JM, and Salmon M (2000) IFN-alpha and IFN-beta: a link between immune memory and chronic inflammation. *Immunol. Today* **21**: 337-342

Akbar AN, and Salmon M (1997) Cellular environments and apoptosis: tissue microenvironments control activated T-cell death. *Immunol. Today* **18**: 72-76

Akbari O, Panjwani N, Garcia S, Tascon R, Lowrie D, and Stockinger B (1999) DNA vaccination: transfection and activation of dendritic cells as key events for immunity. *J. Exp. Med.* **189**: 169-178

Akira S, Takeda K, and Kaisho T (2001) Toll-like receptors: critical proteins linking innate and acquired immunity. *Nat. Immunol.* **2**: 675-680

Alimonti J, Zhang QJ, Gabathuler R, Reid G, Chen SS, and Jefferies WA (2000) TAP expression provides a general method for improving the recognition of malignant cells in vivo. *Nat. Biotechnol.* **18**: 515-520

Altman JD, and Safrit JT (2000). MHC Tetramer Analysis of CD8+ T-cell responses to HIV and SIV.,HIV Molecular Immunology Database, http://hiv-lanl.gov/REVIEWS/articles/safrit.html

Artandi SE, and DePinho RA (2000) Mice without telomerase: what can they teach us about human cancer? *Nat. Med.* **6**: 852-855

Bachmann MF, Barner M, Viola A, and Kopf M (1999) Distinct kinetics of cytokine production and cytolysis in effector and memory T cells after viral infection. *Eur. J. Immunol.* **29**: 291-299

Barth RK, Kim BS, Lan NC, Hunkapiller T, Sobieck N, Winoto A, Gershenfeld H, Okada C, Hansburg D, Weissman IL, and Hood L (1985) The murine T-cell receptor uses a limited repertoire of expressed V beta gene segments. *Nature* **316**: 517-523

Behlke MA, Chou HS, Huppi K, and Loh DY (1986) Murine T-cell receptor mutants with deletions of beta-chain variable region genes. *Proc. Natl. Acad. Sci. U. S. A.* **83**: 767-571

Behlke MA, Spinella DG, Chou HS, Sha W, Hartl DL, and Loh DY (1985) T-cell receptor beta-chain expression: dependence on relatively few variable region genes. *Science* **229**: 566-570

Bell EB, Sparshott SM, and Bunce C (1998) CD4+ T-cell memory, CD45R subsets and the persistence of antigen--a unifying concept. *Immunol. Today* **19**: 60-64

Benner R, Hijmans W, and Haaijman JJ (1981) The bone marrow: the major source of serum immunoglobulins, but still a neglected site of antibody formation. *Clin. Exp. Immunol.* **46**: 1-8

Beverley PC (1990) Is T-cell memory maintained by crossreactive stimulation? *Immunol. Today* **11**: 203-205

Bosslet K, and Schirrmacher V (1982) High-frequency generation of new immunoresistant tumor variants during metastasis of a cloned murine tumor line (ESb). *Int. J. Cancer* **29**: 195-202

Bosslet K, Schirrmacher V, and Shantz G (1979) Tumor metastases and cell-mediated immunity in a model system in DBA/2 mice. VI. Similar specificity patterns of protective anti-tumor immunity in vivo and of cytolytic T cells in vitro. *Int. J. Cancer* **24**: 303-313

Brosterhus H, Brings S, Leyendeckers H, Manz RA, Miltenyi S, Radbruch A, Assenmacher M, and Schmitz J (1999) Enrichment and detection of live antigen-specific CD4(+) and CD8(+) T cells based on cytokine secretion. *Eur. J. Immunol.* **29**: 4053-4059

Bruno L, Kirberg J, and von Boehmer H (1995) On the cellular basis of immunological T-cell memory. *Immunity* **2**: 37-43

Carbone FR, and Bevan MJ (1990) Class I-restricted processing and presentation of exogenous cell-associated antigen in vivo. *J. Exp. Med.* **171**: 377-387

Carosella ED, Rouas-Freiss N, Paul P, and Dausset J (1999) HLA-G: a tolerance molecule from the major histocompatibility complex. *Immunol. Today* **20**: 60-62

Cella M, Sallusto F, and Lanzavecchia A (1997) Origin, maturation and antigen presenting function of dendritic cells. *Curr. Opin. Immunol.* **9**: 10-16

Chizzonite R, Gubler U, Magram J, and Stern AS (1998) *Cytokines* (Mire-Sluis AR, and Thorpe R Eds.) Academic Press, London. 183-203

Cho HJ, Takabayashi K, Cheng PM, Nguyen MD, Corr M, Tuck S, and Raz E (2000) Immunostimulatory DNA-based vaccines induce cytotoxic lymphocyte activity by a T-helper cell-independent mechanism. *Nat. Biotechnol.* **18**: 509-514

Chou HS, Anderson SJ, Louie MC, Godambe SA, Pozzi MR, Behlke MA, Huppi K, and Loh DY (1987) Tandem linkage and unusual RNA splicing of the T-cell receptor beta-chain variable-region genes. *Proc. Natl. Acad. Sci. U. S. A.* **84**: 1992-1996

Cohen PA, Peng L, Plautz GE, Kim JA, Weng DE, and Shu S (2000) CD4+ T cells in adoptive immunotherapy and the indirect mechanism of tumor rejection. *Crit. Rev Immunol.* **20**: 17-56

Costello RT, Gastaut JA, and Olive D (1999) What is the real role of CD40 in cancer immunotherapy? *Immunol. Today* **20**: 488-493

de Maeyer E, and de Maeyer-Guignard J (1998). *Cytokines* (Mire-Sluis, A. R. and Thorpe, R. Eds.) Academic Press, London. 391-400.

Döffinger R, Klein TC, Pepys MB, Casanova JL, and Kyewski BA (1997) The MHC class II-restricted T cell response of C57BL/6 mice to human C-reactive protein: homology to self and the selection of T cell epitopes and T cell receptors. *Mol. Immunol.* **34**: 115-124

Dong C, Juedes AE, Temann UA, Shresta S, Allison JP, Ruddle NH, and Flavell RA (2001) ICOS co-stimulatory receptor is essential for T-cell activation and function. *Nature* **409**: 97-101

Donskov F, Basse PH, and Hokland M (1996) Expression and function of LFA-1 on A-NK and T-LAK cells: role in tumor target killing and migration into tumor tissue. *Nat. Immun.* **15**: 134-146

Emoto M, Emoto Y, and Kaufmann SH (1996) Development of CD8 alpha/beta + TCR alpha beta intestinal intraepithelial lymphocytes in athymic nu/nu mice and participation in regional immune responses. *Immunology* **88**: 531-536

Emoto M, Emoto Y, and Kaufmann SH (1997) CD8 alphabeta+ TCR alphabeta(intermediate) lymphocytes expressing skewed TCRVbeta repertoire in the liver of aged athymic nu/nu mice. *J. Immunol.* **158**: 1041-1050

Faint JM, Annels NE, Curnow SJ, Shields P, Pilling D, Hislop AD, Wu L, Akbar AN, Buckley CD, Moss PA, Adams DH, Rickinson AB, and Salmon M (2001) Memory T cells constitute a subset of the human CD8(+)CD45RA(+) pool with distinct phenotypic and migratory characteristics. *J. Immunol.* **167**: 212-220

Feuerer M, Beckhove P, Bai L, Solomayer EF, Bastert G, Diel IJ, Pedain C, Oberniedermayr M, Schirrmacher V, and Umansky V(2001) Therapy of human tumors in NOD/SCID mice with patient-derived reactivated memory T cells from bone marrow. *Nat. Med.* **7**: 452-8.

Feuerer M, Beckhove P, Mahnke Y, Schwendemann J, Hommel M, Bai L, Kyewski B, Umansky V, and Schirrmacher V (2001) Bone marrow: a secondary lymphoid organ capable of antigen presentation and induction of T-cell responses., submitted

Feurgard C, Boehler N, Ferezou J, Serougne C, Aigueperse J, Gourmelon P, Lutton C, and Mathe D (1999) Ionizing radiation alters hepatic cholesterol metabolism and plasma lipoproteins in Syrian hamster. *Int. J. Radiat. Biol* **75**: 757-766

Finke J, Ferrone S, Frey A, Mufson A, and Ochoa A (1999) Where have all the T cells gone? Mechanisms of immune evasion by tumors. *Immunol. Today* **20**: 158-160

Förg P, von Hoegen P, Dalemans W, and Schirrmacher V (1998) Superiority of the ear pinna over muscle tissue as site for DNA vaccination. *Gene Ther.* **5**: 789-797

Gascoigne NR, Chien Y, Becker DM, Kavaler J, and Davis MM (1984) Genomic organization and sequence of T-cell receptor beta-chain constant- and joining-region genes. *Nature* **310**: 387-391

Gavin MA, Gilbert MJ, Riddell SR, Greenberg PD, and Bevan MJ (1993) Alkali hydrolysis of recombinant proteins allows for the rapid identification of class I MHC-restricted CTL epitopes. *J. Immunol.* **151**: 3971-3980

Goldrath AW, and Bevan MJ (1999) Selecting and maintaining a diverse T-cell repertoire. *Nature* **402**: 255-262

Gosslar U, Jonas P, Luz A, Lifka A, Naor D, Hamann A, and Holzmann B (1996) Predominant role of alpha 4-integrins for distinct steps of lymphoma metastasis. *Proc. Natl. Acad. Sci. U. S. A.* **93**: 4821-4826

Graf L, Koch N, and Schirrmacher V (1985) Expression of Ia antigens in a murine T-lymphoma variant. *Mol. Immunol.* **22**: 1371-1377

Gray D, and Matzinger P (1991) T cell memory is short-lived in the absence of antigen. *J. Exp. Med.* **174**: 969-974

Greenberg AW, Kerr WG, and Hammer DA (2000) Relationship between selectin-mediated rolling of hematopoietic stem and progenitor cells and progression in hematopoietic development. *Blood* **95**: 478-486

Harley CB, and Villeponteau B (1995) Telomeres and telomerase in aging and cancer. *Curr. Opin. Genet. Dev* **5**: 249-55.

He J, Hayes CG, Binn LN, Seriwatana J, Vaughn DW, Kuschner RA, and Innis BL (2001) Hepatitis E virus DNA vaccine elicits immunologic memory in mice. *J. Biomed. Sci.* **8**: 223-226

Hennecke J, Carfi A, and Wiley DC (2000) Structure of a covalently stabilised complex of a human alphabeta T-cell receptor, influenza HA peptide and MHC class II molecule, HLA-DR1. *EMBO J.* **19**: 5611-5624

Hodes RJ, and Abe R (1996) *Current Protocols in Immunology* (Coligan JE, Kruisbeek AM, Margulies DH, Shevach EM, and Strober W Eds.) John Wiley & Sons Inc. New York. A.1F.1-A.1F.5

Holzmann B (2001) Expression of CGRP-receptors on bone marrow derived dormant tumour cells but not on the parental T-lymphoma., personal communication

Hou S, Hyland L, Ryan KW, Portner A, and Doherty PC (1994) Virus-specific CD8+ T-cell memory determined by clonal burst size. *Nature* **369**: 652-654

Hung K, Hayashi R, Lafond-Walker A, Lowenstein C, Pardoll D, and Levitsky H (1998) The central role of CD4(+) T cells in the antitumor immune response. *J. Exp. Med.* **188**: 2357-2368

Igietseme JU, Smith K, Simmons A, and Rayford PL (1995) Effect of gamma-irradiation on the effector function of T lymphocytes in microbial control. *Int. J. Radiat. Biol* **67**: 557-564

Islam D, Wretlind B, Lindberg AA, and Christensson B (1996) Changes in the peripheral blood T-cell receptor V beta repertoire in vivo and in vitro during shigellosis. *Infect. Immun.* **64**: 1391-1399

Iwamoto A, Ohashi PS, Pircher H, Walker CL, Michalopoulos EE, Rupp F, Hengartner H, and Mak TW (1987) T cell receptor variable gene usage in a specific cytotoxic T cell response. Primary structure of the antigen-MHC receptor of four hapten-specific cytotoxic T cell clones. *J. Exp. Med.* **165**: 591-600

Janeway CA, and Travers P (1996) *Immunobiology - The immune system in health and disease*, 2nd edition edition. Current Biology Ltd. London

Jurianz K, von Hoegen P, and Schirrmacher V (1998) Superiority of the ear pinna over a subcutaneous tumour inoculation site for induction of a Th1-type cytokine response. *Cancer Immunol. Immunother.* **45**: 327-333

Kaech SM, and Ahmed R (2001) Memory CD8+ T cell differentiation: initial antigen encounter triggers a developmental program in naive cells. *Nat. Immunol.* **2**: 415-422

Kataoka Y, Iwasaki T, Kuroiwa T, Seto Y, Iwata N, Hashimoto N, Ogata A, Hamano T, and Kakishita E (2001) The role of donor T cells for target organ injuries in acute and chronic graft-versus-host disease. *Immunology* **103**: 310-318

Kell MR, Winter DC, O'Sullivan GC, Shanahan F, and Redmond HP (2000) Biological behaviour and clinical implications of micrometastasis. *Br. J. Surgery* **87**: 1629-1639

Kelsoe G (2000) Remembrance of things past. *Nat. Immunol.* **1**: 375-376

Khazaie K, Prifti S, Beckhove P, Griesbach A, Russell S, Collins M, and Schirrmacher V (1994) Persistence of dormant tumor cells in the bone marrow of tumor cell-vaccinated mice correlates with long-term immunological protection. *Proc. Natl. Acad. Sci. U. S. A.* **91**: 7430-7434

Kipling D, and Cooke HJ (1990) Hypervariable ultra-long telomeres in mice. *Nature* **347**: 400-402

Klein L, Klein T, Ruther U, and Kyewski B (1998) CD4 T cell tolerance to human C-reactive protein, an inducible serum protein, is mediated by medullary thymic epithelium. *J. Exp. Med.* **188**: 5-16

Kornacker M, Verneris MR, Kornacker B, Scheffold C, and Negrin RS (2001) Survivin expression correlates with apoptosis resistance after lymphocyte activation and is found preferentially in memory T cells. *Immunol. Lett.* **76**: 169-173

Krstic RV (1994) *Human Microscopic Anatomy* (AnonymousSpringer Verlag, Heidelberg

Kruger A, Umansky V, Rocha M, Hacker HJ, Schirrmacher V, and von Hoegen P (1994a) Pattern and load of spontaneous liver metastasis dependent on host immune status studied with a lacZ transduced lymphoma. *Blood* **84**: 3166-3174

Kruger A, Schirrmacher V, and von Hoegen P (1994b) Scattered micrometastases visualized at the single-cell level: detection and re-isolation of lacZ-labeled metastasized lymphoma cells. *Int. J. Cancer* **58**: 275-284

Lansdorp PM (1995) Telomere length and proliferation potential of hematopoietic stem cells. *J. Cell Sci.* **108**: 1-6

Larizza L, Schirrmacher V, and Pfluger E (1984) Acquisition of high metastatic capacity after in vitro fusion of a nonmetastatic tumor line with a bone marrow-derived macrophage. *J. Exp. Med.* **160**: 1579-1584

Lau LL, Jamieson BD, Somasundaram T, and Ahmed R (1994) Cytotoxic T-cell memory without antigen. *Nature* **369**: 648-652

Lefrancois L, Parker CM, Olson S, Muller W, Wagner N, Schon MP, and Puddington L (1999) The role of beta7 integrins in CD8 T cell trafficking during an antiviral immune response. *J. Exp. Med.* **189**: 1631-1638

Levesque JP, Zannettino AC, Pudney M, Niutta S, Haylock DN, Snapp KR, Kansas GS, Berndt MC, and Simmons PJ (1999) PSGL-1-mediated adhesion of human hematopoietic progenitors to P-selectin results in suppression of hematopoiesis. *Immunity.* **11**: 369-378

Lutz MB, Kukutsch N, Ogilvie AL, Rossner S, Koch F, Romani N, and Schuler G (1999) An advanced culture method for generating large quantities of highly pure dendritic cells from mouse bone marrow. *J. Immunol. Methods* **223**: 77-92

Mackay CR (1999) Dual personality of memory T cells. *Nature* **401**: 659-660

Male D (1994) *Immunology - an illustrated outline*, 2nd edition edition. Mosby, London.

Masellis-Smith A, Belch AR, Mant MJ, and Pilarski LM (1997) Adhesion of multiple myeloma peripheral blood B cells to bone marrow fibroblasts: a requirement for CD44 and alpha4beta7. *Cancer Res.* **57**: 930-936

Matsuzawa A, and Takeda Y (1996) *Premalignancy and tumor dormancy* (Yefenof, E. and Scheuermann, R. H. Eds.) Springer Verlag, Heidelberg. 89-103

Matter A, and Askonas BA (1976) Protection against murine ascites tumours by lymphoid cell populations with T memory or cytotoxicity. *Transplantation* **22**: 184-189

McMahan CJ, and Fink PJ (2000) Receptor revision in peripheral T cells creates a diverse V beta repertoire. *J. Immunol.* **165**: 6902-6907

Merkenschlager M, Power MO, Pircher H, and Fisher AG (1999) Intrathymic deletion of MHC class I-restricted cytotoxic T cell precursors by constitutive cross-presentation of exogenous antigen. *Eur. J. Immunol.* **29**: 1477-1486

Morahan G, Allison J, Peterson MG, and Malcolm L (1989) Sequence of the V beta 13 gene used by an influenza-specific T cell. *Immunogenetics* **30**: 311-313

Morecki S, and Slavin S (1996) *Premalignancy and tumor dormancy* (Yefenof E, and Scheuermann RH Eds.) Springer Verlag, Heidelberg. 137-146.

Moskophidis D, Lechner F, Pircher H, and Zinkernagel RM (1993) Virus persistence in acutely infected immunocompetent mice by exhaustion of antiviral cytotoxic effector T cells. *Nature* **362**: 758-761

Müerkoster S, Rocha M, Crocker PR, Schirrmacher V, and Umansky V (1999) Sialoadhesin-positive host macrophages play an essential role in graft-versus-leukemia reactivity in mice. *Blood* **93**: 4375-4386

Müllbacher A (1994) The long-term maintenance of cytotoxic T cell memory does not require persistence of antigen. *J. Exp. Med.* **179**: 317-321

Müller M, Gounari F, Prifti S, Hacker HJ, Schirrmacher V, and Khazaie K (1998) EblacZ tumor dormancy in bone marrow and lymph nodes: active control of proliferating tumor cells by CD8+ immune T cells. *Cancer Res.* **58**: 5439-5446

O'Connell J, Bennett MW, O'Sullivan GC, Collins JK, and Shanahan F (1999) The Fas counterattack: cancer as a site of immune privilege. *Immunol. Today* **20**: 46-52

Opferman JT, Ober BT, and Ashton-Rickardt PG (1999) Linear differentiation of cytotoxic effectors into memory T lymphocytes. *Science* **283**: 1745-1748

Opferman JT, Ober BT, Narayanan R, and Ashton-Rickardt PG (2001) Suicide induced by cytolytic activity controls the differentiation of memory CD8(+) T lymphocytes. *Int. Immunol.* **13**: 411-419

Osmond DG (1994) Production and selection of B lymphocytes in bone marrow: lymphostromal interactions and apoptosis in normal, mutant and transgenic mice. *Adv. Exp. Med. Biol* **355:** 15-20

Pannetier C, Cochet M, Darche S, Casrouge A, Zoller M, and Kourilsky P (1993) The sizes of the CDR3 hypervariable regions of the murine T-cell receptor beta chains vary as a function of the recombined germ-line segments. *Proc. Natl. Acad. Sci. U. S. A.* **90**: 4319-4323

Pardoll DM, and Topalian SL (1998) The role of CD4+ T cell responses in antitumor immunity. *Curr. Opin. Immunol.* **10**: 588-594

Pieters J (1997) MHC class II restricted antigen presentation. *Curr. Opin. Immunol.* **9**: 89-96

Pilling D, Akbar AN, Girdlestone J, Orteu CH, Borthwick NJ, Amft N, Scheel-Toellner D, Buckley CD, and Salmon M (1999) Interferon-beta mediates stromal cell rescue of T cells from apoptosis. *Eur. J. Immunol.* **29**: 1041-1050

Pisetsky DS (1996) Immune activation by bacterial DNA: a new genetic code. *Immunity.* **5**: 303-310

Pogany G, Timar F, Olah J, Harisi R, Polony G, Paku S, Bocsi J, Jeney A, and Laurie GW (2001) Role of the basement membrane in tumor cell dormancy and cytotoxic resistance. *Oncology* **60**: 274-281

Price PW, and Cerny J (1999) Characterization of CD4+ T cells in mouse bone marrow. I. Increased activated/memory phenotype and altered TCR Vbeta repertoire. *Eur. J. Immunol.* **29**: 1051-1056

Prowse KR, and Greider CW(1995) Developmental and tissue-specific regulation of mouse telomerase and telomere length. *Proc. Natl. Acad. Sci. U. S. A.* **92**: 4818-4822

Putz E, Witter K, Offner S, Stosiek P, Zippelius A, Johnson J, Zahn R, Riethmuller G, and Pantel K (1999) Phenotypic characteristics of cell lines derived from disseminated cancer cells in bone marrow of patients with solid epithelial tumors: establishment of working models for human micrometastases. *Cancer Res.* **59**: 241-248

Qin D, Wu J, Vora KA, Ravetch JV, Szakal AK, Manser T, and Tew JG (2000) Fc gamma receptor IIB on follicular dendritic cells regulates the B cell recall response. *J. Immunol.* **164**: 6268-6275

Reddehase MJ, Rothbard JB, and Koszinowski UH (1989) A pentapeptide as minimal antigenic determinant for MHC class I-restricted T lymphocytes. *Nature* **337**: 651-653

Rhyu MS (1995) Telomeres, telomerase, and immortality. *J. Natl. Cancer Inst.* **87**: 884-894

Richards CD (1998) *Cytokines* (Mire-Sluis, A. R. and Thorpe, R. Eds.) Academic Press, London. 88-108.

Ridge JP, Di Rosa F, and Matzinger P (1998) A conditioned dendritic cell can be a temporal bridge between a CD4+ T-helper and a T-killer cell. *Nature* **393**: 474-478

Rocha M, Krüger A, Umansky V, von Hoegen P, Naor D, and Schirrmacher V (1996) Dynamic expression changes in vivo of adhesion and costimulatory molecules determine load and pattern of lymphoma liver metastasis. *Clin. Cancer Res.* **2**: 811-820

Rocha M, Umansky V, Schirrmacher V, and Elices MJ (1997) *In situ* downregulation of VLA-4 integrin cell surface expression during lymphoma growth and liver metastasis. *Int. J. Oncol.* **10**: 457-464

Sallusto F, Lenig D, Forster R, Lipp M, and Lanzavecchia A (1999) Two subsets of memory T lymphocytes with distinct homing potentials and effector functions. *Nature* **401**: 708-712

Sanderson CJ, Karlen S, Cornelis S, Plaetinck G, Tavernier J, and Devos R (1998). *Cytokines* (Mire-Sluis, A. R. and Thorpe, R. Eds.) Academic Press, London. 69-85

Schild HJ, Kyewski B, von Hoegen P, and Schirrmacher V (1987) CD4+ helper T cells are required for resistance to a highly metastatic murine tumor. *Eur. J. Immunol.* **17**: 1863-1866

Schirrmacher V (1981) Immunogenetic studies on the resistance of mice to highly metastatic DBA/2 tumor cell variants. I. Effect of incompatibilities at H-2 or non-H-2 genes in normal and nude (nu/nu) mice. *Invasion Metastasis* **1**: 4-21

Schirrmacher V (1995) Biotherapy of cancer: Perspectives of immunotherapy and gene therapy. *J. Canc. Res. Clin. Oncol.* **121**: 443-451

Schirrmacher V (1995) Augmentation of protective immunotherapy against metastatic ESb lymphoma cells by combining immune cell transfer with host irradiation, antigen restimulation and/or anti-TNF? antibody treatment. *Int. J. Oncol.* **6**: 17-25

Schirrmacher V, Shantz G, Clauer K, Komitowski D, Zimmermann HP, and Lohmann-Matthes ML (1979) Tumor metastases and cell-mediated immunity in a model system in DBA/2 mice. I. Tumor invasiveness in vitro and metastasis formation in vivo. *Int. J. Cancer* **23**: 233-244

Schirrmacher V, Leidig S, and Griesbach A (1991) *In situ* activation of syngeneic tumour-specific cytotoxic T lymphocytes: intra-pinna immunization followed by restimulation in the peritoneal cavity. *Cancer Immunol. Immunother.* **33**: 299-306

Schirrmacher V, Schild HJ, Gueckel B, and von Hoegen P (1992) Tumor specific CTL response requiring interactions of four different cell types and dual recognition of MHC class I and class II restricted tumor antigens. *Immunol. Cell. Biol.* **71**: 311-326

Schirrmacher V, and von Hoegen P (1993) Importance of tumour cell membrane integrity and viability for cytotoxic T lymphocyte activation by cancer vaccines. *Vaccine Res.* **2**: 183-196

Schirrmacher V, and Zangemeister Wittke U (1994a) γ-irradiation suppresses T-cell mediated protective immunity against a metastatic tumor in the afferent phase of the immune response but enhances it in the efferent phase when given before immune cell transfer. *Int. J. Oncol.* **4**: 335-346

Schirrmacher V, Griesbach A, Umansky V, and Rocha M (1994b) Adoptive transfer of protective immunity against a high metastatic tumor cell variant by small numbers of tumor-specific *in situ* activated peritoneal effector T-cells. *Int. J. Oncol.* **5**: 141-151

Schirrmacher V, Griesbach A, and Zangemeister Wittke U (1994c) g-irradiated viable tumor cells as whole-cell vaccines can stimulate *in situ* syngeneic antitumor cytotoxic T-lymphocytes and delayed-type hypersensitivity reactivity whereas tumor cell lysates elicit only delayed-type hypersensitivity reactivity. *Vaccine Res.* **3**: 31-48

Schirrmacher V, Jurianz K, and Griesbach A (1997) Intra-pinna induction of specific antitumor immune T-cell functions: effect of ear resection after antigen application. *Int. J. Oncol.* **11**: 227-233

Schirrmacher V (1999) In situ analysis of tumor-specific CTL effector and memory responses elicited by tumor vaccination. *Int. J. Oncol.* **15**: 217-227

Schirrmacher V, Förg P, Dalemans W, Chlichlia K, Zeng Y, Fournier P, and von Hoegen P (2000) Nonviral Transfer Technology: Intra-pinna anti-tumour vaccination with self-replicating infectious RNA or with DNA encoding a model tumour antigen and a cytokine. *Gene Ther.* **7**: 1137-1147

Scott S, Pandolfi F, and Kurnick JT (1990) Fibroblasts mediate T cell survival: a proposed mechanism for retention of primed T cells. *J. Exp. Med.* **172**: 1873-1876

Seliger B, Maeurer MJ, and Ferrone S (2000) Antigen-processing machinery breakdown and tumor growth. *Immunol. Today* **21**: 455-464

Singer PA, McEvilly RJ, Noonan DJ, Dixon FJ, and Theofilopoulos AN (1986) Clonal diversity and T-cell receptor beta-chain variable gene expression in enlarged lymph nodes of MRL-lpr/lpr lupus mice. *Proc. Natl. Acad. Sci. U. S. A.* **83**: 7018-22.

Six A, Jouvin-Marche E, Loh DY, Cazenave PA, and Marche PN (1991) Identification of a T cell receptor beta chain variable region, V beta 20, that is differentially expressed in various strains of mice. *J. Exp. Med.* **174**: 1263-1266

Skinner PJ, Daniels MA, Schmidt CS, Jameson SC, and Haase AT (2000) Cutting edge: In situ tetramer staining of antigen-specific T cells in tissues. *J. Immunol.* **165**: 613-617

Sprent J, Tough DF, and Sun S (1997) Factors controlling the turnover of T memory cells. *Immunol. Rev* **156:79-85.** 79-85

Sprent J, and Tough DF (2001) T cell death and memory. *Science* **293**: 245-248

Surman DR, Dudley ME, Overwijk WW, and Restifo NP (2000) Cutting edge: CD4+ T cell control of CD8+ T cell reactivity to a model tumor antigen. *J. Immunol.* **164**: 562-565

Tanchot C, Lemonnier FA, Perarnau B, Freitas AA, and Rocha B (1997) Differential requirements for survival and proliferation of CD8 naive or memory T cells. *Science* **276**: 2057-2062

Tanchot C, and Rocha B (1998) The organization of mature T-cell pools. *Immunol. Today* **19**: 575-579

Toes RE, Ossendorp F, Offringa R, and Melief CJ (1999) CD4 T cells and their role in antitumor immune responses. *J. Exp. Med.* **189**: 753-756

Tokunaga K, Taniguchi H, Yoda K, Shimizu M, and Sakiyama S (1986) Nucleotide sequence of a full-length cDNA for mouse cytoskeletal beta-actin mRNA. *Nucleic. Acids. Res.* **14**: 2829-2835

Trinchieri G (1995) Interleukin-12: a proinflammatory cytokine with immunoregulatory functions that bridge innate resistance and antigen-specific adaptive immunity. *Annu. Rev. Immunol.* **13**: 251-276

Tripp RA, Topham DJ, Watson SR, and Doherty PC (1997) Bone marrow can function as a lymphoid organ during a primary immune response under conditions of disrupted lymphocyte trafficking. *J. Immunol.* **158**: 3716-3720

Varga SM, Selin LK, and Welsh RM (2001) Independent regulation of lymphocytic choriomeningitis virus-specific T cell memory pools: relative stability of CD4 memory under conditions of CD8 memory T cell loss. *J. Immunol.* **166**: 1554-1561

Veiga-Fernandes H, Walter U, Bourgeois C, McLean A, and Rocha B (2000) Response of naive and memory CD8+ T cells to antigen stimulation in vivo. *Nat. Immunol.* **1**: 47-53

Weber-Arden J, Wilbert OM, Kabelitz D, and Arden B (1996) Inverse PCR amplification of low-abundancy message of gamma delta T cell receptor genes. *J. Immunol. Methods* **197**: 187-192.

Zal T, Volkmann A, and Stockinger B (1994) Mechanisms of tolerance induction in major histocompatibility complex class II-restricted T cells specific for a blood-borne self-antigen. *J. Exp. Med.* **180**: 2089-2099

Zheng P, Sarma S, Guo Y, and Liu Y (1999) Two mechanisms for tumor evasion of preexisting cytotoxic T-cell responses: lessons from recurrent tumors. *Cancer Res.* **59**: 3461-3467

Zimmerman C, Brduscha-Riem K, Blaser C, Zinkernagel RM, and Pircher H (1996) Visualization, characterization, and turnover of CD8+ memory T cells in virus-infected hosts. *J. Exp. Med.* **183**: 1367-1375

Zitvogel L and Lotze MT (1995) Role of interleukin-12 (IL12) as an anti-tumour agent: experimental biology and clinical application. *Res. Immunol.* **146**: 628-638

Appendix

8.1 Abbreviations

aa	aminoacids
Ab, Abs	antibody, antibodies
ADI	adoptive immunotransfer
Ag, Ags	antigen, antigens
AICD	activation-induced cell death
AIP	apoptosis-inhibitory proteins
AP	alkaline phosphatase
APC	Ag presenting cell(s)
ATP	adenosine triphosphate
bp	base pairs
CCR7	chemokine receptor-7
CD..	cluster of differentiation
CD62L	L-selectin; leukocyte selectin
CD95L	CD95 ligand, Fas ligand
cDNA	complementary DNA; single-stranded
CTL	cytotoxic T-lymphocytes
DCs	dendritic cells
ddH_2O	double-distilled water
DEPC	diethyl pyrocarbonate
dH_2O	single-distilled water
DNA	deoxyribonucleic acid
ds cDNA	double-stranded cDNA
DTH	delayed-type hypersensitivity
E. coli	*Escherichia coli*
Eb 288	methyl-cholanthrene induced T-lymphoma of the DBA/2 mouse; L5178Y/E
ECM	extracellular matrix
ELISA	enzyme-linked immunosorbent assay
ELISPOT	enzyme-linked immunospot assay
ER	endoplasmatic reticulum
ESb 289	spontaneous, highly metastatic variant of Eb 288
ESb-L	more aggressive form of ESb 289, isolated from a liver metastasis
ESbL-Gal	bacterial *lacZ* gene transduced Esb-L subline (clone L-Cl.5s)
ESbL-Gal-BM	ESbL-Gal variant isolated from bone marrow resident dormant tumour cells
ESbL-Gal-ET	ESbL-Gal variant isolated from an ear tumour

ESbL-Gal-ST	ESbL-Gal variant isolated from a spleen tumour
ESbL-Gal-TT	ESbL-Gal variant isolated from a throat tumour
FACS	fluorescence-activated cell sorter
FasL	Fas ligand
FCM	fibroblast conditioned medium
Fc-R	Fc-receptor, binding Abs via their Fc-region
FDC	follicular dendritic cells
FDG	fluorescein-di-β-D-galactopyranoside
Fig.	figure
FITC	fluoroisothiocyanate
g	gravitational force; 9.8066 m/s^2
GvH	graft versus host reaction
GvHD	GvH disease
GvL	graft versus leukaemia reaction
Gy	Gray; unit of radioactive dosis; 1 Gy = 100 rad
HLA-...	human leukocyte Ags
HSPC	haematopoietic stem and progenitor cells
HvG	host versus graft reaction
ICAM-1	intracellular adhesion molecule-1
ICOS	inducible co-stimulatory molecule
ICs	Ag : Ab immune complexes
i.d.	intra-dermal injection
i.e.	intra-ear pinna injection
IFN-..	interferon
IL-..	interleukin
IL-2R	IL-2 receptor
i.p.	intra-peritoneal injection
iPCR	inverse PCR
iPEC	immune PEC
ISS	immunostimulatory DNA sequences
IST	*in situ* tetramer staining
i.v.	intra-venous injection
kb	kilobases
LAK	lymphokine-activated killer cells
LFA-1	lymphocyte function-associated Ag-1
LN	lymph nodes
L-selectin	leukocyte selectin; CD62L
mAb	monoclonal antibody/antibodies
MACS	magnet-activated cell sorting
MadCAM-1	mucosal addressin cell adhesion molecule-1
MCMV	murine cytomegalovirus

µCi	micro-Curie
MHC	major histocompatibility complex
MIICs	MHC class II compartments
MMTV	mouse mammary tumour virus
mPEC	memory PEC
mRNA	messenger RNA
N	normality, a measure for the concentration of solutions
NK-cells	natural killer cells
nm	nanometer
NMS	normal mouse serum
nPEC	naive PEC
o/n	overnight
OVA-FITC	FITC-conjugated ovalbumin
P815	methyl-cholanthrene induced mastocytoma of the DBA/2 mouse
P815-Gal	bacterial *lacZ* gene transduced subline of P815; commonly known as P13.1
p.a.	pro analysis
PBL	peripheral blood lymphocytes
PBS	phosphate buffered saline
pCMVβ	plasmid carrying the gene coding for β-galactosidase under the human cytomegalovirus (CMV) immediate early gene promoter
PCR	polymerase chain reaction
PE	see R-PE
PEC	peritoneal exudate cells
PHA	phytohemagglutinin
PI	propidium iodide
PKC-δ	protein kinase C-δ
P-selectin	platelet selectin; CD62P
PSGL-1	P-selectin glycoprotein ligand-1
rLN	regional lymph nodes
RNA	ribonucleic acid
RNase A	ribonuclease A
R-PE	R-phycoerythrin
rpm	rounds per minute
r/t	room temperature
RT-PCR	reverse transcriptase PCR; analysis of RNA expression by PCR after transcription to cDNA
s.c.	sub-cutaneous injection
SEM	standard error mean
Sn	sialoadhesin
SPF	specific pathogen free conditions for experimental animals
SV40	Simian Virus 40

TAA	tumour-associated Ag(s)
TCR	T-cell antigen receptor
TCR-Cβ	constant region of the TCR β-chain
TCR-Dβ	diversity region of the TCR β-chain
TCR-Jβ	joining region of the TCR β-chain
TCR-Vβ	variable region of the TCR β-chain
TGF-β	tumour growth factor-β
TLRs	Toll-like receptors
TMB	tetramethylbenzidine
TNF-α	tumour necrosis factor-α
TRF	telomere restriction fragment(s)
U	units
VCAM-1	vascular cell adhesion molecule-1
v/v	volume per volume
w/v	weight per volume

8.2 Testing of reagents of own production

8.2.1 pCMVβ digest

To test whether the pCMVβ plasmid isolated was intact, the DNA was digested using specific restriction endonucleases. The results are depicted in Fig. 8.1.

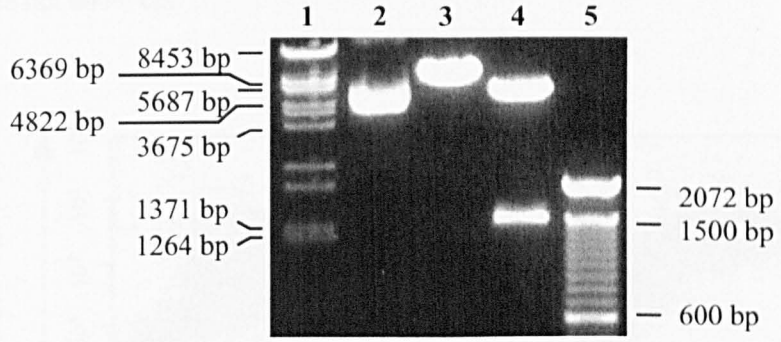

Fig. 8.1 pCMVβ digest with *Xho* I and *Eco* RV. pCMVβ plasmid DNA was left uncut (lane 2), linearised by *Xho* I digest (lane 3) or fragmented by an *Xho* I/*Eco* RV double-digest (lane 4). Lane 1 contains the λ DNA/*Eco* 91I (*Bst* EII) marker and lane 5 contains a 100 bp DNA ladder.

Supercoiled DNA runs faster through an agarose gel than does linearised DNA of the same size. This explains why the uncut pCMVβ plasmid (lane 2) had an apparent size of ~5 kb, while the linearised plasmid (lane 3) ran at the expected 7.2 kb. A double-digest with the restriction endonucleases *Xho* I and *Eco* RV yielded one fragment of 5.8 kb and one of 1.4 kb, indicating that the isolated plasmid DNA had not lost the *lacZ* insert and could therefore be used for experimental purposes.

8.2.2 Phenotype of and Ag-uptake by *in vitro* grown DCs

Myeloid DCs are specialised for the activation of naïve T-cells. Immature DCs are characterised by a high capability for Ag-capture and processing, but low T-cell stimulatory activity. As DCs mature, they express increasing numbers of MHC class II molecules on their surface, owing to reduced internalisation and increased biosynthesis (Cella et al. 1997). Such increased expression allows the loading of many antigenic peptides shortly after an inflammatory stimulus and can be visualised by a higher fluorescence intensity when staining with class II specific mAb. With maturation they also lose their capacity to internalise exogenous Ag, and become increasingly specialised in Ag-processing and -presentation (Lutz et al. 1999).

Lutz and colleagues expanded bone marrow derived DCs in medium supplemented with 10 % FCS. FCS is recognised as a non-self Ag by murine DCs, and is consequently internalised, processed

and presented in conjunction with MHC molecules on the cell surface of DCs. As this could affect the results of Ag-presentation assays, *in vitro* culture of DCs was carried out in the serum-free medium X-vivo 20. Fig 8.2 A demonstrates that this altered culture regimen yielded functional DCs which expressed the DC-marker CD11c, as well as intermediate levels of MHC class I and II, and the co-stimulatory molecules CD80 and CD86. The cultured DCs were able to phagocytose FITC-conjugated ovalbumin (OVA-FITC) at 37°C (Fig. 8.2 B). Incubation of DCs with OVA-FITC on ice also resulted in fluorescently labelled DCs, but in this situation the OVA adhered to the surface of DCs and was not taken up.

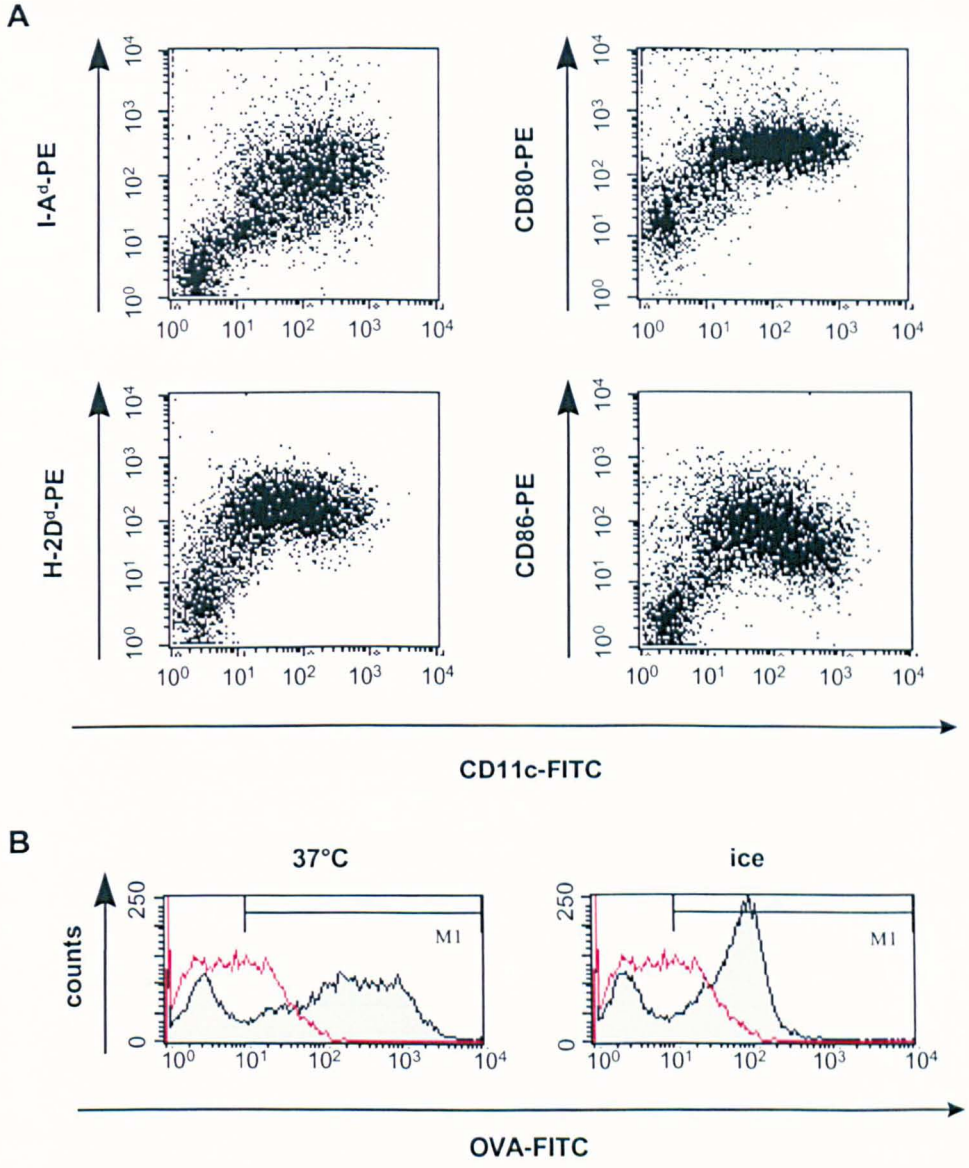

Fig. 8.2 Phenotype of and Ag-uptake by immature DCs. DCs cultured from murine bone marrow were analysed by FACS analysis on d10 of culture. Expression of cell surface MHC class I (H-2D^d) and class II (I-A^d) and of the co-stimulatory molecules CD80 and CD86 was measured and plotted against CD11c expression (A). Ag-uptake capacity was tested by incubating the DC with OVA-FITC either at 37°C or on ice (B).

CD11c$^-$ cells remaining in the cultures are most probably granulocytes, which also expand in GM-CSF containing cultures Lutz et al. 1999).

Expression levels of MHC class II (I-A^d), class I (H-2D^d), CD80 and CD86 molecules is increased on the cell surface of β-gal peptide-pulsed DCs as illustrated in Fig. 8.3, with a marked increase in MHC class II expression. Murine cytomegalovirus (MCMV) peptide-pulsed DCs exhibited a similar cell surface phenotype (data not shown). The Ag-pulsed DCs had matured, expressing elevated levels of co-stimulatory molecules, and therefore appropriate for use in Ag-specific T-cell responses. Maturation of DCs is normally induced by GM-CSF or inflammatory cytokines, such as TNF-α (Cella et al. 1997). Under the present conditions, mere pipetting as well as transfer to fresh culture plates could induce the maturation process, as previously described (Lutz et al. 1999).

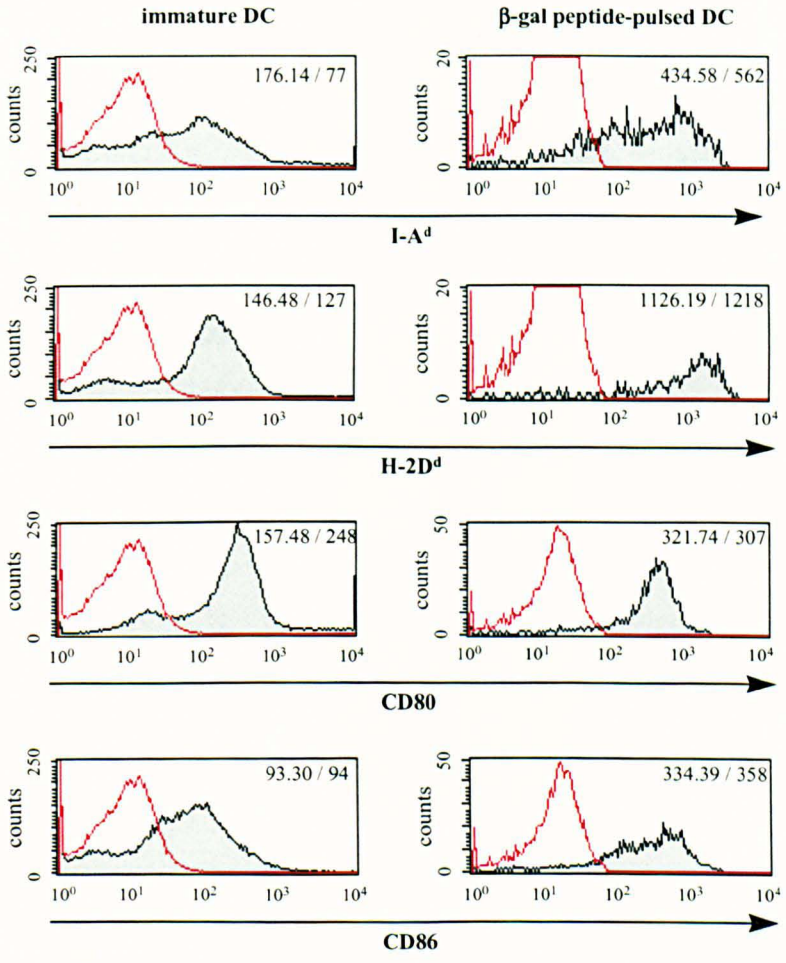

Fig. 8.3 Phenotype of Ag-pulsed DCs. Immature d11 DCs were pulsed o/n with β-gal$^{876-884}$ peptide.Expression levels of cell surface MHC class I (H-2D^d) and class II (I-A^d) and of the co-stimulatory molecules CD80 and CD86 was compared on immature d10 DCs (left) and mature Ag-pulsed d12 DCs (right). The red line (---) depicts the autofluorescence of unstained DCs. Mean fluorescences and peak channels are indicated in the top right corner of every histogram (mean / peak channel).

8.3 Preliminary data

8.3.1 iPCR for TCR-Vβ chains

An inverse PCR (iPCR) for the TCR-Vβ chains would have the advantage of allowing to amplify the transcripts of all Vβ-chains in one reaction and under the same conditions. Quantitative expression analysis could then be carried out using Southern Blot hybridisation with Vβ-chain specific probes as a read-out system.

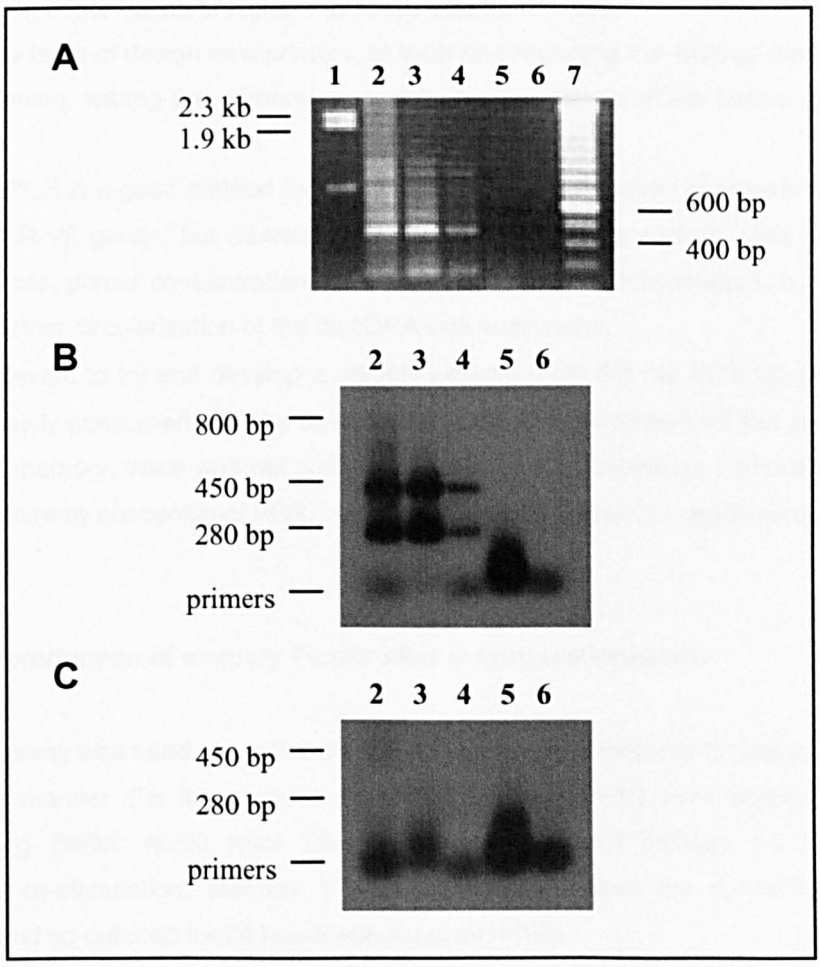

Fig. 8.4 The combination of C_n and BCS primers is unsuitable for iPCR under the present conditions. cDNA from the following probes was amplified in an inverse PCR reaction using the BCS and C_n primers: thymocytes (lane 2), d3 iPEC from ESbL-Gal-immunised DBA/2 (lane 3), $CD4^+$ and $CD8^+$ d3 iPEC (lane 4), naïve PEC (lane 5), and $CD4^+$ and $CD8^+$ immune BM from ESbL-Gal-immunised DBA/2 (lane 6). Lane 1 (λ DNA/*Eco* 91I) and 7 (100 bp DNA-ladder) contain DNA size markers. Shown are an ethidium bromide stained agarose gel (A), a Southern Blot hybridised with a [γ-^{32}P]-ATP labelled BCS-probe (B), and one hybridised with a [γ-^{32}P]-ATP labelled C_n-probe. The BCS but not the C_n primer binds to the amplified DNA-fragments, indicating an iPCR reaction double-primed by the BCS-primer.

In order to develop such a TCR-Vβ iPCR, the both primers were chosen to anneal in the constant region (see 8.4.1.2). Unfortunately, iPCR was unsuccessful under the present conditions (see Fig. 8.4), with the amplification reaction being double-primed by the BCS-primer (no annealing of the C_n-probe was detectable in the Southern Blot). This could indicate that the binding-conditions for C_n are much more stringent than those for BCS, with non-specifically primed sequences competing for amplification during iPCR, suppressing the amplification of specific sequences.
Another indication that the bands visualised by BCS-priming are the result of false priming is the size of the fragments. In an iPCR correctly amplifying the TCR-Vβ sequences one would expect fragment sizes of over 800 nucleotides. Here, the two major bands are at 450 and 280 bp, respectively, with minor bands of higher molecular size up to 1 kb.
One would now have to design new primers, at least one replacing the BCS-primer, and start again from the beginning, testing the primers separately in conventional PCRs before applying them in another iPCR.
Once set up, iPCR is a good method for the simultaneous amplification of several gene sequences as e.g. the TCR-Vβ genes, but developing the ideal conditions is difficult. One can try changing primer sequences, primer concentrations as well as the annealing temperature, but there is no way of knowing whether circularisation of the ds cDNA was successful.
It would be relevant to try and develop a reliably working iPCR for the TCR-Vβ genes, but as my project was mainly concerned with the development of a suitable system for the analysis of tumour specific T-cell memory, there was not sufficient time to do so. Therefore, I decided to analyse the TCR-Vβ repertoire by conventional PCR, using gene-specific primers in combination with C_n (4.3.4).

8.3.2 IFN-γ production of memory T-cells after *in vitro* restimulation

An ELISPOT assay was used to enumerate the *ex vivo* isolated memory T-cells producing IFN-γ in an Ag-specific manner. For this purpose, d3 mPEC (memory PEC) were isolated from ESbL-Gal tumour bearing Balb/c nu/nu mice having received standard therapy 1.5 months prior to intraperitoneal re-stimulation. Memory T-cells were purified from the d3 mPEC using Thy1.2 MACSbeads and co-cultured for 24 hours with Ag-pulsed DCs.
Although the cells had been restimulated *in vivo* 3 days before isolation, this was not expected to cause a high background spot formation as the cytokine-production kinetics of *ex vivo* isolated PEC between d1 and d12 after i.p. restimulation (see Fig. 4.9) indicated a low production of IFN-γ for this time point. Indeed, background levels proved to be very low, with an average of one IFN-γ producing cell per 3401 cells (Fig. 8.5, T-cells without DCs or Ag). In contrast, co-culture with β-gal$^{876\text{-}884}$ peptide-pulsed DCs resulted in a 26.6-fold increase in the number of IFN-γ producing T-cells, giving a frequency of β-gal$^{876\text{-}884}$ specific T-cells within mPEC of 1 : 128. The difference in the frequency of IFN-γ producing cells after a specific stimulus (β-gal$^{876\text{-}884}$ peptide) and a non-specific stimulus (MCMV pp89 peptide 168-176, L^d-restricted) was highly significant ($p = 0.0004$).

Unfortunately, the positive control for T-cell responsiveness, phytohemagglutinin (PHA), failed. Subsequent analysis in the laboratory revealed that the PHA batches used were inactive or only weakly immunogenic, with responses being measurable only at late time points.

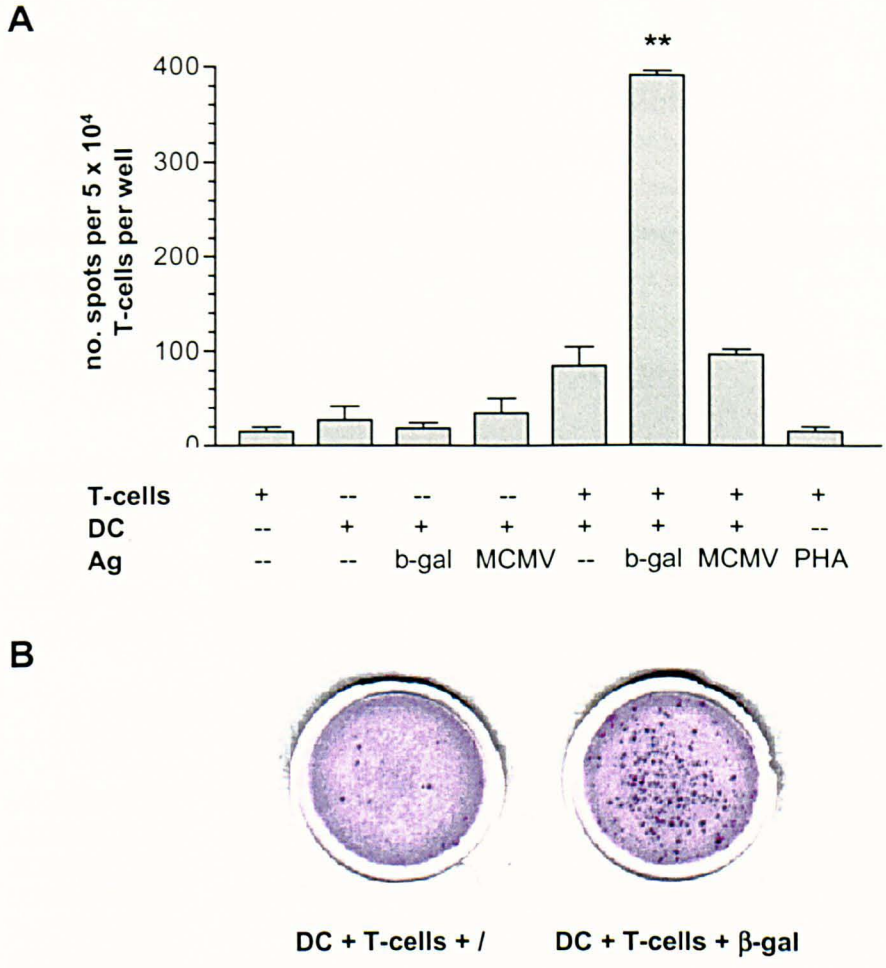

Fig. 8.5 Ag-specific IFN-γ production after *in vitro* restimulation of PEC-derived memory T-cells. 5 DBA/2 mice were primed with 5 x 10^4 ESbL-Gal i.e. 7 days before obtaining a secondary challenge with 1 x 10^7 irradiation inactivated ESbL-Gal i.p. . After 1.5 months the animals received another intraperitoneal challenge. mPEC were isolated 3 days later, and T-cells were isolated from the pooled cells using Thy1.2 MACSbeads. The T-cells were then co-cultured with Ag-pulsed DC for 24 hours and IFN-γ producing cells were measured in an ELISPOT assay. (A) number of IFN-γ producing cells per well (5 x 10^4 T-cells). b-gal: β-gal peptide 876-884; MCMV: MCMV pp89 peptide 168-176. (B) representative wells showing spot formation after co-culture of T-cells with β-gal pulsed DCs, and background IFN-γ production in the presence of non-Ag-pulsed DCs.

All samples were measured in triplicates. ** : significantly higher ($p < 0.005$) than the control groups.

8.4 mRNA sequences of genes analysed by PCR

All sequences are given in a 5' → 3' direction.

8.4.1 Murine TCR mRNA sequences

8.4.1.1 TCR-Vβ segments

TCR-Vβ primers used for PCR amplification in combination with the C_n-primer for the TCR-C region (see 8.4.1.2) are highlighted in blue.

Vβ1 (Barth et al. 1985, EMBL accession no.: X02778)

```
  1 AACACTAAAA TTACTCAGTC ACCAAGATAT CTAATCCTGG GAAGAGCAAA
 51 TAAGTCTTTG GAATGTGAGC AACATCTGGG ACATAATGCT ATGTACTGGT
101 ATAAACAGAG CGCTGAGAAG CCGCCAGAGC TCATGTTTCT CTACAATCTT
151 AAACAGTTGA TTCGAAATGA GACGGTGCCC AGTCGTTTTA TACCTGAATG
201 CCCAGACAGC TCCAAGCTAC TTTTACATAT ATCTGCCGTG GATCCAGAAG
251 ACTCAGCTGT CTATTTTTGT GCCAGCAGC
```

Vβ2 (Barth et al. 1985, EMBL accession no.: X02780)

```
  1 GTGACTTTGC TGGAGCAAAA CCCAAGGTGG CGTCTGGTAC CACGTGGTCA
 51 AGCTGTGAAC CTACGCTGCA TCTTGAAGAA TTCCCAGTAT CCCTGGATGA
151 GCTGGTATCA GCAGGATCTC CAAAAGCAAC TACAGTGGCT GTTCACTCTG
201 CGGAGTCCTG GGGACAAAGA GGTCAAATCT CTTCCCGGTG CTGATTACCT
251 GGCCACACGG GTCACTGATA CGGAGCTGAG GCTGCAAGTG GCCAACATGA
301 GCCAGGGCAG AACCTTGTAC TGCACCTGCA GT
```

Vβ4 (Barth et al. 1985, EMBL accession no.: X02781)

```
  1 GACCCGAAAA TTATCCAGAA ACCAAAATAT CTGGTGGCAG TCACAGGGAG
 51 CGAAAAAATC CTGATATGCG AACAGTATCT AGGCCACAAT GCTATGTATT
101 GGTATAGACA AAGTGCTAAG AAGCCTCTAG AGTTCATGTT TTCCTACAGC
151 TATCAAAAAC TTATGGACAA TCAGACTGCC TCAAGTCGCT TCCAACCTCA
201 AAGTTCAAAG AAAAACCATT TAGACCTTCA GATCACAGCT CTAAAGCCTG
251 ATGACTCGGC CACATACTTC TGTGCCAGCA GC
```

Vβ5.1 (Barth et al. 1985, EMBL accession no.: X02782)

```
  1 AATTCTGGGG TTGTCCAGTC TCCAAGATAC ATAATCAAAG GAAAGGGAGA
 51 AAGGTCCATT CTAAAATGTA CTCCCATCTC TGGACATCTC TCTGTGGCCT
101 GGTATCAACA GACTCAGGGG CAGGAACTAA AGTTCTTCAT TCAGCATTAT
151 GATAAAATGG AGAGAGATAA AGGAAACCTG CCCAGCAGAT TCTCAGTCCA
201 ACAGTTTGAT GACTATCACT CTGAGATGAA CATGAGTGCC TTGGAGCTAG
251 AGGACTCTGC CGTGTACTTC TGTGCCAGCT CTG
```

Vβ5.2 (Iwamoto et al. 1987, EMBL accession no.: X05737)

```
  1 GATTCTGGGG TTGTCCAGTC TCCAAGACAC ATAATCAAAG AAAAGGGAGG
 51 AAGGTCCGTT CTGACGTGTA TTCCCATCTC TGGACATAGC AATGTGGTCT
101 GGTACCAGCA GACTCTGGGG AAGGAATTAA AGTTCCTTAT TCAGCATTAT
151 GAAAAGGTGG AGAGAGACAA AGGATTCCTA CCCAGCAGAT TCTCAGTCCA
201 ACAGTTTGAT GACTATCACT CTGAAATGAA CATGAGTGCC TTGGAACTGG
251 AGGACTCTGC TATGTACTTC TGTGCCAGCT CTCTCG
```

Vβ8.1 (Barth et al. 1985, EMBL accession no.: X02783)

```
  1 GAGGCTGCAG TCACCCAAAG TCCAAGAAGC AAGGTGGCAG TAACAGGAGG
 51 AAAGGTGACA TTGAGCTGTC ACCAGACTAA TAACCATGAC TATATGTACT
101 GGTATCGGCA GGACACGGGG CATGGGCTGA GGCTGATCCA TTACTCATAT
151 GTCGCTGACA GCACGGAGAA AGGAGATATC CCTGATGGGT ACAAGGCCTC
201 CAGACCAAGC CAAGAGAATT TCTCTCTCAT TCTGGAGTTG GCTTCCCTTT
251 CTCAGACAGC TGTATATTTC TGTGCCAGCA GT
```

The sequence highlighted in green is the primer BV8 used for testing the C_n-primer prior to application in iPCR.

Vβ8.2 (Barth et al. 1985, EMBL accession no.: X02784)

```
  1 GAGGCTGCAG TCACCCAAAG CCCAAGAAAC AAGGTGGCAG TAACAGGAGG
 51 AAAGGTGACA TTGAGCTGTA ATCAGACTAA TAACCACAAC AACATGTACT
101 GGTATCGGCA GGACACGGGG CATGGGCTGA GGCTGATCCA TTATTCATAT
151 GGTGCTGGCA GCACTGAGAA AGGAGATATC CCTGATGGAT ACAAGGCCTC
201 CAGACCAAGC CAAGAGAACT TCTCCCTCAT TCTGGAGTTG GCTACCCCCT
251 CTCAGACATC AGTGTACTTC TGTGCCAGC
```

The sequence highlighted in green is the primer BV8 used for testing the C_n-primer prior to application in iPCR.

Vβ8.3 (Chou et al. 1987)

```
  1 AGGCTGCAGT CACCCAAAGC CCTAGAAACA AGGTGACAGT AACAGGAGGA
 51 AACGTGACAT TGAGCTGTCG CCAGACTAAT AGCCACAACT ACATGTACTG
101 GTATCGGCAG GACACTGGGC ATGGGCTGAG GCTGATCCAT TACTCATATG
151 GTGCTGGCAA CCTTCGAATA GGAGATGTCC CTGATGGGTA CAAGGCCACC
201 AGAACAACGC AAGAAGACTT CTTCCTCCTG CTGGAATTGG CTTCTCCCTC
251 TCAGACATCT TTGTACTTCT GTGCCAGCAG TGATG
```

The sequence highlighted in green is the primer BV8 used for testing the C_n-primer prior to application in iPCR.

Vβ10 (Behlke et al. 1985)

```
  1 TCCTATTGGT ACAAGCAAGA CTCTAAGAAA TTGCTGAAGA TTATGTTTAG
 51 CTACAATAAT AAGCAACYCA TTGTAAACGA AACAGTTCCA AGGCGCTTCT
101 CACCTCAGTC TTCAGATAAA GCTCATTTGA ATCTTCGAAT CAAGTCTGTA
151 GAGCCGGAGG ACTCTGCTGT GTATCTCTGT GCCAGCAGCG CCC
```

Vβ13 (Morahan et al. 1989, EMBL accession no.: M25913)

```
  1 GTACTGTCTG AAGCTGGAGT CACCCAGTCT CCCAGATATG CAGTCCTACA
 51 GGAAGGGCAA GCTGTTTCCT TTTGGTGTGA CCCTATTTCT GGACATGATA
101 CCCTTTACTG GTATCAGCAG CCCAGAGACC AGGGGCCCCA GCTTCTAGTT
151 TACTTTCGGG ATGAGGCTGT TATAGATAAT TCACAGTTGC CCTCGGATCG
201 ATTTTCTGCT GTGAGGCCTA AAGGAACTAA CTCCACTCTC AAGATCCAGT
251 CTGCAAAGCA GGGCGACACA GCCACCTATC TCTGTGCCAG
```

Vβ14 (Behlke et al. 1986, EMBL accession no.: M11858)

```
  1 GCTCAGACTA TCCATCAATG GCCAGTTGCC GAGATCAAGG CTGTGGGCAG
 51 CCCACTGTCT CTGGGGTGTA CCATAAAGGG GAAATCAAGC CCTAACCTCT
101 ACTGGTACTG GCAGGCCACA GGAGGCACCC TCCAGCAACT CTTCTACTCT
151 ATTACTGTTG GCCAGGTAGA GTCGGTGGTG CAACTGAACC TCTCAGCTTC
201 CAGGCCGAAG GACGACCAAT TCATCCTAAG CACGGAGAAG CTGCTTCTCA
251 GCCACTCTGG CTTCTACCTC TGTGCCTGGG
```

Vβ15 (Behlke et al. 1986, EMBL accession no.: M11859)

```
  1 GGAGCACTCG TCTATCAATA TCCCAGAAGA ACCATCTGTA AGAGTGGAAC
 51 TTCCATGAGG ATGGAGTGTC AAGCTGTGGG TTTTCAGGCA ACTTCCGTAG
101 CTTGGTATCG TCAATCGCCT CAAAAGGCAT TTGAACTGAT AGCACTTTCT
151 ACTGTGAACT CAGCAATCAA ATATGAACAA AATTTTACCC AGGAAAAATT
201 TCCCATCAGT CATCCCAACT TATCCTTTTC ATCTATGACA GTTTTAAATG
251 CATATCTTGA AGACAGAGGC TTATATCTCT GTGGTGCGG
```

Vβ16 (Behlke et al. 1986, EMBL accession no.: M11860)

```
  1 GGACCCAAAG TCTTACAGAT CCCAAGTCAT CAAATAATAG ATATGGGGCA
 51 GATGGTGACC CTCAATTGTG ACCCAGTTTC TAATCACCTA TATTTTTATT
101 GGTATAAACA GATTTTAGGA CAGCAGATGG AGTTTCTGGT TAATTTCTAC
151 AATGGTAAAG TCATGGAGAA GTCTAAACTG TTTAAGGATC AGTTTTCAGT
201 TGAAAGACCA GATGGTTCAT ATTTCACTCT GAAAATCCAA CCCACAGCAC
251 TGGAGGACTC AGCTGTGTAC TTCTGTGCCA GCAGCTTAC
```

Vβ18 (Singer et al. 1986, EMBL accession no.: M14294)

```
  1 TCTTTGGAGC CAAGTTCCAG GAACAGAGCT TGATGCTCAT GGCAACTGCA
 51 AATGAAGGCT CTGAAGCCAC ATACGAGAGT GGATTCACCA AGGACAAGTT
101 TCCAATCAGC CGGCCAAACC TAACATTCTC AACGTTGACA GTGAACAATG
151 CAAGGCCTGG AGACAGCAGT ATCTATTTCT GTAGTTCTC
```

Vβ20 (Six et al. 1991)

```
  1 GGCTCTTTTG ATGCTGCAGT TACACAGAAG CCAAGATATT TGATCAAAAT
 51 GAAAGGCCAG GAAGCAGAGA TGAAATGTAT CCCTGAAAAG GGGCACACTG
101 CTGTTTTCTG GTATCAACAA AAGCAGAGCA AAGAATTAAA GTTCCTGATT
151 TACTTTCAGA ATCAACAGCC TCTTGATCAA ATAGACATGG TCAAGGAGAG
201 ATTCTCAGCT GTGTGCCCCT CCAGCTCACT CTGCAGCCTG GGAATCAGAA
251 CGTGCGAAGC AGAAGACTCA GCACTGTACT TGTGCTCCAG CAGT
```

8.4.1.2 The TCR-Cb segment

(Gascoigne et al. 1984)

```
                                Cn-primer (antisense)
  1 GAGGATCTGA GAAATGTGAC TCCACCCAAG GTCTCCTTGT TTGAGCCATC
    (1)
 51 AAAAGCAGAG ATTGCAAACA AACAAAAGGC TACCCTCGTG TGCTTGGCCA
101 GGGGCTTCTT CCCTGACCAC GTGGAGCTGA GCTGGTGGGT GAATGGCAAG
151 GAGGTCCACA GTGGGGTCAG CACGGACCCT CAGGCCTACA AGGAGAGCAA
201 TTATAGCTAC TGCCTGAGCA GCCGCCTGAG GGTCTCTGCT ACCTTCTGGC
251 ACAATCCTCG CAACCACTTC CGCTGCCAAG TGCAGTTCCA TGGGCTTTCA
                                BCS-primer (sense)
301 GAGGAGGACA AGTGGCCAGA GGGCTCACCC AAACCTGTCA CACAGAACAT
351 CAGTGCAGAG GCCTGGGGCC GAGCAGACTG TGGGATTACC TCAGCATCCT
                           (2)                  (3)
401 ATCAACAAGG GGTCTTGTCT GCCACCATCC TCTATGAGAT CCTGCTAGGG
451 AAAGCCACCC TGTATGCTGT GCTTGTCAGT ACACTGGTGG TGATGGCTAT
501 GGTCAAAAGA AAGAATTCAT GAAGTCAGAT GTGAAGATGA ATACAAGAGC
     (4)                (5)
551 TGACAACACA TTGTGTTAAT ACAGATTTTC TTCTCCCAGA ACTTCTGAA
                                          UTA-primer (antisense)
601 GAGCTATTCT CATTTGTCTG TGCATCCCAA ATTCTGCCTA CTAGTCACGC
651 ATAGGTGCAT TTGTATGTCT GAAATTCTTG TGACCTAGAA AATGCCTACA
701 CTTACAATCA AACCAATAAA CATGTTCTAG GACGGCCTG - poly (A)
```

Underlined bases mark the first codon of the respective exon, with exon 1 (1) being the external part of the TCR-Cβ, exon 2 (2) the hinge-like region, exon 3 (3) the transmembrane domain and exon 4 (4) the cytoplasmic tail. The next underlined codon (5) indicates the beginning of the 3' untranslated region, which contains the poly (A) addition signal, highlighted in green.

8.4.2 The murine cytoskeletal β-actin mRNA sequence

(Tokunaga et al. 1986, EMBL accession no.: X03672)

```
   1 CCGGTCGAGT CGCGTCCACC CGCGAGCACA GCTTCTTTGC AGCTCCTTCG
  51 TTGCCGGTCC ACACCCGCCA CCAGTTCGCC ATGGATGACG ATATCGCTGC
 101 GCTGGTCGTC GACAACGGCT CCGGCATGTG CAAAGCCGGC TTCGCGGGCG
 151 ACGATGCTCC CCGGGCTGTA TTCCCCTCCA TCGTGGGCCG CCCTAGGCAC
 201 CAGGGTGTGA TGGTGGGAAT GGGTCAGAAG GACTCCTATG TGGGTGACGA
 251 GGCCCAGAGC AAGAGAGGTA TCCTGACCCT GAAGTACCCC ATTGAACATG
 301 GCATTGTTAC CAACTGGGAC GACATGGAGA AGATCTGGCA CCACACCTTC
 351 TACAATGAGC TGCGTGTGGC CCCTGAGGAG CACCCTGTGC TGCTCACCGA
 401 GGCCCCCCTG AACCCTAAGG CCAACCGTGA AAAGATGACC CAGATCATGT
 451 TTGAGACCTT CAACACCCCA GCCATGTACG TAGCCATCCA GGCTGTGCTG
 501 TCCCTGTATG CCTCTGGTCG TACCACAGGC ATTGTGATGG ACTCCGGAGA
 551 CGGGGTCACC CACACTGTGC CCATCTACGA GGGCTATGCT CTCCCTCACG
 601 CCATCCTGCG TCTGGACCTG GCTGGCCGGG ACCTGACAGA CTACCTCATG
 651 AAGATCCTGA CCGAGCGTGG CTACAGCTTC ACCACCACAG CTGAGAGGGA
 701 AATCGTGCGT GACATCAAAG AGAAGCTGTG CTATGTTGCT CTAGACTTCG
 851 AGCAGGAGAT GGCCACTGCC GCATCCTCTT CCTCCCTGGA GAAGAGCTAT
 801 GAGCTGCCTG ACGGCCAGGT CATCACTATT GGCAACGAGC GGTTCCGATG
 851 CCCTGAGGCT CTTTTCCAGC CTTCCTTCTT GGGTATGGAA TCCTGTGGCA
 901 TCCATGAAAC TACATTCAAT TCCATCATGA AGTGTGACGT TGACATCCGT
 951 AAAGACCTCT ATGCCAACAC AGTGCTGTCT GGTGGTACCA CCATGTACCC
1001 AGGCATTGCT GACAGGATGC AGAAGGAGAT TACTGCTCTG GCTCCTAGCA
1051 CCATGAAGAT CAAGATCATT GCTCCTCCTG AGCGCAAGTA CTCTGTGTGG
1101 ATCGGTGGCT CCATCCTGGC CTCACTGTCC ACCTTCCAGC AGATGTGGAT
1151 CAGCAAGCAG GAGTACGATG AGTCCGGCCC CTCCATCGTG CACCGCAAGT
1201 GCTTCTAGGC GGACTGTTAC TGAGCTGCGT TTTACACCCT TTCTTTGACA
1251 AAACCTAACT TGCGCAGAAA AAAAAAAAAT AAGAGACAAC ATTGGCATGG
1301 CTTTGTTTTT TTAAATTTTT TTTAAAGTTT TTTTTTTTTT TTTTTTTTTT
1351 TTTTTTTTAA GTTTTTTTGT TTTGTTTTGG CGCTTTTGAC TCAGGATTTA
1401 AAAACTGGAA CGGTGAAGGC GACAGCAGTT GGTTGGAGCA AACATCCCCC
1451 AAAGTTCTAC AAATGTGGCT GAGGACTTTG TACATTGTTT TGTTTTTTTT
1501 TTTTTTTGGT TTTGTCTTTT TTTAATAGTC ATTCCAAGTA TCCATGAAAT
1551 AAGTGGTTAC AGGAAGTCCC TCACCCTCCC AAAAGCCACC CCCACTCCTA
1601 AGAGGAGGAT GGTCGCGTCC ATGCCCTGAG TCCACCCCGG GGAAGGTGAC
1651 AGCATTGCTT CTGTGTAAAT TATGTACTGC AAAAATTTTT TTAAATCTTC
1701 CGCCTTAATA CTTCATTTTT GTTTTTAATT TCTGAATGGC CCAGGTCTGA
1751 GGCCTCCCTT TTTTTTGTCC CCCCAACTTG ATGTATGAAG GCTTTGGTCT
1801 CCCTGGGAGG GGGTTGAGGT GTTGAGGCAG CCAGGGCTGG CCTGTACACT
1851 GACTTGAGAC CAATAAAAGT GCACACCTTA CCTTACACAA AC
```

Indicated in blue are the docking sites of the primers used (Klein et al. 1998), which yield a fragment of 349 bp.

8.4.3 The genetic code

1st position (5'-end)	2nd position				3rd position (3'-end)
	U	C	A	G	
U	Phe	Ser	Tyr	Cys	U
	Phe	Ser	Tyr	Cys	C
	Leu	Ser	STOP	STOP	A
	Leu	Ser	STOP	Trp	G
C	Leu	Pro	His	Arg	U
	Leu	Pro	His	Arg	C
	Leu	Pro	Gln	Arg	A
	Leu	Pro	Gln	Arg	G
A	Ile	Thr	Asn	Ser	U
	Ile	Thr	Asn	Ser	C
	Ile	Thr	Lys	Arg	A
	Met	Thr	Lys	Arg	G
G	Val	Ala	Asp	Gly	U
	Val	Ala	Asp	Gly	C
	Val	Ala	Glu	Gly	A
	Val	Ala	Glu	Gly	G

U = uracil; C = cytosine; A = adenine; G = guanine

In DNA molecular complexes, the complementary nucleotide for adenine (A) is not uracil (U) as in RNA, but thymine (T).

8.4.4 The amino acids

amino acid	3-letter code	single-letter code
alanine	Ala	A
cysteine	Cys	C
aspartic acid	Asp	D
glutamic acid	Glu	E
phenylalanine	Phe	F
glycine	Gly	G
histidine	His	H
isoleucine	Ile	I
lysine	Lys	K
leucine	Leu	L
methionine	Met	M
asparagine	Asn	N
proline	Pro	P
glutamine	Gln	Q
arginine	Arg	R
serine	Ser	S
threonine	Thr	T
valine	Val	V
tryptophane	Trp	W
tyrosine	Tyr	Y

Contributions to scientific publications and meetings

Y. Mahnke, V. Schirrmacher, Longevity and functional characteristics of memory T-cells in a murine graft versus leukaemia adoptive immunotherapy (ADI) model, 2nd International Conference on Tumour Microenvironment: Progression, Therapy and Prevention, Tiberias (Israel), Nov 2000 (conference cancelled due to political insecurities)

Y. Mahnke, V. Schirrmacher, Localisation and longevity of memory T-cells in a murine graft versis leukaemia adoptive immunotherapy (ADI) model, 2nd Invasion and Metastasis Conference (IIAR, International Institute of Anticancer Research), Athens (Greece), June 2001

M. Feuerer, P. Beckhove, Y. Mahnke, J. Schwendemann, M. Hommel, L. Bai, B. Kyewski, V. Umansky, V. Schirrmacher, Bone marrow: a secondary lymphoid organ capable of antigen presentation and induction of T-cell responses, submitted

Declaration

I hereby declare that this thesis has been composed solely by myself and has not been accepted in any previous application for candidature for a higher degree. All work presented in this thesis, was, unless acknowledged, initiated and executed by myself. All sources of information in the text have been acknowledged by reference.

Yolanda D. Mahnke

Acknowledgements

I am grateful to have had the opportunity to work and learn in the laboratories of my immediate supervisor, Prof. Volker Schirrmacher, as well as for his ideas and thorough reading of my PhD-thesis.
Many thanks to my secondary supervisor, Prof. Jonathan Lamb, who provided me with a lot of encouragement, as well as many helpful comments and constructive criticism during the writing of my thesis.

I would like to thank Dr. Bernhard Arden of the Dermatology Clinic, Heidelberg, who kindly offered help and experience in establishing the iPCR for the TCR-Vβ segments (which, unfortunately, did not work).

Many thanks go to Andreas Griesbach who offered practical assistance in the many adoptive transfer experiments, to Klaus Hexel for his mastery of the FACSvantage, and to Mariana Bucur who was always generous with tips, sweets, and good humour.

I am very grateful to Dr. Katerina Chlichlia for the many discussions and her revision of early drafts of this thesis, as well as for the co-operation during Maxi Preps.

I would like to thank Dr. Axel Benner who kindly offered support with biostatistical analyses. Special thanks go to all the personnel of the central animal facilities in the "Barriere IV" and the isolator premises for keeping my mice happy with abundant food and drink.

Thanks to all my colleagues, past and present, of the Department of Immunology who provided a good working atmosphere and many fun moments outside the lab. Special thanks goes to Dr. Natalio Garcia Garbi for productive tips and tricks, and the many relaxing cooking sessions.

I am most grateful to my family who supported me at all times.

Curriculum vitae

PERSONAL DATA

Name:	Yolanda Dagmar Mahnke
Address:	Beethovenstrasse 20, 69214 Heidelberg, Germany
Date of birth:	4th October 1975
Place of birth:	Ludwigshafen am Rhein, Germany

EDUCATION

June 1994	European Baccalaureate European School of Brussels I, Brussels, Belgium
Oct 1994 - June 1997	BSc in Biology Associate of the Royal College of Science (ARCS) Dept. of Biology, Imperial College of Science, Technology and Medicine, University of London, London, UK
April 1997 - June 1997	Final Year Research Project 'Analysis of T-cell responses to a major allergen of house dust mite, Der p1, in transgenic mice expressing MHC class II on their T-cells - an *in vitro* investigation' in the laboratories of Prof. Jonathan R Lamb, Respiratory Medicine Unit, The University of Edinburgh Medical School, Edinburgh, UK
Feb 1998 - today	PhD-thesis 'A novel model system for the study of anti-tumour T-cell memory' in the laboratories of Prof. Volker Schirrmacher, Dept. of Cellular Immunology, German Cancer Research Centre (DKFZ), Heidelberg, Germany submitted to the Dept. of Biology at The Open University, London, UK